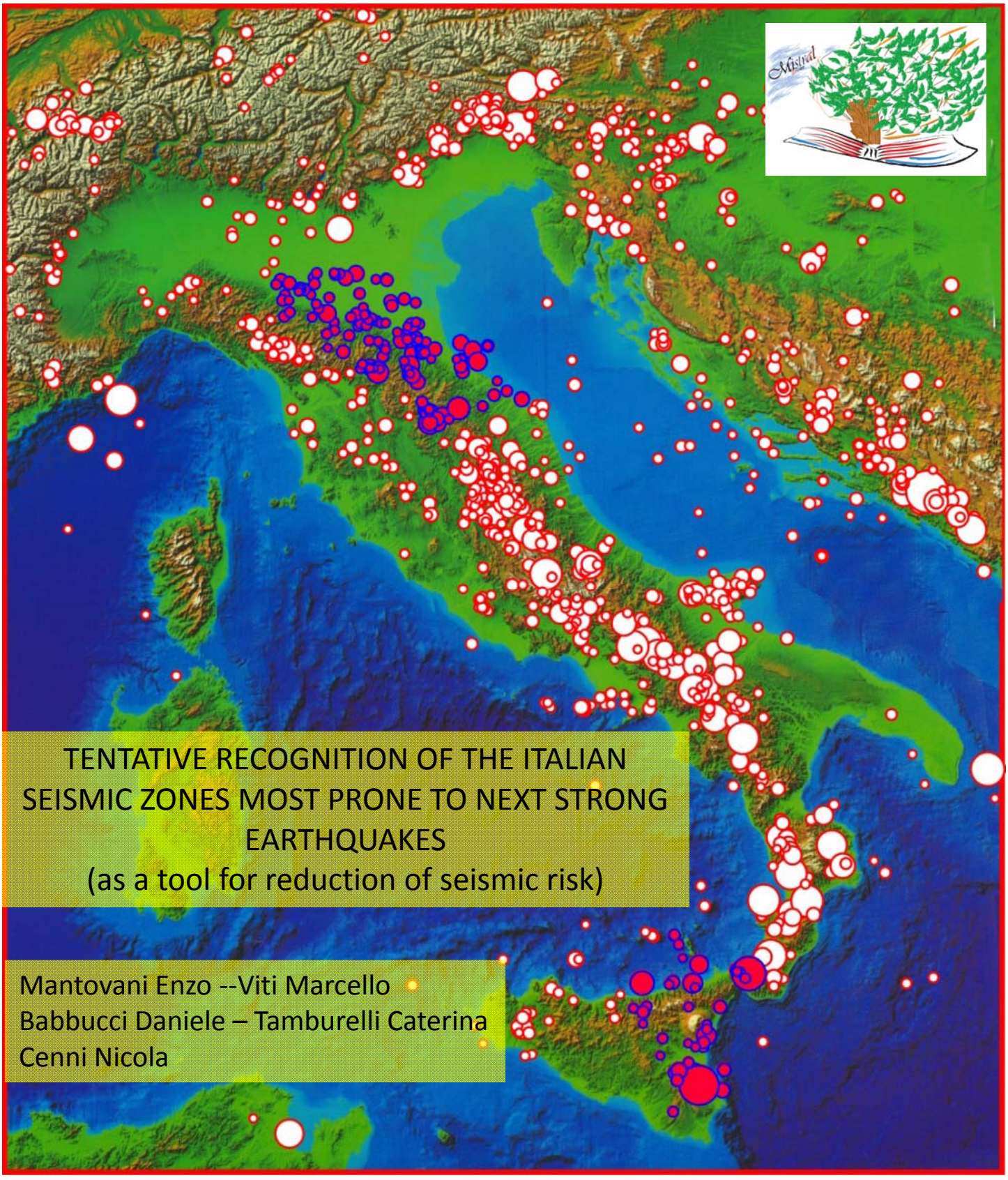

TENTATIVE RECOGNITION OF THE ITALIAN SEISMIC ZONES MOST PRONE TO NEXT STRONG EARTHQUAKES

(as a tool for reduction of seismic risk)

Mantovani Enzo --Viti Marcello
Babbucci Daniele – Tamburelli Caterina
Cenni Nicola

Cover figure

Circles indicate the earthquakes that have occurred since 1000 A.D.(e.g. Rovida et al., 2011). The full red in the symbols identifies the zones (Umbria-Marche-Romagna Apennines and eastern Sicily) that, on the basis of the evidence and arguments described in this report, are recognized as the most prone to next strong shocks. This relative evaluation implies a priority respect to the Italian seismic zones, except the Western Alps, the western Po valley, the inner (Tyrrhenian) side of the Apennine belt and the Apulian high, where the proposed approach cannot be applied yet. Since no indication is provided about the expected occurrence time of major shocks in the proposed priority zones, this report does not involve any warning. It only aims at facilitating the best management of resources for the mitigation of seismic risk in Italy.

Tentative recognition of the Italian seismic zones most prone to next strong earthquakes (as a tool for reduction of seismic risk)

Mantovani Enzo, Viti Marcello, Babbucci Daniele, Tamburelli Caterina
Dipartimento di Scienze Fisiche , della Terra e dell'Ambiente – Università di Siena
Cenni Nicola
Dipartimento di Fisica e Astronomia – Università di Bologna

Published by
Mistral Service sas
Via U. Bonino, 3,
98100 Messina (Italy)

This book is distributed as an Open Access work. All users can download copy and use the present volume as long as the author and the publisher are properly cited. The content of this manuscript has been revised by our international Editorial Board members.

Important Notice
The publisher does not assume any responsibility for any damage or injury to property or persons arising out of the use of any materials, instructions, methods or ideas contained in this book. Opinions and statements expressed in this book are those of the authors and not those of the publisher. Furthermore, the publisher does not take any responsibility for the accuracy of information contained in the present volume.

First published: June, 2016
Prepared in Italy

© **Mantovani Enzo, Viti Marcello, Babbucci Daniele, Tamburelli Caterina, Cenni Nicola**

A free online copy of this book is available at www.mistralservice.it

Tentative recognition of the Italian seismic zones most prone to next strong earthquakes (as a tool for reduction of seismic risk)
Mantovani Enzo, Viti Marcello, Babbucci Daniele, Tamburelli Caterina, Cenni Nicola
ISBN: 978-88-98161-23-2

Contents

Premise: objective of the study, methodology, results obtained and their possible social impact

A large portion of the building heritage in Italy has not been realized to resist the seismic shaking caused by earthquakes occurred in the past. Thus, the limited economic resources now available are largely insufficient to obtain a significant reduction of the seismic risk throughout the whole country. A way to achieve such objective might be identified by exploiting the fact that most probably in the next tens of years only few Italian zones will be hit by strong earthquakes and that, consequently, for such period the restoration of weak buildings and critical infrastructures will be urgent only in a very limited portion of the national territory. Thus, if the present scientific knowledge allowed us to reliably identify the location of the next major shocks, a significant reduction of the of seismic risk in Italy could become economically and operationally feasible.

The hope of realizing such very attractive possibility should strongly increase the attention of Civil Protection authorities towards the researches that may provide the information cited above. As a first contribution towards that objective, this report describes a procedure that might allow the recognition of the Italian zone most prone to the next strong earthquake.

Since it is well known that earthquakes are deterministic phenomena, closely connected with the progressive development of crustal deformations, any attempt at recognizing the future path of seismicity in the study area can provide reliable results only when it is carried out by an adequate deterministic approach and it can dispose of a profound knowledge of the ongoing kinematic/tectonic context. Thus, this volume starts with a synthetic description of the above elements, making reference to the publications that report more complete descriptions. Then, in support to the tectonic context here adopted, it is pointed out that its expected short-term development can coherently and plausibly account for the spatio-temporal distribution of major earthquakes that have occurred in the periAdriatic regions since 1400 A.D. and reported in the Appendix 2.

Using the knowledge so acquired about the past seismotectonic behaviour of the system, one can try to predict the future pattern of seismicity, taking into account the present situation created by the recent distribution of major shocks. In particular, hypotheses are advanced about where crustal strain and stress, and thus earthquake probability, may be highest at present. This procedure has led to identify some zones of the northern Apennines and eastern Sicily, where the employment of the resources eventually available for the reduction of seismic risk could be privileged with respect to the other Italian regions.

The proposed approach, being aimed at tentatively recognizing the zones where the stress has recently undergone and still undergoes a significant increase, can be flanked by experimental observations that may confirm or refute the proposed predictions. For instance, insights into this problem could be provided by the analysis of the distribution of minor seismicity, even though the interpretation of this signal is not simple. In general, it is reasonable to think that an increase of this background activity is caused by an enhancement of the tectonic load. However, to understand the complex distribution of such seismicity one must consider that each fault system is constituted either by segments where the slip is poorly resisted and by segments where instead frictional forces are higher than tectonic forces.

In the first type of fault segment the slip is almost continuous (being mainly aseismic) and the accumulation of elastic strain is very limited. Such segment can anyhow generate small seismic fractures when the relative motion between the opposite sides of the fault overcomes the rate that is allowed by the rheological properties of the structure. In the fault segments characterized by high values of friction slip is almost negligible while strain accumulation is relatively fast. During this phase, stress increases up to reach the rupture value, when a sudden slip occurs along the fault. Thus, to identify the zones where a major shock could occur it is necessary to recognize both the free faults segments (marked by accelerations of minor seismicity) and the blocked segments (sites of historical earthquakes). This report provides a discussion about the various aspects of the above

problem and an analysis of the distribution of the minor seismicity that has occurred in the study area since 1981 (the most complete and reliable data set). The results of this investigation point out that the priority zones identified on the basis of the seismotectonic evidence described earlier are affected by the highest level of minor seismicity.

Another information that may help to recognize where favorable conditions to the seismic activation of faults are being developing, could be provided by space geodetic monitoring (GPS), which may help to determine the velocity field and the related strain rate field. Since the interpretation of this last information is not simple, being not yet clear how this parameter can condition the probability of major shocks, this volume reports a discussion about the main aspects of this problem and the possible implications of the geodetic observations that have been carried out over the last 15 years. In addition, it is pointed out the importance of geodetic monitoring for evidencing the perturbations of the strain/stress fields triggered by major earthquakes in the central Mediterranean region, which could induce seismic activity in the Italian region.

Since the decision of taking or not taking into account the indications here proposed will be obviously conditioned by the degree of confidence that the authorities may grow on the adopted approach, this report ends up with a discussion about the uncertainties that might affect the results obtained.

However, one should consider that notwithstanding possible ambiguities in the identification of the priority seismic zones, the strategy of privileging seismic risk reduction in few priority zones would anyway be convenient. In case the next shock does not occur in one of the zones identified (eventuality that can not be excluded, given the complexity of the problem involved) the negative consequences of such failure would be not very important for the epicentral zone, where a negligible improvement of safety would have been allowed by an homogeneous distribution of resources. Instead, in case the next earthquake occurs in one of the proposed priority zones, the practical advantages would be remarkable, since the significant improvement of safety obtained for such zone could allow an appreciable reduction of casualties and damages.

Furthermore, the plausibility of the arguments here presented in support of the proposed approach strongly encourages to think that the resources devoted to seismic risk mitigation in the proposed zones can hardly be considered a waste.

It is finally opportune to point out that no information can actually be provided about when the priority zones here recognized may be hit by major earthquakes. This underlines that the only purpose of this attempt is favouring the best management of public resources devoted to seismic risk mitigation in Italy and to inform the people living in the proposed priority zones. This last awareness may at least stimulate the restoration of the most vulnerable buildings in the zones involved and, more in general, all the operations that can improve the resistance of buildings.

1. Present tectonic setting and recent geological evolution in the central Mediterranean region

The ongoing tectonic context in the central Mediterranean area is sketched in Fig.1.

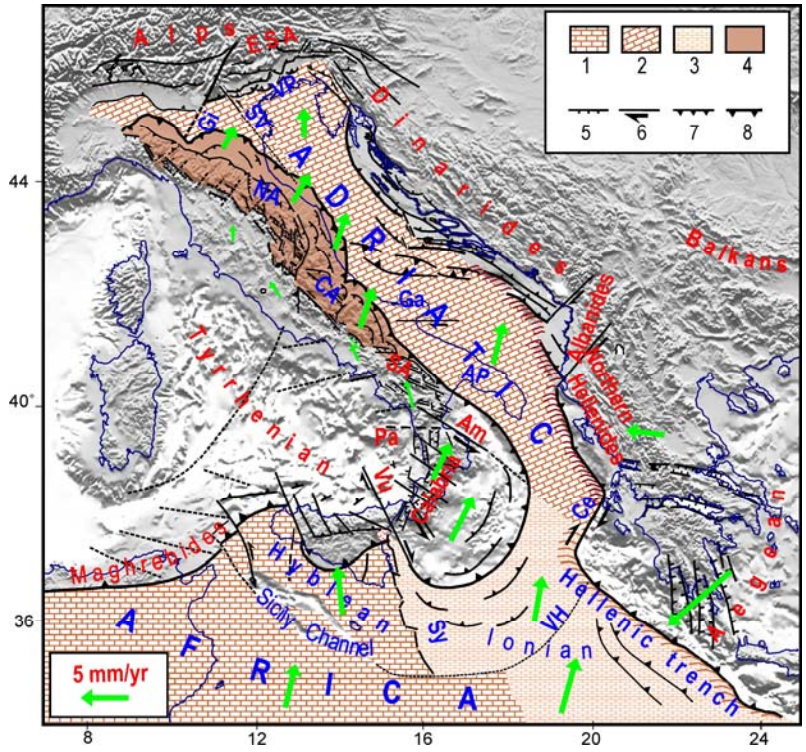

Fig. 1. *Sketch of the tectonic/kinematic setting in the central Mediterranean region (Mantovani et al., 2006, 2007a, 2009, Viti et al. 2006, 2011)* ***1,2)*** *African and Adriatic continental domains respectively* ***3)*** *Ionian oceanic domain* ***4)*** *Outer sector of the Apennine belt dragged and stressed by the Adriatic plate* ***5,6,7)*** *Major extensional, transcurrent and compressional tectonic features respectively* ***8)*** *Outer front of Neogenic belts. Green arrows indicate the proposed kinematic pattern with respect to Eurasia (Mantovani et al., 2007a; Viti et al., 2011). Am=Amendolara fault, Ap=Apulia, CA=Central Apennines, Ce=Cephalonia fault, ESA=Eastern Southern Alps, Ga=Gargano, Gi=Giudicarie fault system, NA=Northern Apennines, Pa=Palinuro fault, SA=Southern Apennines, SV= Schio-Vicenza fault system, Sy=Syracuse fault system, VH=Victor Hensen discontinuity, VP=Venetian Plain, Vu=Vulcano fault system.*

Tectonic activity in the study area is mainly driven by the motions of Africa and the Anatolian-Aegean-Balkan system with respect to Eurasia, as argued in several papers (Mantovani et al., 2006, 2007a, 2009, 2014; Viti et al. 2006, 2011). Such plate convergence is primarily accommodated by the tectonic interactions of the Adriatic plate (Adria) with the surrounding belts. Along its eastern and northern margins that plate underthrusts the Northern Hellenides, the Southern Dinarides and the Eastern Southern Alps (e.g., Louvari et al., 2001; Bressan et al., 2003; Galadini et al., 2005; Benetatos and Kiratzi, 2006; Aliaj, 2006; Kokkalas et al., 2006; Kastelic et al., 2013). The relative motion between the northern part of Adria and the Northern Dinarides is allowed by a system of dextral transpressional faults (e.g., Markusic and Herak, 1999; Kuk et al., 2000; Poljak et al., 2000; Burrato et al., 2008). The underthrusting of Adria beneath the Alpine edifice mainly develops to the east of the Schio-Vicenza fault system (e.g., Galadini et al., 2005; Burrato et al., 2008).

The interaction of Adria with the Apennine belt is instead characterized by a more complex tectonic pattern, that has mainly developed since the middle Pleistocene (e.g., Viti et al., 2006; Mantovani et al., 2009), as schematically illustrated by perspective images in figure 2.

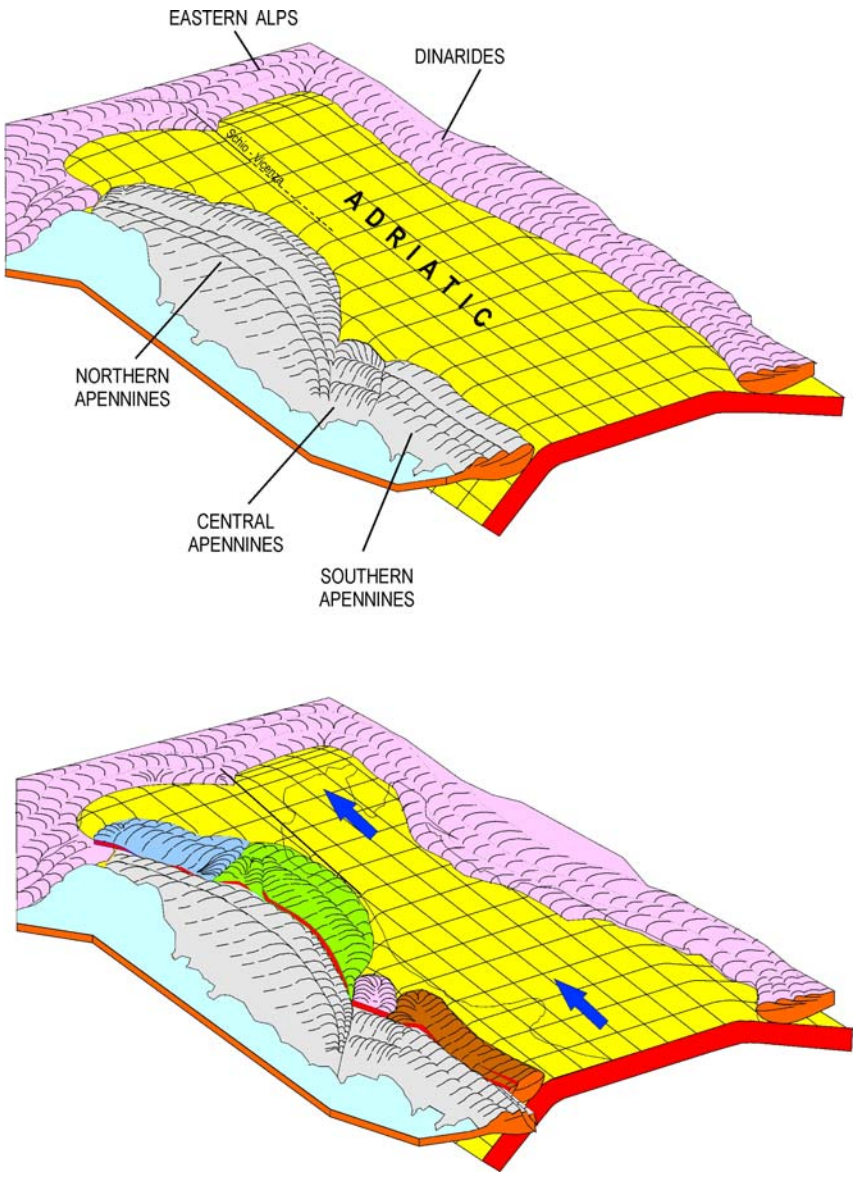

Fig.2. *Perspective sketch of the Adria plate and its margins buried under the surrounding belts.* ***A)*** *Structural tectonic setting in the lower Pleistocene, evidencing the configuration of the Apennine belt that overlay the western subducted margin of Adria* ***B)*** *Since the middle Pleistocene, the outermost sector of the Apennine belt, stressed by Adria, has undergone belt-parallel shortening, accommodated by uplift and lateral escape of some wedges (evidenced by colours, as in figure 3), driven by the motion of the Adriatic plate (blue arrows). The dynamics that determined this process is described in the text and in some publications (e.g., Viti et al., 2006; Mantovani et al., 2009). The separation between the outer mobile Apennine belt and the inner one has generated extensional and transtensional features in the axial portion of the chain.*

Stressed to the south by Adria and resisted to the north by fixed structures in the Western Alps, the outer sector of the Apennines, has undergone belt parallel shortening, which has caused its uplift and outward extrusion of wedges, at the expense of the adjacent Adriatic domain (Viti et al., 2006, 2011; Mantovani et al., 2006, 2009, 2016; Cenni et al., 2012). The main extruding wedges, the Molise-Sannio (MS), Eastern Latium-Abruzzi carbonate Platform (ELA), Laga (La), Romagna-Marche-Umbria (RMU) and Tuscany-Emilia (TE), are evidenced by colours in figure 3. The escaping material has only involved the sedimentary cover, decoupled from its crustal basement at

seismogenic depth (of the order of 6-10 km) by mechanically weak crustal horizons (e.g., Finetti et al., 2005; Mirabella et al., 2008). In particular, a late Triassic evaporitic layer (Burano formation, e.g., Martinis and Pieri, 1964), forms the base of the Meso-Cenozoic sedimentary cover of the RMU and TE wedges (e.g., Anelli et al., 1994; Ciarapica and Passeri, 2002, 2005). The overall weakness of the Burano formation is related to the presence of soft evaporite (anydhrite) levels among stiffier dolostones (e.g., De Paola et al., 2008).

The sinistral transtensional decoupling between the outer escaping Apennine wedges and the inner belt has mainly been accommodated by the formation of several intramontane basins along the axial part of the chain (e.g., Piccardi et al., 2006 and references therein). On the other hand, compressional deformation has occurred at the outer front of the extruding wedges, which are overthrusting the Adriatic domain (e.g., Scisciani and Calamita, 2009; Boncio and Bracone, 2009; Mazzoli et al., 2014, 2015).

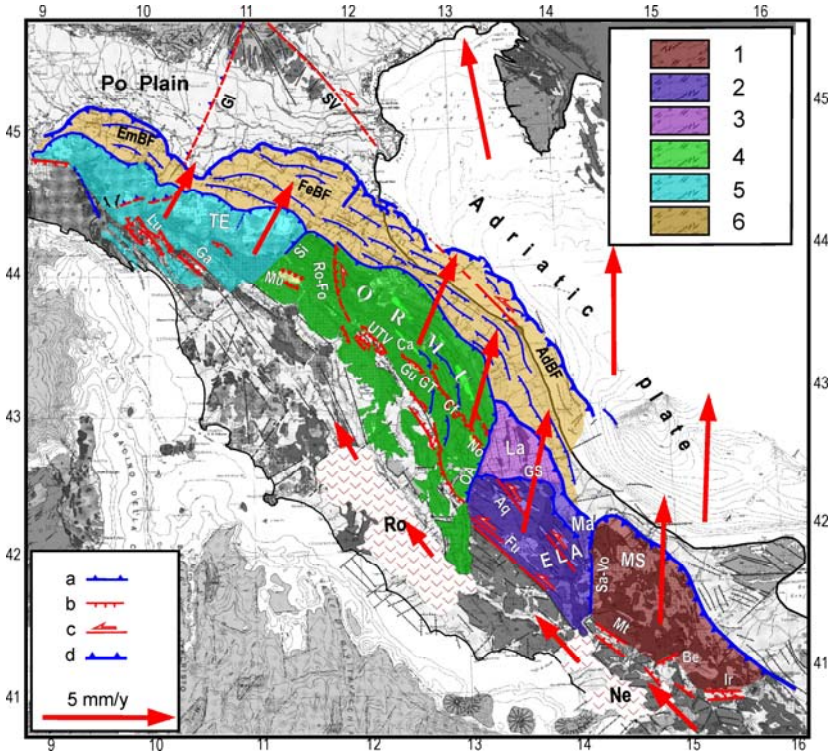

Fig. 3*. Orogenic wedges that constitute the outer mobile sector of the Apennine belt:* ***1****) Molise-Sannio (MS),* ***2****) Eastern Latium-Abruzzi (ELA),* ***3****) Laga (La),* ***4****) Romagna–Marche–Umbria (RMU), 5) Tuscany-Emilia (TE) 6) Outermost buried thrusts and folds. The outermost sector of the RMU wedge (ORMU) is delimited on the inner side by the Norcia-Colfiorito-Gualdo Tadino-Gubbio (No-Cf-GT-Gu) and Romagna-Forlì (Ro-Fo) fault systems. a,b,c) Main compressional, extensional and transcurrent features, d) Outer front of the belt. Arrows indicate the presumed long-term average kinematics of Adria and Apennine wedges. AdBF=Adriatic buried folds, Aq=L'Aquila fault system, Be=Benevento fault system, Ca=Cagli zone, EmBF=Emilia buried folds; FeBF=Ferrara buried folds; Fu=Fucino fault system, Ga=Garfagnana tectonic trough, GS=Gran Sasso Arc, Ir=Irpinia fault system, Lu=Lunigiana trough, Ma=Maiella, Mt=Matese fault system, Mu=Mugello trough, OA=Olevano-Antrodoco thrust front, Ro, Ne=Roman and Neapolitan Quaternary volcanism, Si=Sillaro thrust zone, Sa-Vo=Sangro-Volturno thrust front, UTV=Upper Tiber Valley fault system. Other symbols and abbreviations as in figure 1.*

In the southern Apennines, the MS wedge has decoupled from the inner belt by transtensional deformation that has generated a system of faults in the Irpinia, Matese and Benevento zones (e.g., Ascione et al., 2003, 2007; Brozzetti, 2011; Amoroso et al., 2014). In the central Apennines, the

decoupling between the outer mobile sector and the western part of the belt is accommodated by two major SE-NW sinistral transtensional fault systems (L'Aquila and Fucino, e.g., Cello et al., 1997, 1998; Amoruso et al., 1998; Piccardi et al., 1999, 2006; Elter et al., 2012). Since the late Pleistocene, the outermost sector of the RMU wedge (ORMU in figure 3) has decoupled from the inner belt by the Norcia-Colfiorito-Gualdo Tadino-Gubbio (No-Cf-GT-Gu), Upper Tiber Valley (UTV) and Romagna-Forlì (Ro-Fo) fault systems (e.g., Boncio and Lavecchia, 2000; Piccardi et al., 2006).

The fact that several major earthquakes have occurred along a roughly N-S, narrow zone of the Romagna Apennines (Fig.4) suggests the presence of a major fault system (Ro-Fo in figure 3). Most probably, the development of this fracture has allowed the sector of the RMU wedge that is almost parallel to the Adriatic plate (Umbria-Marche) to decouple from the remaining part of the Northern Apennines which, being roughly oriented E-W, can hardly be dragged by the Adriatic plate (Mantovani et al., 2009, Viti et al., 2012). The lack of clear geological/morphological evidence in the above fault system may be due to its very young age (late Pleistocene). The generation of this tectonic feature has most probably occurred in close connection with the formation of the No-Cf-GT-Gu and UTV fault systems, allowing the decoupling of the ORMU wedge from the inner Apennine structures (Fig.3).

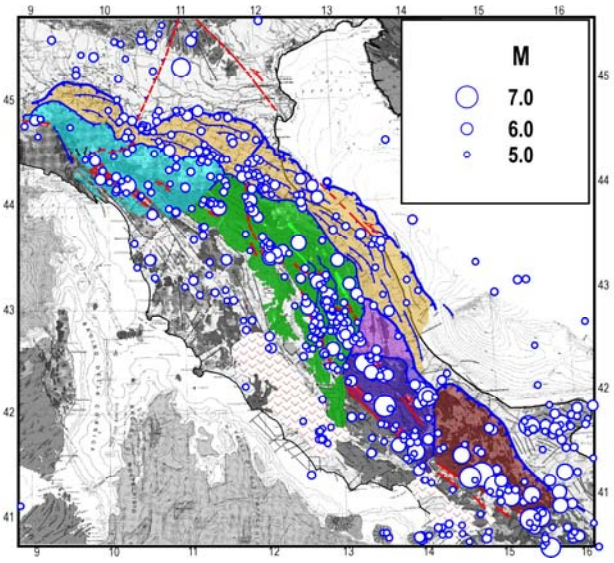

Fig.4. *Major earthquakes (M≥5.0) that have occurred in the Apennine belt since 1000 A.D. Data from Rovida et al. (2011).*

As argued in several works (e.g., Viti et al., 2006, 2011; Mantovani et al., 2007b, 2009), the proposed geodynamic context, in particular the hypothesis that tectonic activity in the Apennines is driven by belt parallel compression, can provide plausible explanations for major features of the observed Quaternary deformation pattern , as synthetically discussed in the following.

- Rapid uplift of the outer Apennine belt has occurred since the middle Pleistocene (Calamita et al., 1999; Ghisetti and Vezzani, 1999; Argnani et al., 2003; Bartolini, 2003; Mayer et al., 2003), also indicated by space geodetic measurements (e.g., Devoti et al., 2011; Cenni et al., 2013).
- Several thrust fronts oriented perpendicularly to the belt (i.e., the Sangro-Volturno and the Olevano-Antrodoco thrust fronts, e.g., Mazzoli et al., 2005; Ascione et al., 2008), are located at the boundaries between the main wedges (Molise-Sannio, Lazio-Abruzzi and Romagna-Marche-Umbria, Fig.3).
- Several arcs, compatible with the action of a belt parallel compression, can be recognized within the Apennine belt. In particular, the Campania-Lucania, Matese-Benevento and Gran Sasso arcs, as discussed by Viti et al., (2006).
- A number of authors (Castellarin et al., 1982; Costa, 2003, Elter et al., 2012, Piccardi et al., 2006) suggest that the Quaternary tectonic setting in the Northern Apennines can be plausibly explained as an effect of belt-parallel compression. In particular, the large tectonic window lying southeast of the

Sillaro thrust front has resulted from the erosion of the 2-4 km of the overlying Ligurian units, mostly interpreted as an effect of local crustal thickening induced by belt parallel shortening and upward flexure, which has accelerated since the middle Pleistocene (e.g., Cerrina Ferroni et al., 2001; Boccaletti and Martelli, 2004; Boccaletti et al., 2010).

- As argued by Viti et al. (2006), Tamburelli et al. (2000) and Mantovani et al. (2009), the location and timing of the abundant Quaternary volcanism in the Roman and Neapolitan magmatic provinces (Fig.3, Peccerillo, 2005) is fairly compatible with the transtensional regime induced in those areas by the outward escape of the Molise-Sannio and Romagna-Marche-Umbria wedges.

A very detailed description of the late Quaternary tectonic features that are compatible with the geodynamic interpretation here proposed is given by Viti et al. (2006).

The relative motion between the Molise-Sannio wedge and the Calabrian wedge (Fig. 5) is accommodated by the system of NW-SE sinistral strike-slip faults recognized in the Lucanian Apennines (e.g., Catalano et al., 2004; Viti et al., 2006; Caputo et al., 2008; Ferranti et al., 2009). To the South, this fault system is confined by the Palinuro fault (e.g., Finetti and Del Ben, 1986, 2005; Viti et al., 2006; Del Ben et al., 2008).

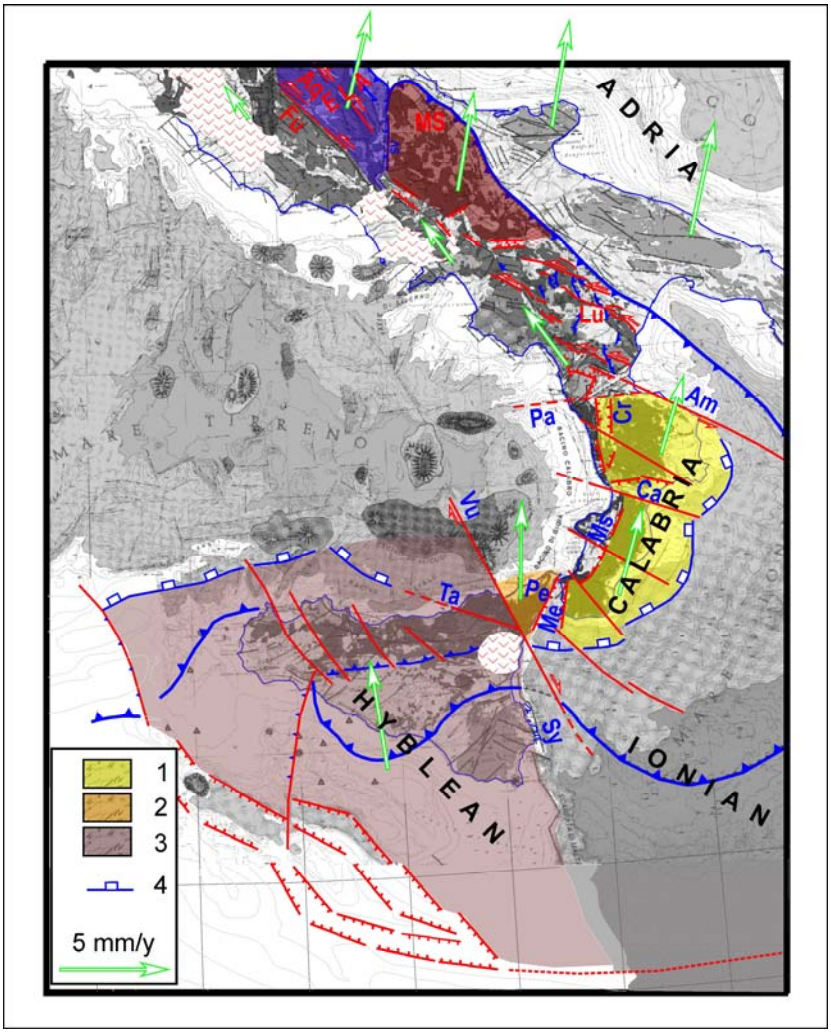

Fig.5. *Tectonic sketch of the southernmost Italian region. 1) Calabrian wedge 2) Peloritani block 3) Hyblean wedge 4) Outer front of the Alpine belt. Green arrows indicate the presumed kinematics with respect to Eurasia. Am=Amendolara fault system, Ca=Catanzaro fault system, Cr=Crati trough, Lu=Lucania fault system, Me=Messina trough, Ms=Mesima trough, Pa=Palinuro fault, Pe=Peloritani block, Sy=Syracuse fault, Ta=Taormina fault system, Vu=Vulcano fault. Other symbols and abbreviations as in figures 1 and 3.*

In southernmost Italy, tectonic activity is mainly connected with the opposite extrusions of the Calabrian and Hyblean wedges (Fig. 5), driven by convergence between the confining plates (Africa, Eurasia and the Aegean-Balkan system)**.** The lateral escape of the Calabrian wedge, bounded by the Vulcano and Amendolara fault systems, occurs at the expense of the Ionian oceanic

domain (Finetti, 2005; Guarnieri, 2006; Del Ben et al., 2008). Belt parallel shortening has also been accommodated by uplift and considerable fragmentation of Calabria, which has generated longitudinal (Crati and Mesima troughs) and transversal (as, i.e., Catanzaro) tectonic features, where major earthquakes have occurred (Fig.6).

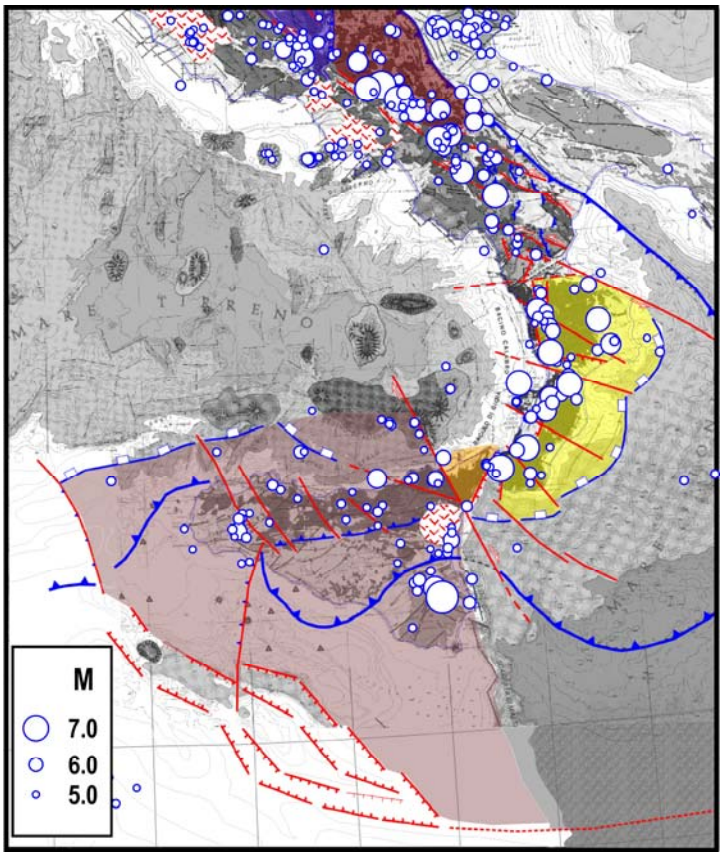

Fig.6. Major earthquakes (M≥5.0) that have occurred in southern Italy since 1000 A.D. Data from Rovida et al. (2011). The epicentral location of the strongest event in southeastern Sicily (1693, M= 7.4) is still object of discussion (e.g., Gutscher et al., 2006).

The Hyblean wedge (including Sicily) is undergoing a roughly north to NNWward extrusion, which induces a compressional strain/stress field at the northern boundary of that wedge and dextral strike slip movements at its eastern boundary (Fig.5), as documented by earthquake focal mechanisms (e.g., Giunta et al., 2004; Neri et al., 2005).

The tectonic features and kinematic pattern reported in figure 1, and with more detail in the figures 3 and 5, are compatible with the observed recent/present deformations, but important constraints on the ongoing context have also been inferred from the evolutionary reconstruction described in some papers (e.g., Mantovani et al. 2006, 2009, 2014; Viti et al., 2006, 2009, 2011). Thus, to provide this information to the reader, a synthetic description of such reconstruction, mainly concerning the central Mediterranean region, is reported in the following.

The evolution of the Mediterranean region since the lower-middle Miocene has been driven by the roughly NNE ward motion of Africa (Nubia, De Mets et al., 2010) and of the roughly westward motion of the Anatolian-Aegean-Balkan system with respect to Eurasia (Fig. 7, Mantovani et al., 2006, 2007a,b, 2009, 2014). This plate convergence has been mainly accommodated by the tectonic processes that involved the minimum resistance from gravitational forces and friction, in line with the minimum action principle (Cloos, 1993; Masek and Duncan, 1998; Mantovani et al., 2006, 2009, 2014). Most often, this condition was fulfilled by the consumption of the least buoyant lithosphere that was present in the Mediterranean area, i.e. the Tethyan oceanic domain. Until the late Miocene, the convergence between Adria and the Anatolian-Aegean system was accommodated by the consumption of the thinned oceanic Ionian zone (Mercier et al., 1987). However, after the complete consumption of that domain such subduction process encountered

stronger and stronger resistance from gravitational forces, creating a critical situation. This required a drastic reorganization of the tectonic setting in the central Mediterranean region, that involved a number of major tectonic events. The main effect was the decoupling of the Adriatic-Ionian-Hyblean plate from Nubia (Fig. 7b), which was allowed by the activation of the Victor-Hensen and Sicily Channel strike-slip/transtensional discontinuities. To accommodate the roughly E-W shortening required by the convergence between the Adria-Ionian plate and the Northwestern Nubia domain (Tunisia), the Hyblean wedge underwent a roughly NW ward extrusion. The indentation of this extruding wedge then caused the outward escape of wedges from the Apennine-Alpine belt (which at that time lay to the east of Sardinia), at the expense of the thinned continental Adriatic margin and the oceanic Ionian domain (Fig. 7b). The decoupling of the Hyblean wedge from the Adria-Ionian plate has been allowed by transtensional and transcurrent tectonics at the Syracuse fault system (Finetti, 2005; Del Ben et al., 2008). The proposed evolution can account for the present shape of the Alpine belt lying along the northern boundary of the Hyblean wedge (Fig.5).

As argued by Mantovani et al. (2009, 2014), the above context can plausibly and coherently account for the complex spatio-temporal distribution of major tectonic events that almost simultaneously started in the late Miocene and then developed until the upper Pliocene in the central Mediterranean area, as listed in the following:

- formation of the Sicily Channel and Victor-Hensen fault systems, two major discontinuities that did not exist before the late Miocene
- extensional activity in the central Tyrrhenian area, which led to the formation of the Magnaghi-Vavilov basin
- acceleration of orogenic activity in the Apennine belt
- activation of a major strike-slip discontinuity in the northern Adriatic area, the Schio-Vicenza fault system
- roughly northward displacement of the sector of the Maghrebian-Alpine belt which lay north of the Hyblean wedge.

The evidence about the tectonic events mentioned above is reported in the references given by Mantovani et al. (2009, 2014) and Viti et al. (2006, 2011).

This evolutionary phase developed until the late Pliocene-early Pleistocene (Fig. 7c), when the entering of thick Adriatic continental lithosphere at the Southern Apennines trench zones, caused that Apennine sector to stop its lateral escape. Since then, the only sector of the belt that was allowed to escape laterally, being adjacent to a remnant of the Ionian oceanic domain, was the Calabrian Arc. The extensional tectonic that developed in the wake of the escaping Calabrian wedge, bounded by the Palinuro and Vulcano strike-slip guides, caused the formation of the southernmost Tyrrhenian (Marsili basin), while accretionary activity occurred along the outer front of the wedge, with the formation of the External Calabrian Arc. In response to the belt parallel compression that drove such extrusion, the Calabrian wedge underwent rapid uplift and major fracturation (e.g., Westaway, 1993; Van Dijk and Sheepers, 1995), that generated several transversal and belt parallel fault systems.

During the same evolutionary stage, the southern Adria sector, contemporaneously stressed by the westward push of the Balkan peninsula and the roughly NNE ward push of Nubia (transmitted by the Calabrian Arc), underwent upward flexure (e.g., Moretti and Royden, 1988; Argnani et al., 2001). The fact that only the southern portion of Adria was stressed by the westward push of the Anatolian-Aegean-Balkan system might have induced a dextral shear stress in the central part of that plate, in good correspondence to the Gargano zone, where the Mattinata fault system was reactivated with a dextral movement (e.g., Chilovi et al., 2000; Di Bucci and Mazzoli, 2003; Tondi et al., 2005). The particular location of that fault in the Gargano area could be due to the fact that in such elevated sector the confining pressure is lower than in the surrounding zones, implying a lower resistance to fracturing.

Since the early Pleistocene (Fig. 7d**),** the direct contact between the northern part of the Calabrian wedge and the thick continental Adria domain caused a significant slow down of Calabria's escape. This phenomenon, recognized by a number of authors (e.g., Zecchin et al., 2015

and references therein), emphasized the decoupling of the northern sector of Calabria (slowed down) from the southern one (still extruding). Furthermore, the orientation of the Calabrian escape changed from about ESE to SE ward (Del Ben et al., 2008).

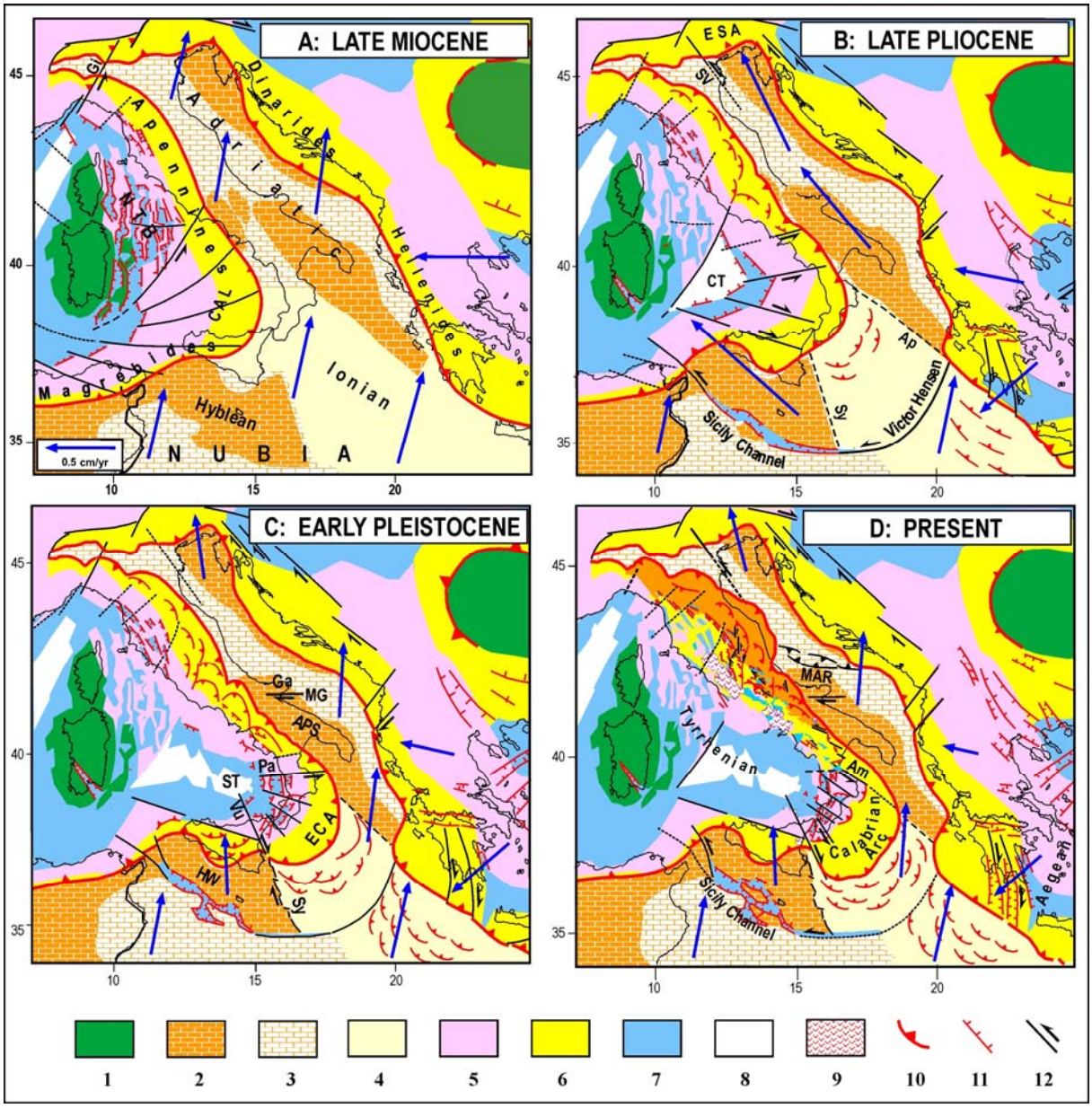

Fig.7. *Evolutionary reconstruction of the central Mediterranean region proposed by Mantovani et al. (2009, 2014)* ***A) Late Miocene.*** *CAL=Calabria, Gi=Giudicarie fault system, NTB=Northern Tyrrhenian basin* ***B) Late Pliocene.*** *Ap=Apulian escarpment, CT=Central Tyrrhenian (Magnaghi and Vavilov basins), ESA=Eastern Southern Alps, SV=Schio-Vicenza fault system, Sy=Syracuse escarpment* ***C) Early Pleistocene.*** *APS=Apulian Swell, ECA=External Calabrian Arc, Ga=Gargano, HW=Hyblean wedge, MG=Mattinata-Gondola fault, Pa=Palinuro fault, ST=Southern Tyrrhenian (Marsili basin), Vu=Vulcano fault.* ***D) Present*** *Am=Amendolara ridge, MAR=Mid Adriatic Ridge* ***1)*** *European continental domain* ***2,3)*** *Africa-Adriatic continental and thinned continental domains* ***4****) Neotethys oceanic domain* ***5****) Alpine belt* ***6)*** *Neogenic accretionary belts* ***7,8****) Neogenic extensional basins and oceanized zones* ***9****) Quaternary magmatism* ***10, 11, 12)*** *Major compressional, extensional and transcurrent tectonic features. Thin lines identify the present geographical contours. The paleoposition of the Tunisian coast (thick line) is reported for reference in the evolutionary maps. Blue arrows indicate plate motions with respect to Eurasia (Mantovani et al., 2009; Viti et al., 2011).*

After the slowdown of Northern Calabria, the Palinuro decoupling fault system became almost inactive. However, the outward escape of Northern Calabria has not completely ceased, since in the late Pleistocene, the activation of a new NW-SE transpressional tectonic zone lying offshore Northern Calabria (Amendolara ridge, Fig. 7d, Ferranti et al., 2014), has allowed such block to maintain some movement towards the Ionian oceanic domain. This extrusion, accompanied by a counterclockwise rotation, could be responsible for the extensional regime that has developed the Crati trough in Northern Calabria (e.g., Tansi et al., 2005; Zecchin et al., 2015).

Since the late Pleistocene (Fig. 7d), the relative motion of the Adria-Ionian plate with respect to Nubia has undergone a considerable slowdown, due to the increasing resistance to shortening along the surrounding buoyant orogenic structures (Hellenides, Dinarides, Alps and Apennines). This trend suggests that at present the motion of Nubia cannot be significantly different from that of southern Adria.

As described earlier, the proposed reconstruction provides that since the middle Pleistocene the outer sector of the Apennine belt, stressed by Adria, has undergone belt parallel shortening, which has been accommodated by outward extrusion and uplift (Fig. 3).

The proposed geodynamic interpretation (Viti et al., 2006; Mantovani et al., 2009, 2014) also suggests that some mobility also characterizes the inner sector of the Apennines, even though such motion develops at lower rates and with a roughly northwestward orientation with respect to the outer belt (Fig. 5). This process is driven by the push of Nubia, transmitted by the Calabrian wedge.

2. Velocity field in the Italian area by geodetic observations (GPS)

The space geodetic (GPS) observations obtained from more than 500 continuous stations operating in the Italian area and surroundings (Fig. 8) over the period January 1, 2001-July 30, 2015 have been considered in order to estimate the present horizontal kinematic field. The phase and pseudo-code data for each station have been analyzed by the GAMIT software version 10.5 (Herring et al. 2010a) adopting a distributed procedure (Dong et al. 1998), as described by Cenni et al. (2012, 2013). The whole network has been divided into 43 clusters, following a simple geographic criterion, while maintaining the shortest baseline as possible. Loose constraints (100 m) have been assigned to the daily position coordinates of each station belonging to all clusters. The International GPS service for Geodynamics *(*IGS) precise orbital solutions from Scripps Orbit and Permanent Array Center have been included in the processing with tight constraints, such as the Earth Orientation Parameter. The daily loosely constrained solutions have been combined into a unique solution by the GLOBK software (Herring et al. 2010b), and aligned into the ITRF2008 reference frame (Altamimi et al., 2012) by a weighted six parameters transformation (three translations and three rotations), using the ITRF2008 coordinates and velocities of the 13 high-quality common IGS stations shown in the inset of figure 8. Then, the time series have been analyzed to estimate the north, east and vertical components of the geographical position of each site, following the procedure described by Cenni et al. (2012, 2013). Only the sites with a minimum observation length of 2.5 years have been included in the processing, in order to avoid biases generated by unreliable estimated seasonal signals (Blewitt and Lavallée, 2002) and/or by rate uncertainties, due to short time series (Bos et al. 2008). As argued in several papers (e.g. Hackl et al. 2011, Bos et al. 2008; 2010; Santamaria-Gomez et al. 2011; Williams, 2004), the noise in time series can be described as a power law process. Different methods have been developed to characterize noise in GPS time series and its impact on velocity uncertainties (Bos et al. 2013; Hackl et al. 2011; Santamaria-Gomez et al. 2011; Williams 2008). We have used the reformulated computation method of the Maximum Likelihood Estimation introduced by Bos et al. (2013), in order to obtain a reliable recognition of the noise and the uncertainties associated with velocity values. The resulting ITRF2008 horizontal velocity vectors with respect to the adopted Eurasian frame (Altamini et al. 2012) are reported in the Appendix 1 and mapped in figure 8.

It is worth noting that the velocity field delineated by the above data is fairly compatible with the

long-term kinematics deduced from the Pleistocene deformation pattern (Figs.1 and 7d). In the Apennine belt, the present GPS field confirms the main feature of the long-term kinematics, i.e. the fact that the outer sector of the belt moves faster (4-5 mm/y) and with a larger eastward component with respect to the inner (Tyrrhenian) belt (1-2 mm/y). To better illustrate this similarity, the two velocity fields in the Apennines are both reported in figure 9.

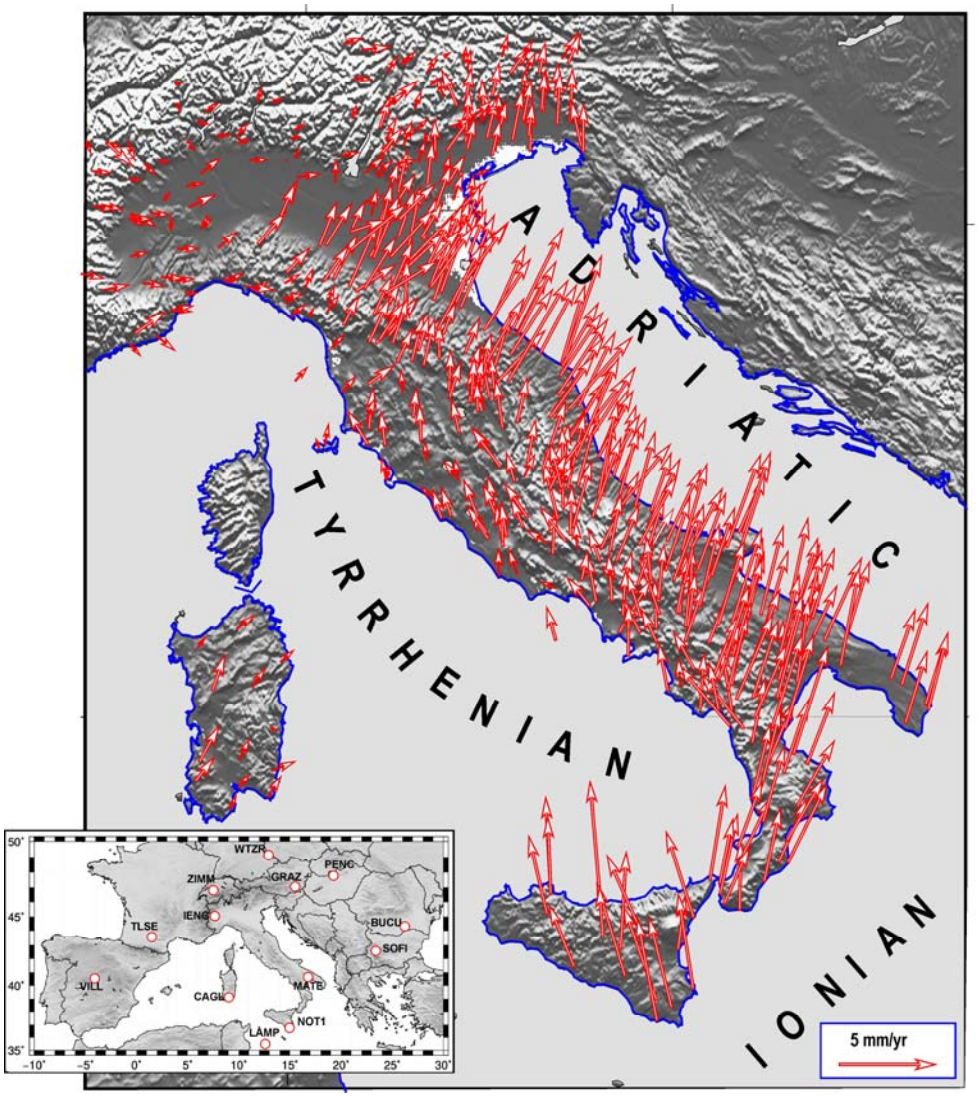

Fig. 8. *Horizontal velocities (red vectors) of the GPS sites with respect to a fixed Eurasian frame (absolute Euler pole of Eurasia at 54.23°N, 98.83°W, ω = 0.257°/Myr, Altamimi et al., 2012). The inset shows the location of the 13 IGS stations that have been used to align the daily solutions of the network to the ITRF 2008 references frame (Altamimi et al., 2012).*

The considerable variation of velocity from the outer to the inner sectors is illustrated in greater detail in figure 9b, which depicts a tentative identification of roughly homogeneous kinematic domains. The highest velocities (3-5 mm/y) and a prevailing NE ward orientation of vectors characterize the outermost belt, including the buried thrusts and folds under the Po Plain, while the lowest velocities (< 2 mm/y), with NW ward to Northward orientation, are observed in the innermost belt. These two sectors are separated by an axial zone, characterized by intermediate velocity values and orientations.

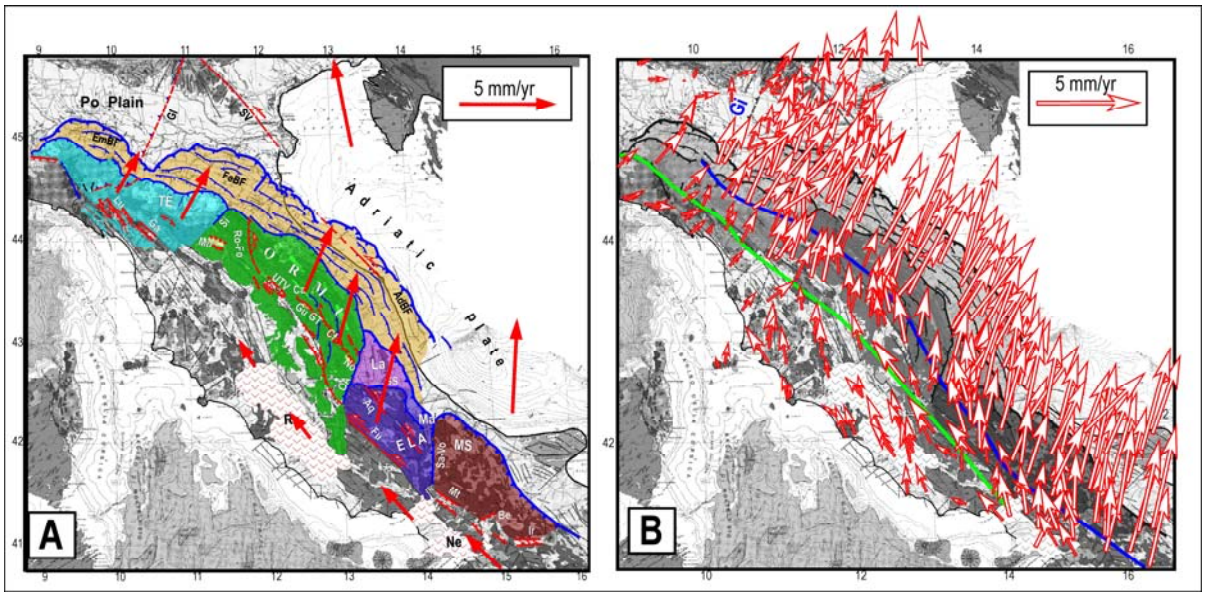

Fig.9. *Comparison of the long-term geological (A) and short-term geodetic (B) kinematic patterns in central and northern Italy. The blue and green lines in B tentatively delimitate roughly homogeneous kinematic domains in the Apennine belt. See text for comments. Symbols and abbreviations as in figure 3.*

In the Padanian zone lying north of the buried Apennine folds velocity values show a significant decrease, with respect to the outer Apennine belt. It can be noted that in the Padanian zone that lies west of the Giudicarie fault system the trends and rates of GPS vectors are significantly different from the ones in the main Adriatic domain (Fig.8). A discussion about the possible tectonic causes of this evidence is given by Cenni et al. (2013).

The distribution of seismicity in the Apennine belt (Fig.10) shows an interesting correspondence between the alignments of major earthquakes and the transition zones from higher to lower geodetic velocities (Fig. 9).

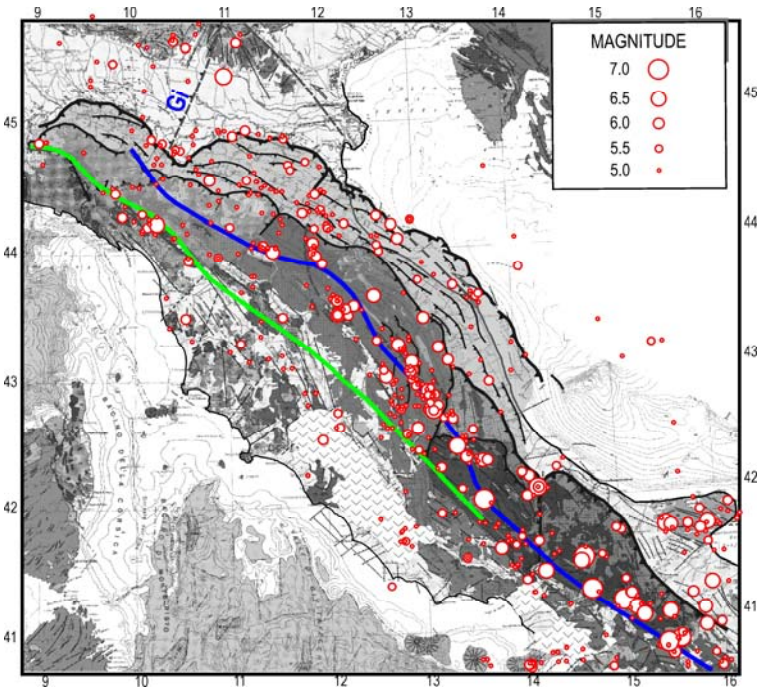

Fig.10 *Distribution of major seismicity (M>5) that has occurred in the Apennine belt since 1000 A.D. (Rovida et al., 2011). The blue and green lines are taken from figure 9.*

In southern Italy (Fig.11), the geodetic field confirms the long-term roughly NE ward motion trend of Calabria and the NNW ward motion trend of the Hyblean wedge (including Sicily). The roughly NE ward motion of Calabria may be interpreted as the result of two components, one (roughly NNE ward) compatible with the motion of Nubia, and the other (roughly SE ward) due to the escape of this wedge towards the Ionian domain.

The roughly NNW ward motion of the Hyblean wedge may instead result from the combination of a roughly NNE ward motion of Nubia and a roughly NW ward escape of that wedge.

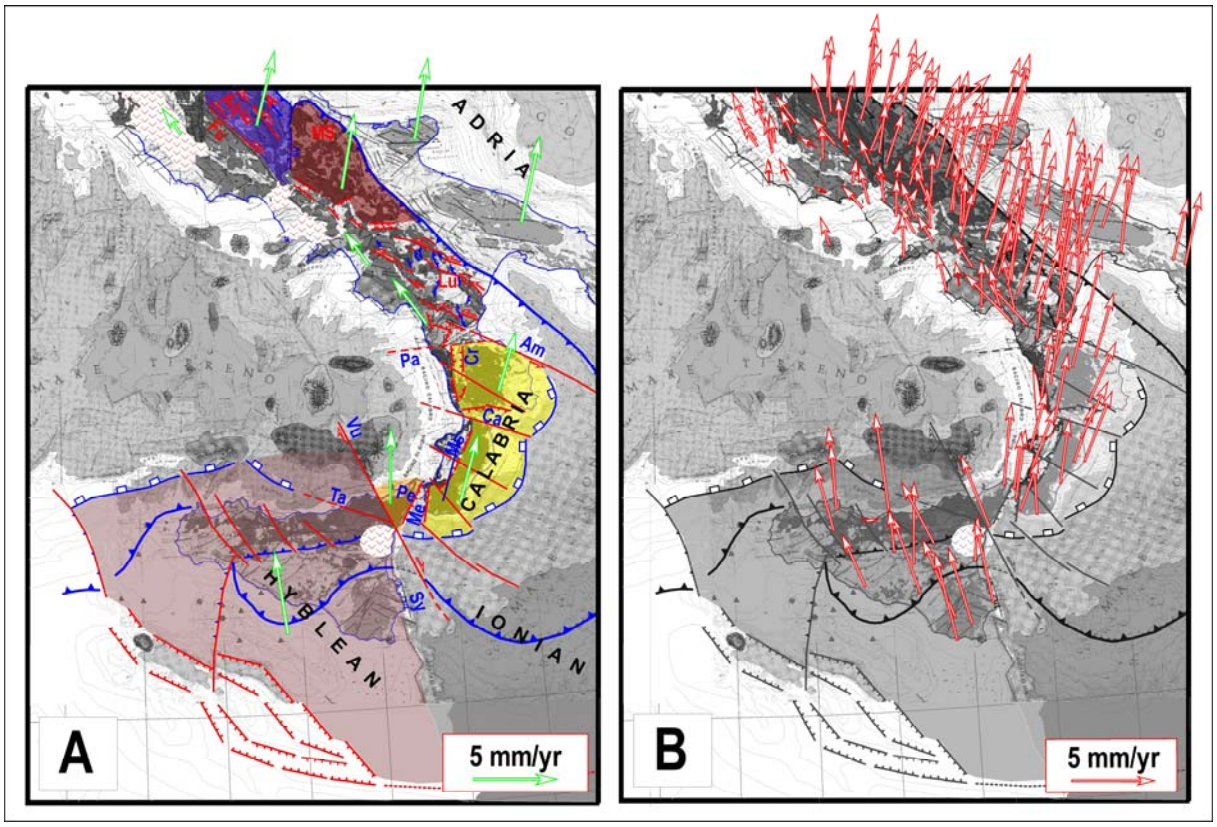

Fig.11. *Comparison of the long-term geological (A) and short-term geodetic (B) kinematic patterns in the Calabrian and Hyblean wedges. Symbols and abbreviations as in figure 5.*

3. Short-term kinematics of the Adria plate and spatio-temporal distribution of major earthquakes in the surrounding zones

The geodynamics and present tectonic context described above suggests that the Adriatic plate, stressed by the convergence of the confining plates (Africa, Eurasia and Anatolian-Aegean system), tends to move with respect to the surrounding structures (Fig.1). Such motion is supposed to be very slow during quiescent periods, while it locally accelerates (during co-seismic and post-seismic phases) in response to major decoupling earthquakes along the periAdriatic boundaries (Fig. 12), in line with the well-known concept of *accelerated plate tectonic*s suggested by a number of authors (e.g., Bott and Dean, 1973; Anderson, 1975; Pollitz, 2003; Heki and Mitsui, 2013).

Each strong shock in a periAdriatic zone triggers a perturbation of the strain/stress fields, generally defined as post-seismic relaxation (e.g., Pollitz et al 2006; Ryder et al 2007; Ergintav et al 2009; Ozawa et al., 2011) that propagating through the plate may reach mature faults (i.e., favorably oriented and prone to failure) at the contiguous boundary sectors, where stress, and consequently

the probability of seismic activation, may significantly increase (Rydelek and Sacks 1990; Pollitz et al 1998, 2004, 2012; Mikumo et al 2002; Viti et al., 2003, 2012, 2013; Freed 2005; Freed et al., 2007; Mantovani et al., 2008, 2010, 2012; Brodski, 2009; Lay et al., 2009; Durand et al., 2010; Luo and Liu, 2010).

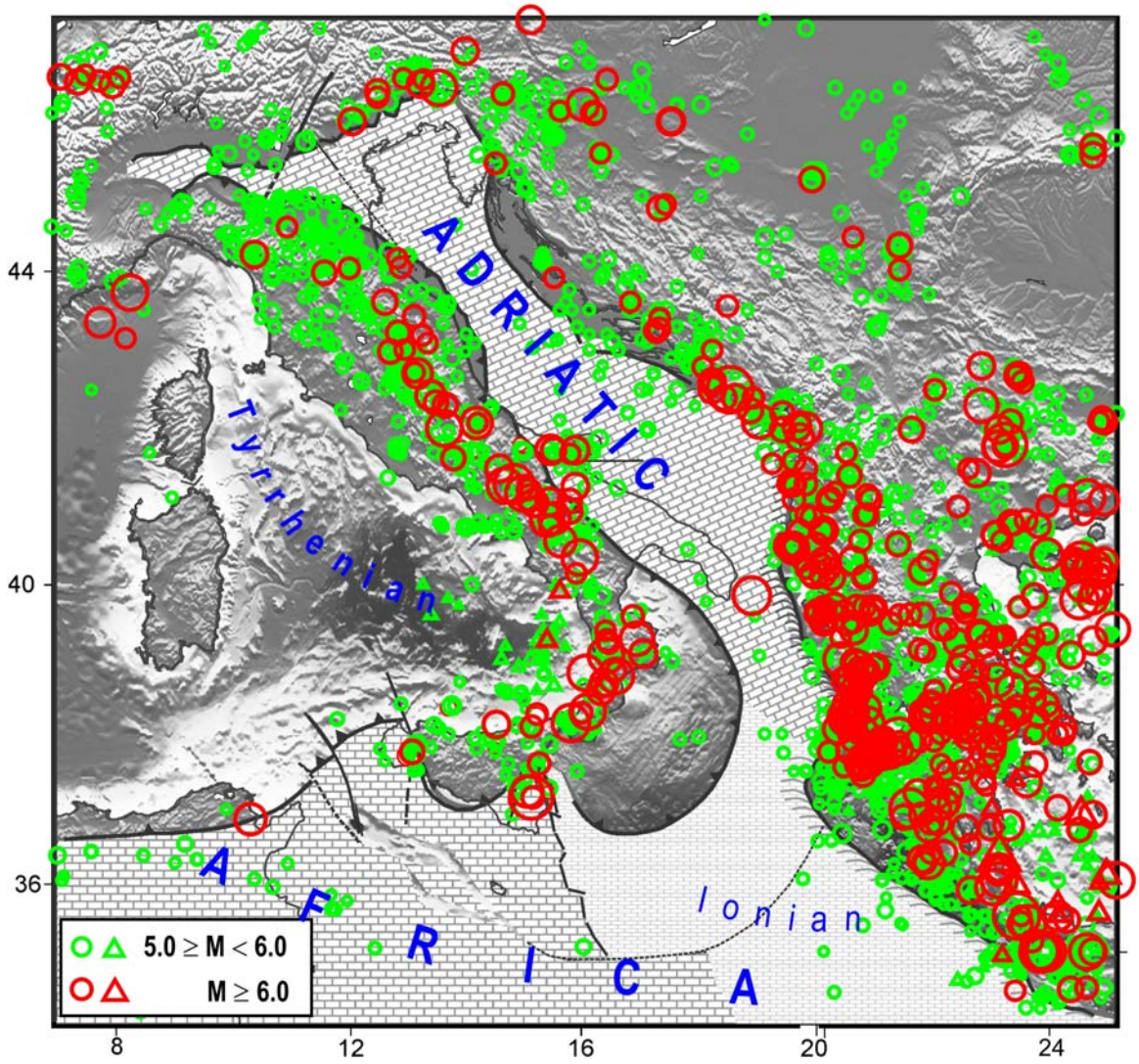

Fig.12. *Distribution of major seismicity in the central Mediterranean area. Circles and triangles respectively indicate the shallow and deep (h > 60 km) earthquakes that have occurred since 1400. Seismicity data from: Ergin et al. (1967); Rothé (1971); Ben-Menahem (1979); Papazachos and Comninakis, 1982; Iannaccone et al. (1985); Comninakis and Papazachos (1986); Ambraseys and Finkel (1987); Anderson and Jackson (1987); Eva et al. (1988); Jackson and McKenzie (1988); Benouar (1994); Godey et al. (2006); ISC Catalogue (http://www.isc.ac.uk/iscbulletin/) and references cited in Appendix 2. See caption of figure 1.*

Taking into account the above tectonic context and in particular the fact that the seismic activation of a periAdriatic sector may influence the tectonic load and thus the probability of strong shocks in the other boundary zones, one could expect to observe regularities in the spatio-temporal distribution of seismicity along the periAdriatic zones. To check the reliability of this hypothesis, we have analysed the time patterns of seismic activity in the main periAdriatic zones since 1400 A.D. (Fig. 13). In this regard, one could display the release of seismic energy over time, but we think that reporting the annual sum of seismic slips, inferred from a suitable slip-magnitude

relationship (Wells and Coppersmith, 1994), provides an information more representative of the effects of major decoupling earthquakes on the local motion of the Adriatic plate with respect to the surrounding structures (Fig.13). The same diagrams also show the total seismic slip over intervals of ten years, in order to give insights into how such effect has concentrated over time. This last information may be useful to recognize how rapidly the surrounding structures have been stressed by the effects of the triggering earthquakes. In this regard, it must be considered that as the induced strain rate increases, the brittle and frictional behaviour of rocks and thus the probability of seismic sliding increases as well (Kato et al., 2003; Niemeijer and Spiers 2007; Savage and Marone 2007).

The time patterns shown in figure 13 point out that in the zones considered seismicity is mostly discontinuous over time, with periods of high activity separated by almost quiescent phases. Furthermore, one could tentatively recognize a progressive northward migration of seismic crises, through the eastern (Northern Hellenides and Southern Dinarides) and western (Apennines) boundaries of Adria, up to reach the northernmost boundary zones (Eastern Southern Alps and Northern Dinarides). In figure 13, the presumed migrating sequences are tentatively marked by different colours (grey, orange, green, yellow and blue). This could suggest that the periAdriatic decoupling earthquakes involved in each sequence may have allowed the whole Adria plate to make a further step (roughly 1-2 meters) towards Europe.

Some traces of a first possible sequence (grey in figure 13) could be recognized in the central and northern periAdriatic zones, where a significant increase of seismic activity took place, from about the middle of the XV century in the Albania and Southern Dinarides zone, to the beginning of the XVI century in the northern Adriatic front (Fig.13). The comparison of the seismicity pattern that have occurred since 1456 (Fig.14a) and the one related to the previous period (Fig. 14b) points out the considerable increase of activity that the central and northern periAdriatic zones underwent after the occurrence of major seismic crises in the Albania-Southern Dinarides (1444-1451) and Southern Apennines (1456). Since the information on seismic activity in the Northern Hellenides and Calabria is very scanty for the time prior to 1600, the starting phase of this presumed sequence can hardly be recognized. This sequence was followed by a long period of moderate activity in most periAdriatic zones (Fig.13).

The first presumably complete sequence (green in figure 13) may have been triggered by a considerable increase of seismic activity in the Northern Hellenides sector during the first decades of the XVII century. This triggering crisis was followed by a significant increase of seismic activity in almost all other periAdriatic zones, up to reach the northern front of Adria in the second half of the XVIII century (Fig.13). In this last zone, major seismic activity lasted up to about the end of the XVIII century and then underwent a drastic reduction for a relatively long period, until 1870.

A drastic increase of seismic activity in the Northern Hellenides in the last decades of the XVIII century may have determined the beginning of a new seismic sequence (yellow in figure 13). Other seismic periods occurred in the same zone up to the middle of the XIX century. This sequence continued to develop with several major events in the Albania, Southern Dinarides and Southern Apennines. In the Central Apennines, a relatively long period of moderate seismic activity was interrupted by a very strong shock in 1915 (Fucino, M=7.0), which was followed by several strong earthquakes in the Northern Apennines in the period 1916-1920. The space-time distribution of major events during the above seismic sequence (1915-1920) is consistent with the tectonic implications of the proposed tectonic context in the Apennine belt, as argued by Mantovani et al. (2010, 2012). In particular, the quantification of the effects of the post-seismic relaxation induced by the 1915 Fucino and subsequent (1916-1920) strong earthquakes shows that each event of such crisis occurred when the respective source zone was reached by the highest values of the strain and strain rate perturbation induced by the previous shocks (Viti et al., 2012, 2013). Moreover, such results point out that the strain regimes associated with post-seismic perturbations roughly agree with the styles of seismic faulting recognized in the Apennine zones activated during the 1916-1920 sequence.

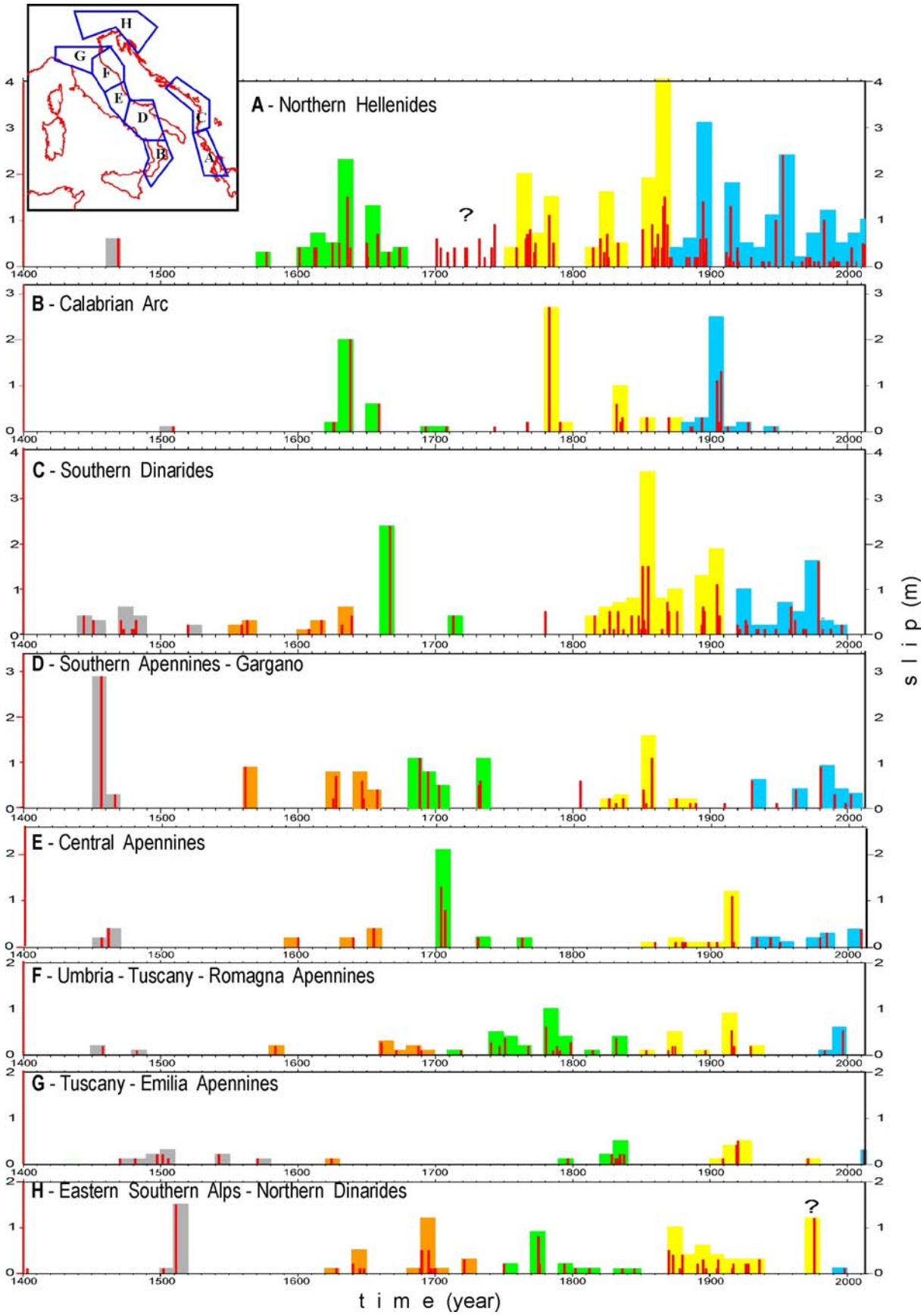
A - Northern Hellenides
B - Calabrian Arc
C - Southern Dinarides
D - Southern Apennines - Gargano
E - Central Apennines
F - Umbria - Tuscany - Romagna Apennines
G - Tuscany - Emilia Apennines
H - Eastern Southern Alps - Northern Dinarides
?
s l i p (m)
t i m e (year)

***Fig.13**. Time patterns of seismic slip associated with major shallow seismicity ((h≤30 k and M ≥ 5.5) that has occurred in the main periAdriatic seismic zones since 1400 A.D. The geometries of the zones considered are shown in the inset. Red bars in the diagrams indicate the total seismic slip (metres) occurred during the related year, computed by the relation log u = - 4.8 + 0.69M, where u is the average seismic slip on the fault (in metres) and M is the earthquake magnitude (Wells and Coppersmith, 1994). Vertical coloured bands indicate the sum of seismic slips over decades. Colours tentatively evidence the seismic sequences during which major decoupling earthquakes have undergone a progressive migration from the southern to the northern periAdriatic zones (see text for comments). Seismicity data from Appendix 2.*

The last presumed seismic sequence (blue in figure 13) was triggered by a phase of very high seismic activity in the Northern Hellenides around the end of the XIX century. As in previous cases (1638 during the green sequence and 1783 during the yellow sequence) the above crisis was accompanied by strong earthquakes in Calabria (1905 M=6.9, 1908 M=7.2).

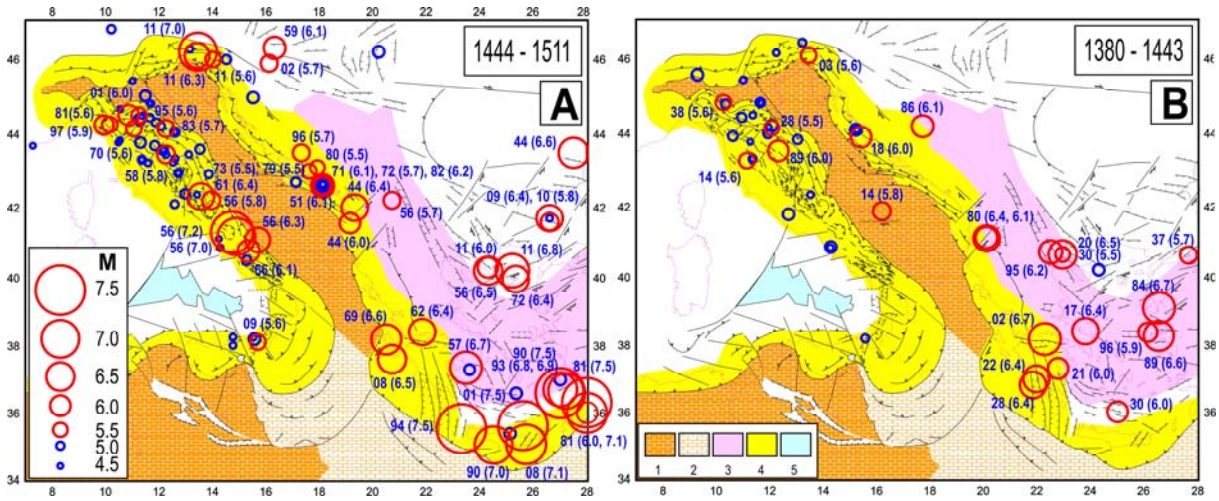

***Fig.14. A**) Distribution of major earthquakes that have occurred in the time interval 1444-1511, presumably related to the first seismic sequence shown in figure 13. Numbers indicate the year of occurrence and magnitude for events with M ≥ 5.5. **B**) Seismic activity that preceded (1380-1443) the seismic phase shown in (A). 1) Africa-Adriatic domain 2) Oceanic Ionian domain 3) Alpine metamorphic belt 4) Orogenic belts 5) Tyrrhenian bathyal plain. Seismicity data as in the caption of figure 12. Other symbols as in figure 1.*

Then, seismic activity occurred in the southern and central sectors of the Dinarides and Apennines, whereas the northern sectors of those belts have so far been affected by scarce activity, only constituted by one major seismic crisis in the Eastern Southern Alps (1976, M=6.5, 6.0) and few shocks (1971, M=5.7 and 2012, M=5.9, 5.8) in the northernmost Apennines. This evidence could imply that the ongoing sequence has not yet undergone a full development, as is also suggested by the spatial distribution of major earthquakes in the last 3 sequences (Fig. 15).

Thus, if seismic activity in the periAdriatic zones were really affected by a systematic tendency to migrate from south to north, the evidence shown in figures 13 and 15 would indicate that at present the probability of hosting the next major shocks is higher in the northern periAdriatic zones

(Northern Apennines, Northern Dinarides and Eastern Southern Alps) than in the southern zones (Calabria and Southern Apennines).

Since in the central Apennines a significant seismic activity has already occurred in the ongoing sequence, even if less intense than in the previous sequences, one can plausibly expect that the probability of major earthquakes is lower than in the northern Apennines, even if the occurrence of significant seismic activity in this zone can hardly be excluded.

Other insights into the most probable location of next major earthquakes in the Italian peninsula may be gained by considering two significant correlations so far recognized between major seismic crises in southern Italian zones and Hellenic/Dinaric sectors (Viti et al., 2003; Mantovani et al., 2008, 2010, 2012), as discussed in the next two sections.

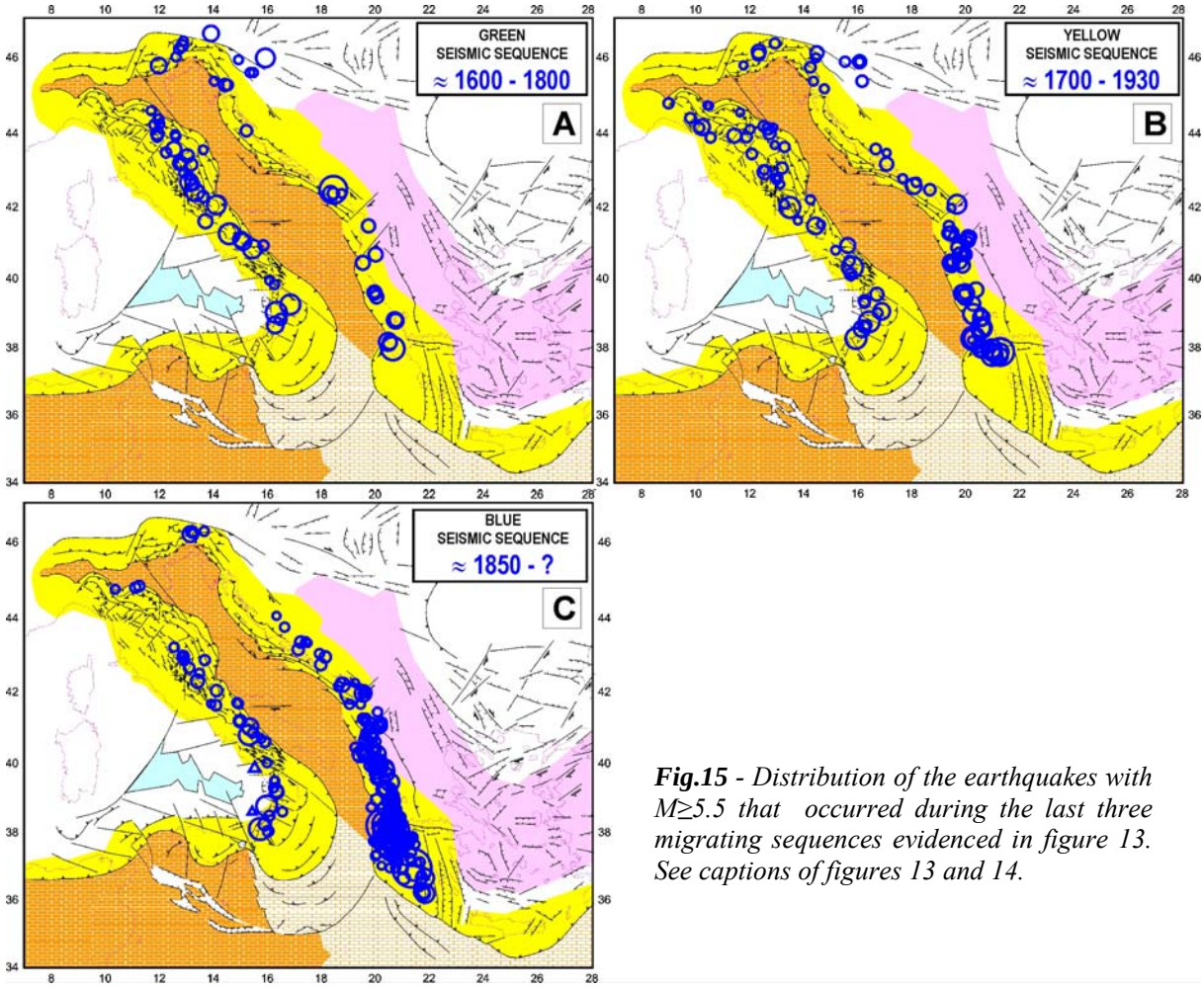

Fig.15 *- Distribution of the earthquakes with M≥5.5 that occurred during the last three migrating sequences evidenced in figure 13. See captions of figures 13 and 14.*

4. Interaction between southern Dinaric and southern Apennine seismic sources

The possibility that the occurrence of major earthquakes in the first zone favours seismic activity in the second zone was first suggested by the fact that the strong earthquake (M=7.0) of April 1979 in the Montenegro area of the Southern Dinarides was followed on November 1980 by a major event (M=6.9) in the Irpinia zone of the Southern Apennines (Fig. 16). This possibility has then been reinforced by the implications of the tectonic setting of the study area (sketched in the section of figure 16) and the results obtained by the quantification of the post-seismic relaxation triggered by the 1979 Montenegro event, as synthetically described in the following.

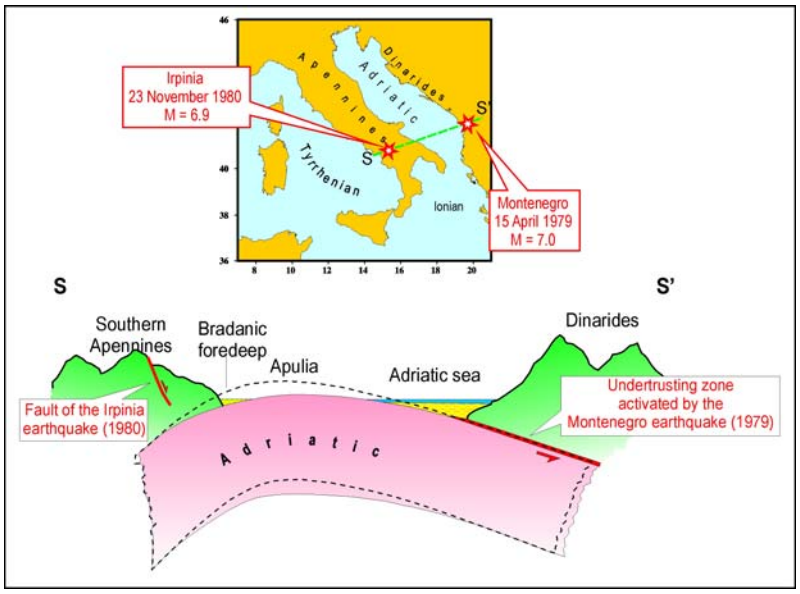

Fig. 16. *Structural sketch, through a transversal section in the Southern Adriatic (S-S'), which shows the vertical flexure of the Adriatic lithosphere overthrusted by the Dinaric belt, on one side, and by the Apennine belt on the other side (e.g., Moretti and Royden, 1988; De Alteriis 1995). The vertical scale is exaggerated in order to make more evident the possible effect of a seismic slip (red arrow) at the subduction fault zone beneath the Dinaric belt. The dashed lines indicate the presumed profile of the Adriatic lithosphere before the Montenegro seismic slip. The epicentres of the 1979 (M=7.0) Montenegro and 1980 (M= 6.9) Irpinia earthquakes and the trace of the section are shown in the map.*

The occurrence of a major seismic slip at a thrust fault beneath the Southern Dinarides, such as the one that developed with the 1979 Montenegro event (estimated to be 1-2 metres, e.g. Benetatos and Kiratzi 2006), implies a displacement of the adjacent Adria domain, which causes a reduction of the vertical flexure in the southern Adriatic domain, as sketched in the section of figure 16. Such process is expected to induce extensional strain in the Southern Apennines, which may favour the activation of the belt parallel normal faults recognized in that zone, as for instance the one that generated the 1980 strong earthquake in the Irpinia zone (e.g., Ascione et al 2007).

This hypothesis is confirmed by the results of numerical modelling of the strain perturbation that was presumably induced in the Irpinia zone by the 1979 Montenegro event (Viti et al 2003; Mantovani et al 2010, 2012). In particular, by the fact that the strain rate induced by the Montenegro earthquake is expected to reach its maximum amplitude in the Southern Apennines about 1-2 years after the triggering event, i.e. a delay fairly consistent with the time interval that elapsed between the April 1979 Montenegro and November 1980 Irpinia shocks. The possible relationship between stress/strain rate increase and triggering of seismic activity has been pointed out in several works (e.g., Pollitz et al 1998; Toda et al 2002; Viti et al 2003, 2012, 2013).

The possibility that the interaction between Southern Dinaric and Southern Apennine seismic sources is a systematic phenomenon is suggested by the comparison of the series of major shocks that have occurred in such zones in the last two centuries.

From the list given in figure 17, it is possible to note that in the period considered all the shocks with M≥6.0 in the Southern Apennines have been preceded within few years (less than 5) by one or more earthquakes with M≥6 in the Southern Dinarides. Since the probability that such a regular correspondence merely occurs by chance is very small (Mantovani et al 2010, 2012), it is plausible to suppose that the observed interrelation results from a tectonic connection between the two zones. The above correspondence does not change significantly if a lower threshold (M=5.5) is considered, since only one of the 15 Southern Apennine events was not preceded by comparable seismicity in the Southern Dinarides. This evidence may indicate that a fault in the first zone can

hardly activate without the contribution of a post-seismic perturbation triggered by one or more major shocks in the other zone.

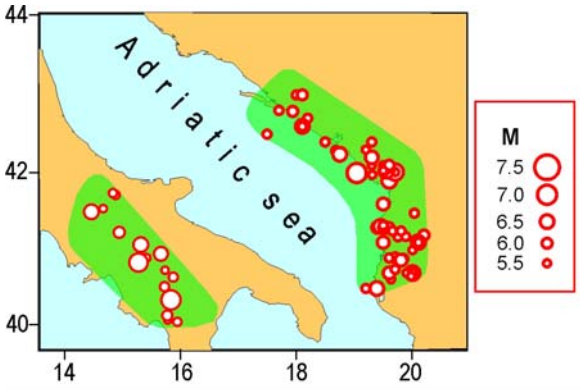

Southern Dinarides (M > 5.5)	Southern Apennines (M ≥ 5.5)
1823 (5.7)	1826 (5.8)
1827 (6.5), 1830 (5.6)	1831 (5.5)
1833 (6.5)	**1836 (6.0)**
1843 (5.6, **6.2**),**1848 (6.4)**, 1850 (5.6) **1851** (6.3, 6.2, 6.6, 6.0), **1852 (6.2)**,	**1851 (6.4)**,1853 (5.6)
1853 (5.7), **1855 (6.6, 6.8)**	**1857 (7.0)**
1869 (5.6, **6.0**, **6.2**), **1870 (6.5)**	
1876 (6.3, 5.6)	1885 (5.5)
1894 (5.9), **1895 (6.2)**,**1896** (5.9, **6.2**)	
1905 (6.6, 6.0), 1906 (6.4), 1907 (5.7, **6.2**)	1910 (5.7)
1920 (5.6, 5.6), 1921 (5.6), 1922 (5.6) 1926 (5.8, 5.8), **1927 (6.0)**	**1930 (6.6)**
1934 (5.6),1935 (5.6)	
1958 (5.6), **1959** (5.9, **6.2**, 5.6), **1962 (6.2)**,	**1962** (5.7, **6.1**)
1979 (6.4, 5.7, **7.0)**	**1980 (6.9)**
1982 (5.7), 1988 (5.7)	1990 (5.5, 5.8)
1996 (6.0)	1998 (5.6)

Fig.17. *Geometry of the zones implied in the presumed interrelation between Southern Dinaric and Southern Apennine seismic sources and list of the major seismic events that have occurred since 1810 (table). The events with M≥6.0 are red. Seismicity data from Appendix 2.*

The fact that this significant time correlation can be recognized for the most recent**,** complete and reliable part of the seismic catalogue gives good reasons to hope that this phenomenon may provide a tool for recognizing the periods when the probability of strong shocks in Southern Apennines may undergo a significant increase. In this view, the fact that no major earthquakes have occurred in the Southern Dinarides since 1996 would imply that at present the probability of major shocks in the Southern Apennines is relatively low. A more detailed description of the seismic correlation cited above and a discussion about its possible uncertainties are reported in previous papers (Viti et al 2003; Mantovani et al 2010, 2012).

5. Interaction between Calabrian and Hellenic seismic sources

Another significant correlation has been recognized between the major earthquakes of Calabria and those of the Hellenides sector lying between the Ionian islands and Albania (Fig.18). The hypothesis that a strong seismic activation of the Hellenic thrust zone may increase the probability of major earthquakes in Calabria is consistent with the structural/tectonic setting sketched in the section of figure 18 (right upper panel). Indeed, such scheme suggests that a significant seismic slip

at the Hellenic thrust zone is expected to produce a reduction of the upward vertical flexure of the Adriatic lithosphere, which may help the overthrusting of the Calabrian wedge, that is the process which is accommodated by the seismic activation of normal and strike-slip faults in Calabria (Mantovani et al 2008, 2009, 2012).

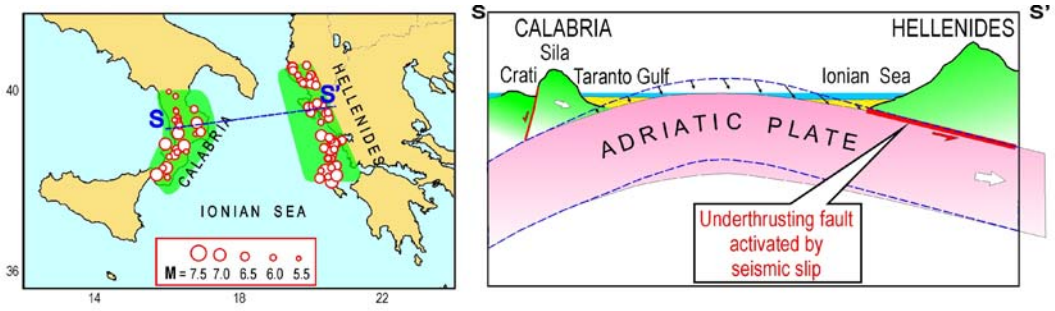

Hellenides (M ≥ 6.0)	Calabria (M ≥ 5.5)
1601 (6.3)	
1612 (6.3), 1613 (6.3)	
1625 (6.5)	**1626 (6.0)**
1630 (6.5), 1636 (7.2)	**1638 (6.9, 7.0)**
1638 (6.3)	
1650 (6.2), **1658 (6.7)**	**1659 (6.6)**
1666 (6.2), 1674 (6.3)	
	1693 (5.7)
1701 (6.6), 1704 (6.4)	1708 (5.5)
1709 (6.2), 1714 (6.3)	
1722 (6.3),1723 (6.3), **1732 (6.6)**	
1736 (6.0), 1741 (6.3), **1743 (6.9)**	1743 (5.7), 1744 (5.7)
1759 (6.3), **1766 (6.6), 1767 (6.7)**	**1767 (6.0)**
1769 (6.8), 1772 (6.1)	
1773 (6.5)	**1783 (7.0, 6.6, 7.0)**
1783 (6.5, 6.6), 1786 (6.5)	**1791 (6.0)**
1815 (6.3), **1820 (6.6)**	
1823 (6.3), **1825 (6.7)**	**1832 (6.6)**

Hellenides (M ≥ 6.0)	Calabria (M ≥ 5.5)
1833 (6.5)	1835 (5.8), **1836 (6.2)**
1851 (6.8)	**1854 (6.2)**
1858 (6.0, 6.2, 6.4), 1859 (6.0)	
1860 (6.4), 1862 (6.4, 6.2) 1865 (6.3), **1866 (6.6,** 6.3, 6.4) **1867 (7.2), 1869** (6.0, **6.7**)	**1870 (6.1)**
1872 (6.0)	
1885 (6.0)	1886 (5.6), 1887 (5.5)
1893 (6.6)	**1894 (6.1)**
1895 (6.2, **6.5**, 6.2, 6.2), **1897 (6.6).** 1912 (6.1)	**1905 (7.0),** 1907 (5.9), **1908 (7.1).** 1913 (5.7)
1915 (6.0, 6.3, 6.1), 1920 (6.0)	1928 (5.8)
	1947 (5.7)
1948 (6.5, 6.5)	
1953 (**7.0,** 6.2, **6.6**)	
1983 (6.7, 6.0)	
2003 (6.2)	
2014 (6.1, 6.1), **2015 (6.5)**	

Fig.18. *The geometry of the presumably interrelated Calabrian and Hellenic seismic zones (map, left panel) and the trace of the section (S-S', right panel) are shown in the map. Red circles indicate the epicenters of the earthquakes that have occurred in the two zones since 1600 A.D (Table). The events with M≥6.0 in Calabria and M≥6.5 in Hellenides are in red. The section illustrates a tentative reconstruction (vertically exaggerated) of the reduction of vertical flexure of the Adriatic plate (dashed line), which may occur in response to a strong decoupling earthquake at the Hellenic thrust zone. This effect may favour the outward escape of the uplifted Calabrian wedge towards the Ionian domain. The non uniform displacement of this wedge may involve the activation of its main transversal and belt-parallel fault systems. Sources of seismicity data from Appendix 2.*

The above interpretation and its implications on the interaction of the Calabrian and Hellenic seismic sources is consistent with the quantification of the effects of post-seismic relaxation induced by strong earthquakes in the Hellenides (Mantovani et al 2008, 2012), which indicates that such phenomenon may have influenced the Calabrian shocks that occurred some years after the Hellenic triggering events. The possibility that the above phenomenon has a systematic character is supported by the comparison of the seismic histories of the two zones involved (Fig. 18), which

points out that all Calabrian shocks with M≥6.0 have been preceded, within 10 years, by at least one event with M≥6.5 in the Hellenides. If lower magnitudes (M≥5.5) are considered, the correspondence remains fairly significant, since only 2 (out of 26) Calabrian events have not been preceded by equivalent shocks in the Hellenides. The above evidence supports the hypothesis that a major Calabrian earthquake can hardly occur without being preceded by significant seismic activity in the Hellenic zone (Mantovani et al 2012).

On the other hand, considering the opposite aspect of the presumed interrelation, one can note that only 12, out of 20, Hellenic seismic crises with M≥6.5 were followed by a Calabrian earthquake with M≥6.0. This indicates that the role of the Hellenic events as precursors of Calabrian shocks may be affected by uncertainty. In this regard, it is worth noting that since 1948 no Hellenic events with M≥6.5 have been followed by an event in Calabria. This drastic increase of false alarms coincides with the latest period (since 1947) during which no earthquakes with M≥5.5 have occurred in Calabria (Fig. 18). Such long quiescence (68 years) is rather anomalous with respect to the previous behavior, in particular with the fact that from 1626 to 1947 the average inter-event time between M≥5.5 shocks was 12 years and never longer than 41 years.

In order to find a possible explanation of the present long quiescence and of the fact that since the middle of the XX century the correspondence between Hellenic and Calabrian earthquakes has undergone a considerable worsening, we advance the hypothesis that such anomalous behavior is an effect of a rare major tectonic event that has drastically changed the strain and stress fields in the above zones. It concerns the large westward displacement that the Anatolian-Aegean system (Fig. 19) underwent in response to the activation of the whole North Anatolian Fault system (NAF) that

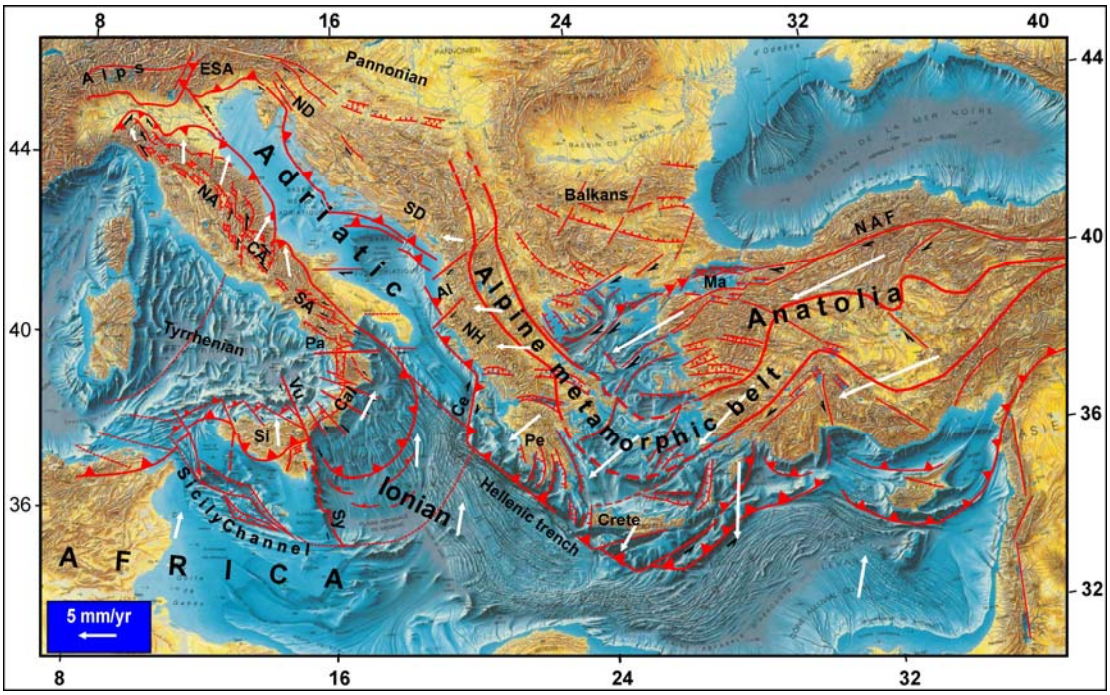

Fig.19. *Proposed plate/microplate configuration and kinematic pattern in the Central Mediterranean and Aegean-Western Anatolian region (Viti et al., 2011). White arrows indicate the presumed velocity field with respect to Eurasia. Land and seafloor morphological features from Le Pichon and Biju-Duval (1990). Thick red lines delimitate for reference the inner part of the Alpine metamorphic belt (see Fig. 20). Al=Albanides; Cal=Calabrian Arc, Ma=Marmara, NAF=North Anatolian fault system, ND=Northern Dinarides, NH=Northern Hellenides, SD=Southern Dinarides, Si=Sicily. Other symbols and abbreviations as in figure 1.*

was triggered by the very strong earthquake (M=8) occurred in the easternmost sector of such fault in 1939 (e.g., Barka, 1996). While activations of the easternmost and westernmost (Marmara zone)

sectors of such fault occurred other times in the past centuries (e.g., Ambraseys and Jackson 1998), the rare event was the fact that the post-1939 crisis involved an activation of the central sector of that fault, which had been almost silent for a long time. This event favoured the westward displacement of the whole Anatolian wedge, which noticeably strengthened the E-W compressional regime in the Aegean area (squeezed between the Anatolia system and the Adria/Africa plate)

Important information on the ongoing tectonic context in the above area may be taken from the reconstruction of its post late Miocene evolution (Fig. 20)

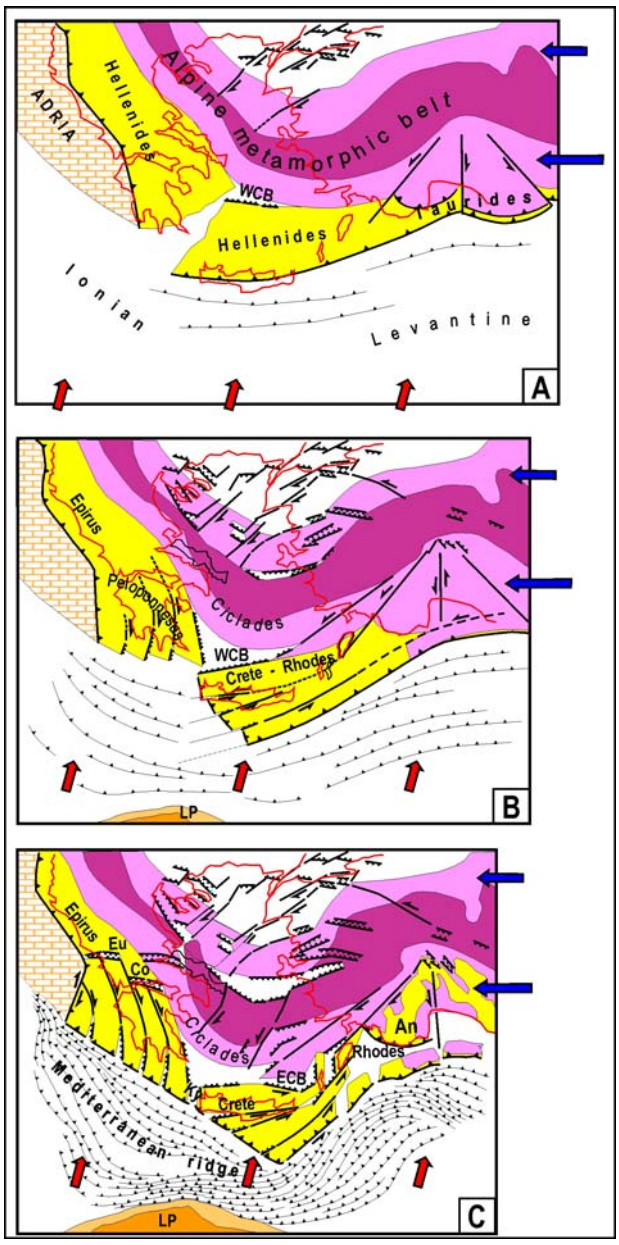

Fig.20. *Tentative reconstruction of the post-late Miocene evolution of the Alpine metamorphic belt (dark and light violet) in the Anatolian-Aegean-Balkan system and of the younger orogenic belts (yellow), which transmitted the push of the Anatolian wedge (blue arrows) to the southern Adria plate (After Viti et al., 2011, modified).* **A) *Late Miocene***: *The convergence between the Anatolian block (undergoing a westward lateral escape driven by the indentation of Arabia) and the Adriatic promontory is accommodated by the longitudinal shortening and southward bending of the metamorphic belt. As a consequence of this deformation, the Hellenic belt undergoes a major break in the zone of maximum bending, giving rise to two segments. This process triggers an extensional tectonics in the wake of the bending arc, generating the western Creta basin (WCB).* **B) *Middle Pliocene***: *the divergence between the metamorphic belt and the two Hellenic segments (Peloponnesus and Creta-Rhodes) generates further extension in the western Creta basin.* **C) *Since the early Pleistocene***: *due to its collision with the continental African domain (Lybian promontory=LP), the Creta-Rhodes segment (stressed by the push of Anatolia) undergoes further fracturing and southward bending, at the expense of the oceanic Levantine domain. In the wake of this bending, extensional deformation developes, generating the Eastern Creta basin (ECB). Squeezed between the metamorphic belt and the southern Adria domain, the Peloponnesus Hellenic segment undergoes a strong fragmentation. The various slices resulting from this phase have then undergone rotation and oblique southward escape at the expense of the Ionian oceanic domain. The divergence between the extruding slices and the structures lying to the north (Epirus) generates troughs roughly E-W oriented, as the Corinth (Co) and Eubea (Eu) ones. An=Antalya extruding wedge. Red arrows indicate the motion of Africa with respect to Eurasia. The present coast lines are reported in the figures (red) for reference. Other symbols as in figure 14.*

Considering the minimum-action principle (e.g., Cloos, 1993; Masek and Duncan, 1998; Mantovani et al., 2006, 2014), it is reasonable to suppose that the fast shortening required by such sudden increase of E-W compression was mainly accommodated by the outward extrusion of the Aegean zones (Peloponnesus and central Aegean domain) which face the low buoyancy Ionian oceanic domain. Instead, the shortening of the Northern Hellenides and the southernmost Adriatic plate, being confined by high buoyancy orogenic and continental structures, has encountered much higher resistance. This hypothesis is compatible with the fact that since about 1945 seismic activity has mainly affected the Aegean structures lying south of the Cephalonia fault system and of the North Aegean trough, whereas only minor seismic activity has occurred at the Northern Hellenic thrust zone (Fig. 21).

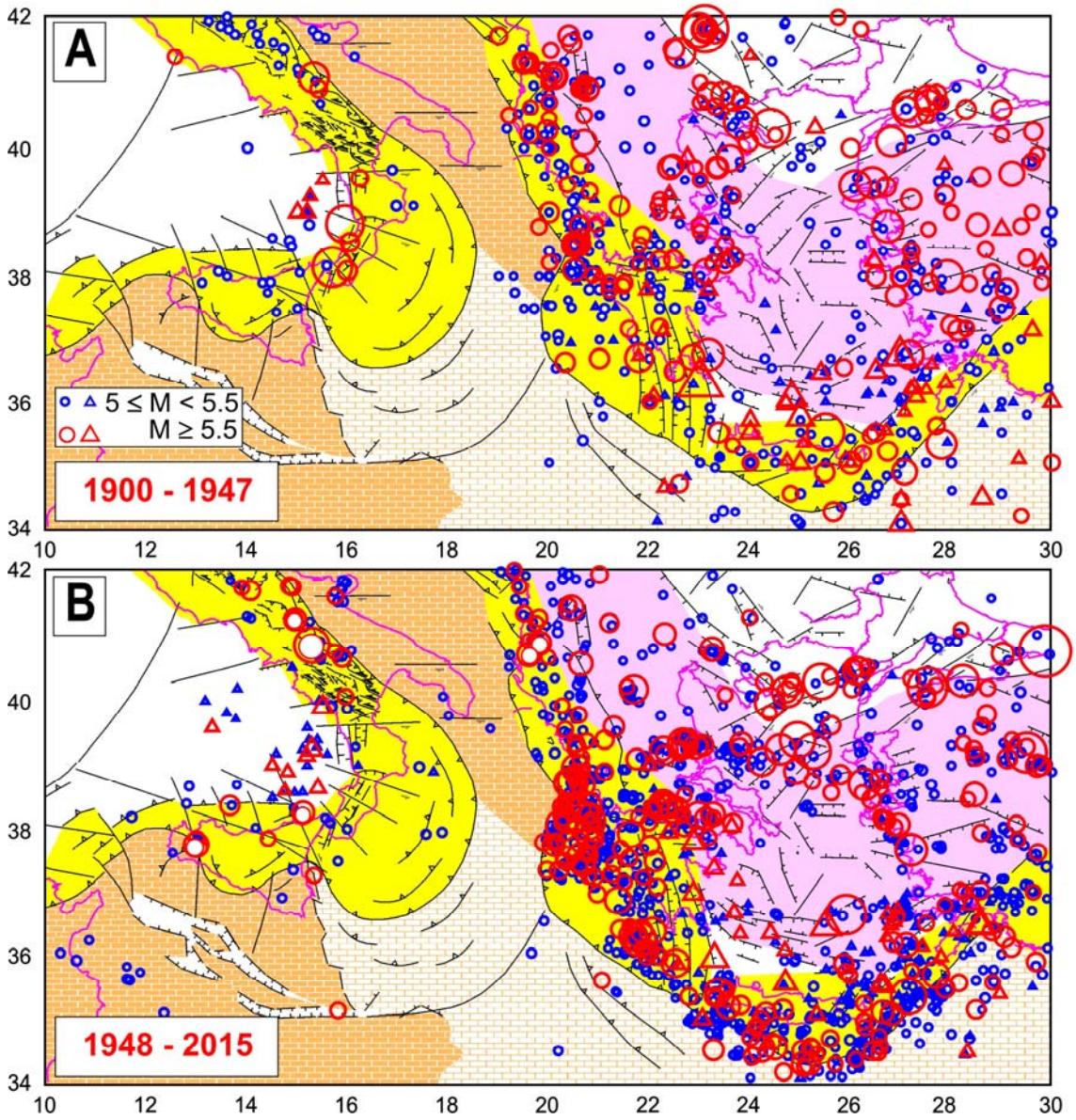

Fig. 21 *- Distribution of major earthquakes that have occurred in two time intervals (1900-1947,* ***A****) and (1948-2015,* ***B****), which respectively preceded and followed the arrival in the Aegean area of the effects of the large westward displacement of the Anatolian wedge, triggered by the strong earthquake (M=8) that occurred in 1939 at the easternmost sector of the North Anatolian fault system (Mantovani et al., 2001; Cenni et al., 2002). Circles and triangles respectively indicate focal depths lower and greater than 60 km.*

It is reasonable to think that E-W shortening to the north of the Cephalonia fault has been mainly accommodated by thickening and uplift of the Southern Adriatic domain, a process that may increase resistance against the outward sliding of Calabria and the associated internal fracturation (and related seismicity) of that wedge. This context could explain why since 1947 no major earthquakes have occurred in Calabria (Fig. 18). During this period, the major earthquakes that occurred in the transpressional Cephalonia fault system (1953 M= 7.0, 6.6 and 1983 M= 6.7) might have been only connected with the SW ward displacement of the Peloponnesus wedge, which has presumably minor influence on the kinematics of the Northern Hellenides and consequently on the tectonic mechanism responsible for the activation of main faults in Calabria (Fig. 21).

On the basis of the evidence and arguments described above, one could expect that at present the stress/strain field in Calabria is not similar to the one that characterized such zone when it was hit by strong historical earthquakes. One could expect that the present condition may persist until the occurrence of a new significant increase of seismic activity in the Hellenic thrust zone that lies north of the Cephalonia fault system.

6. Migration of seismicity along the Apennine belt

Being particularly interested in recognizing seismicity regularity patterns in the Italian territory, we have carried out a careful analysis of the distribution of major earthquakes that occurred in the Apennine belt during the periAdriatic sequences shown in figure 13. This study mainly aims at checking the compatibility between the spatio-temporal distribution of main shocks and the implications of the proposed short-term tectonics of the most mobile sector of the Apennine chain (Mantovani et al., 2009, 2012, 2014; Viti et al., 2011, 2015a), as synthetically described in the following.

When a major decoupling earthquake occurs in the Southern Apennines (Irpinia, Matese or Benevento extensional/transtensional zones), the Molise-Sannio wedge is supposed to undergo a sudden acceleration, which strengthen its belt parallel push on the eastern sector of the Lazio-Abruzzi platform (ELA wedge) in the Central Apennines (Fig. 3). This causes a strengthening of shear stress between the stressed and non-stressed sectors of the LA platform, making more likely seismic sliding at the main belt-parallel faults sytems (L'Aquila and Fucino). When such context ends up with a major shock at one of those faults, the respective decoupled sector of LA accelerates, increasing its tectonic load on the RMU wedge in the Northern Apennines, with a consequent increase of stress, and thus of earthquake probability, at the boundaries of that wedge. The effect that this sudden stress increase can produce in the RMU wedge depends on which fault system is activated in the Central Apennines. When seismic decoupling occurs at the L'Aquila fault, the sector of ELA that undergoes acceleration is relatively narrow, mainly concerning the Gran Sasso Arc (Fig. 3). Correspondingly, the sector of the RMU wedge that is stressed by such accelerated push is narrow as well. This interpretation may explain why a major belt parallel fault system, roughly running along the northward prosecution of the L'Aquila fault system (Norcia-Colfiorito-Gualdo Tadino-Gubbio), has developed within the RMU wedge in the Quaternary. Such major fracture and its northward prosecution by the Upper Tiber Valley and Romagna Apennines/Forlì zones might represent the inner extensional/transtensional border of a wedge that will be hereafter recalled as Outer Romagna-Marche-Umbria or ORMU (Fig.3).

When, instead, the Fucino fault system is activated, the decoupled and accelerated sector of the LA platform is wider. Consequently, the stressed sector of the RMU wedge in the Northern Apennines is wider as well (Fig. 3). An idea about the possible consequences of this case may be gained by considering the peculiar pattern of seismicity which followed the strong earthquake (M=7) that activated the Fucino fault system in 1915 (Fig. 22).

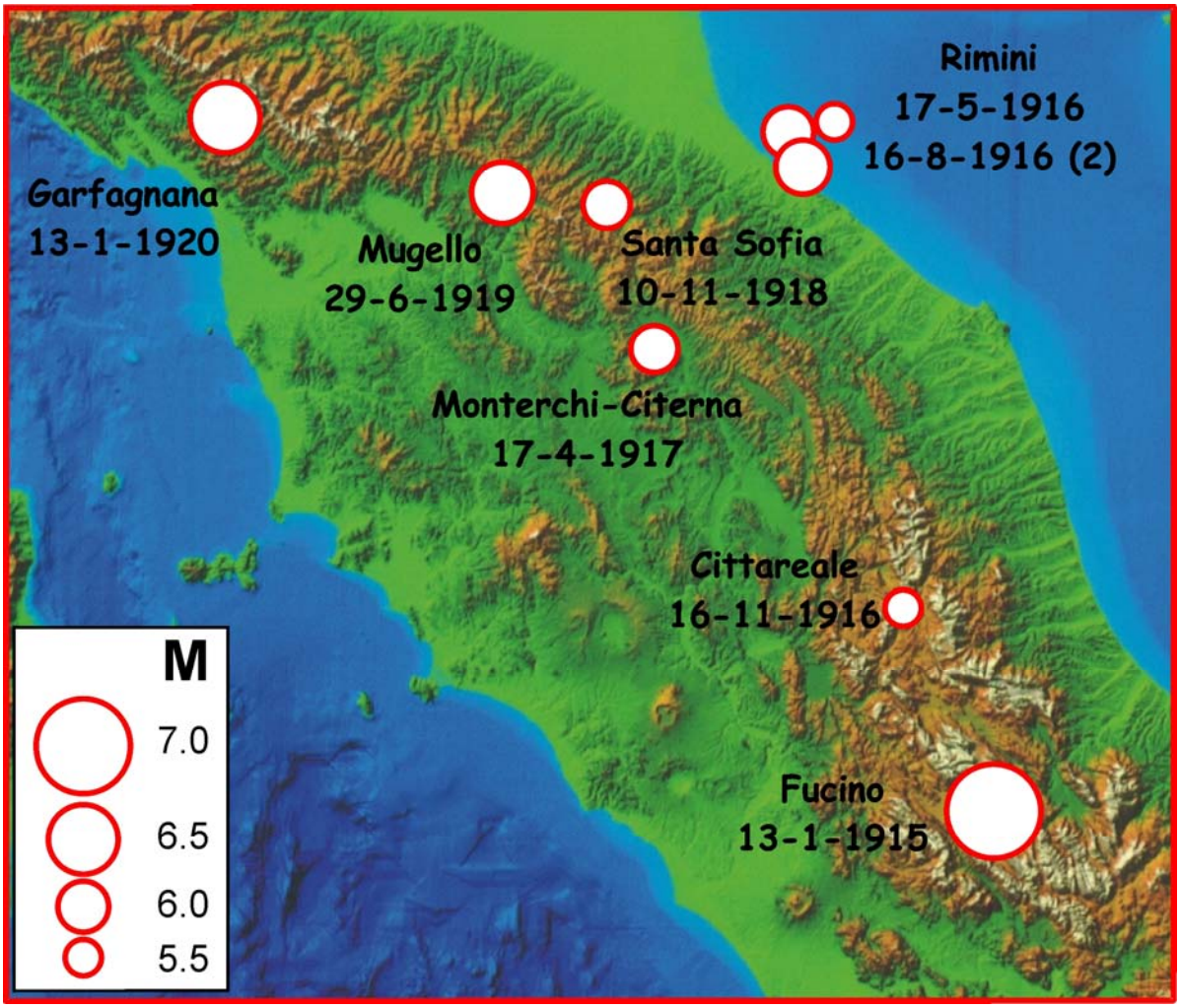

Fig.22. *Distribution of major earthquakes (M≥5.5) in the Northern Apennines after the 1915 strong shock in the Fucino zone. Data from Rovida et al. (2011).*

A possible reconstruction of the short-term development of the tectonic/kinematic setting that determined the distribution of major shock in the period 1915-1920 in the Northern Apennines is illustrated in figure 23 and related caption.

One major difference with respect to the other seismic sequences (when the L'Aquila fault system was involved) is the fact that no sector of the No-Cf-GT-Gu fault system was activated during that period (Fig. 22 and 23). The hypothesis that the accelerated RMU wedge after the 1915 Fucino earthquake moved as an almost unique body (without major internal discontinuities) is supported by the fact that in the subsequent few years (1916-1920) 8 strong shocks (M≥5.5) took place at the main seismic boundaries of the northern part of that sector and of the TE wedge, i.e. the 1916 Rimini, 1917 Upper Tiber Valley, 1918 Romagna Apennines, 1919 Mugello and 1920 Garfagnana/Lunigiana events (Viti et al., 2012, 2013).

In the following, we discuss on how the tectonic setting described above may have influenced the migration of seismicity along the Apennine belt, during the periAdriatic seismic sequences shown in Fig. 13.

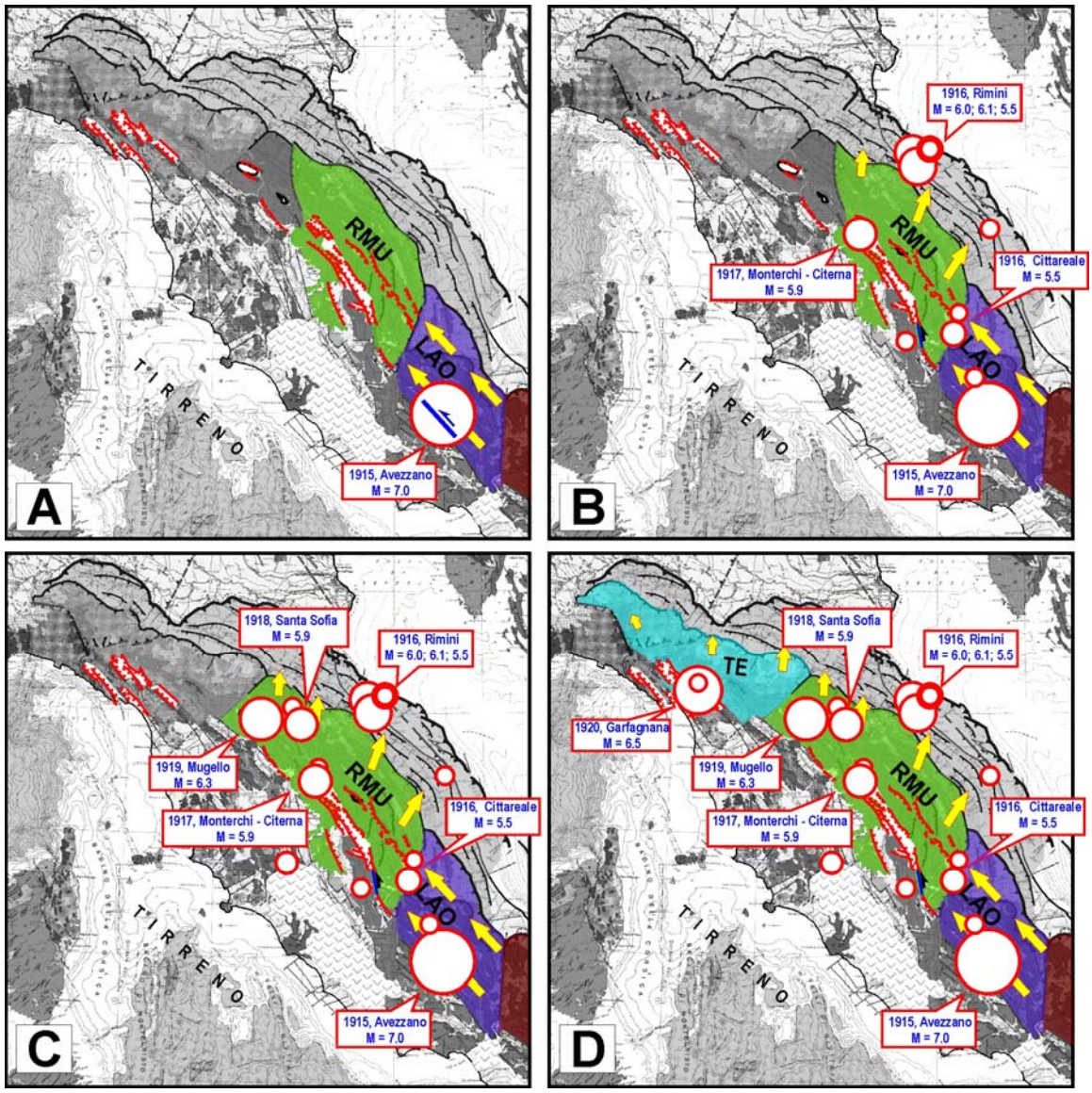

Fig.23. *Tectonic implications of the seismic sequence that occurred in the Central and Northern Apennines during the period 1915-1920 (Fig.22).* ***A****) After the strong 1915 decoupling earthquake (M=7.0) in the Fucino fault system, the eastern sector of the Lazio-Abruzzi platform (ELA, violet) accelerates, increasing its belt-parallel push on the RMU wedge (green).* ***B)*** *In response to the above dynamic context, stresses enhanced along the boundaries of the RMU wedge, where in fact major shocks occurred, involving the outer front of the wedge (Rimini 1916) and the inner extensional/transtensional zone (Upper Tiber Valley, 1917).* ***C)*** *The mobility of the RMU wedge caused the activation of the other major fault systems within that block (Romagna Apennines 1918 and Mugello 1919).* ***D)*** *The compressional strain induced by the mobility of the RMU wedge induces extensional strain at the inner border of the Toscana-Emilia wedge (blue), at the Lunigiana and Garfagnana troughs (1920). The tectonic connection among the seismic sources that were activated during this sequence has been enhanced by the amplitude of the seismic slip of the triggering 1915 Fucino earthquake (about 1-2 metres, Amoruso et al., 1998; Viti et al., 2012). Numerical experiments have shown that the timing of the various events that occurred during the above sequence can be plausibly explained as an effect of post-seismic relaxation (Viti et al., 2012, 2013).*

The first sequence (grey in Fig. 13) was presumably triggered in 1456 by the occurrence of strong earthquakes in the Southern Apennines (Molise, M=7.2, 7.0, 6.3, Fig. 24A), followed by another major shock in Irpinia in 1466, M=6.1). In the same period, strong shocks occurred in the Central

Apennines (Aquila zone 1456, M=5.8; 1461, M=6.4) and in the Marche-Umbria Apennines (Upper Tiber Valley, 1458, M=5.8).

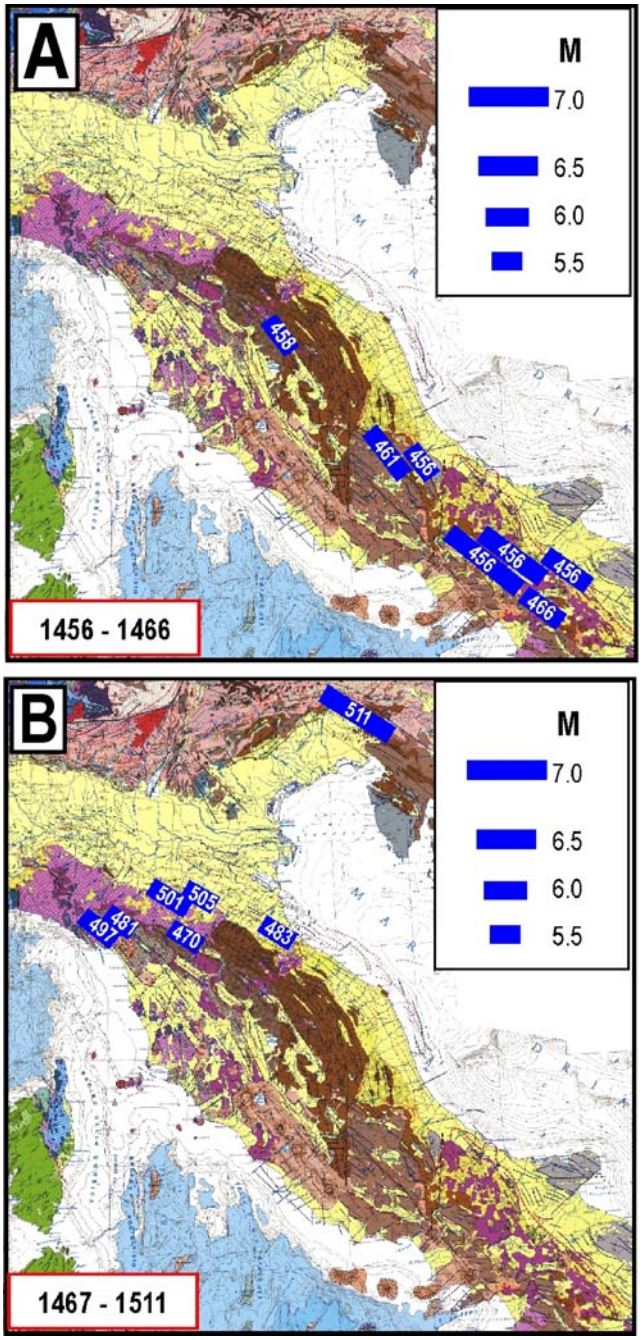

y-m-d	Lat	Long	M	I
1456-12-5	41.30	14.71	7.2	11
1456-12-5	41.18	14.87	7.0	11
1456-12-5	42.20	13.93	5.8	10.5
1456-12-5	41.08	15.67	6.3	9
1458-4-26	43.46	12.24	5.8	8.5
1461-11-27	42.31	13.54	6.4	10
1466-1-15	40.76	15.33	6.1	8.5
1470-4-11	44.16	11.04	5.6	8
1481-5-7	44.27	10.13	5.6	8
1483-8-11	44.16	12.23	5.7	8
1497-3-3	44.25	9.92	5.9	8.5
1501-6-5	44.52	10.84	6.0	9
1505-1-3	44.51	11.23	5.6	8
1511-3-26	46.20	13.43	7.0	9

Fig.24. *Distribution of major earthquakes (M≥5.5) in the Apennine belt during the first periAdriatic sequence given in figure 13. The seismicity pattern in the Apennines is divided in two phases: A (1456-1466) and B (1467-1511), in order to point out the progressive northward migration of seismicity. The numbers within the blue strips indicated the years after 1000 A.D. The date, location, magnitude (M) and macroseismic intensity (I, in the Mercalli-Cancani-Sieberg scale) are given in the table (Rovida et al, 2011; Guidoboni and Comastri, 2005).*

The prosecution of this seismic sequence (Fig. 24B) presents a clear northward migration, involving the inner and outer borders of the Romagna and Toscana-Emilia Apennines (southern Romagna 1483, M=5.7; Garfagnana 1481, M=5.6; Lunigiana 1497, M=5.9; Modena Apennines 1501, M=6.0; Bologna 1505, M=5.6). Strong seismicity reached the northern Adria border (Northern Dinarides) around the beginning of the following century (1511 Slovenia, M=7.0).

The second sequence (orange in figure 13) did not involve very strong earthquakes that instead occurred in the other sequences). Furthermore, the northward migration of seismicity in the study area is rather uncertain. One could tentatively recognize two sub-sequences, as shown in the figures 25A and 25B,C respectively.

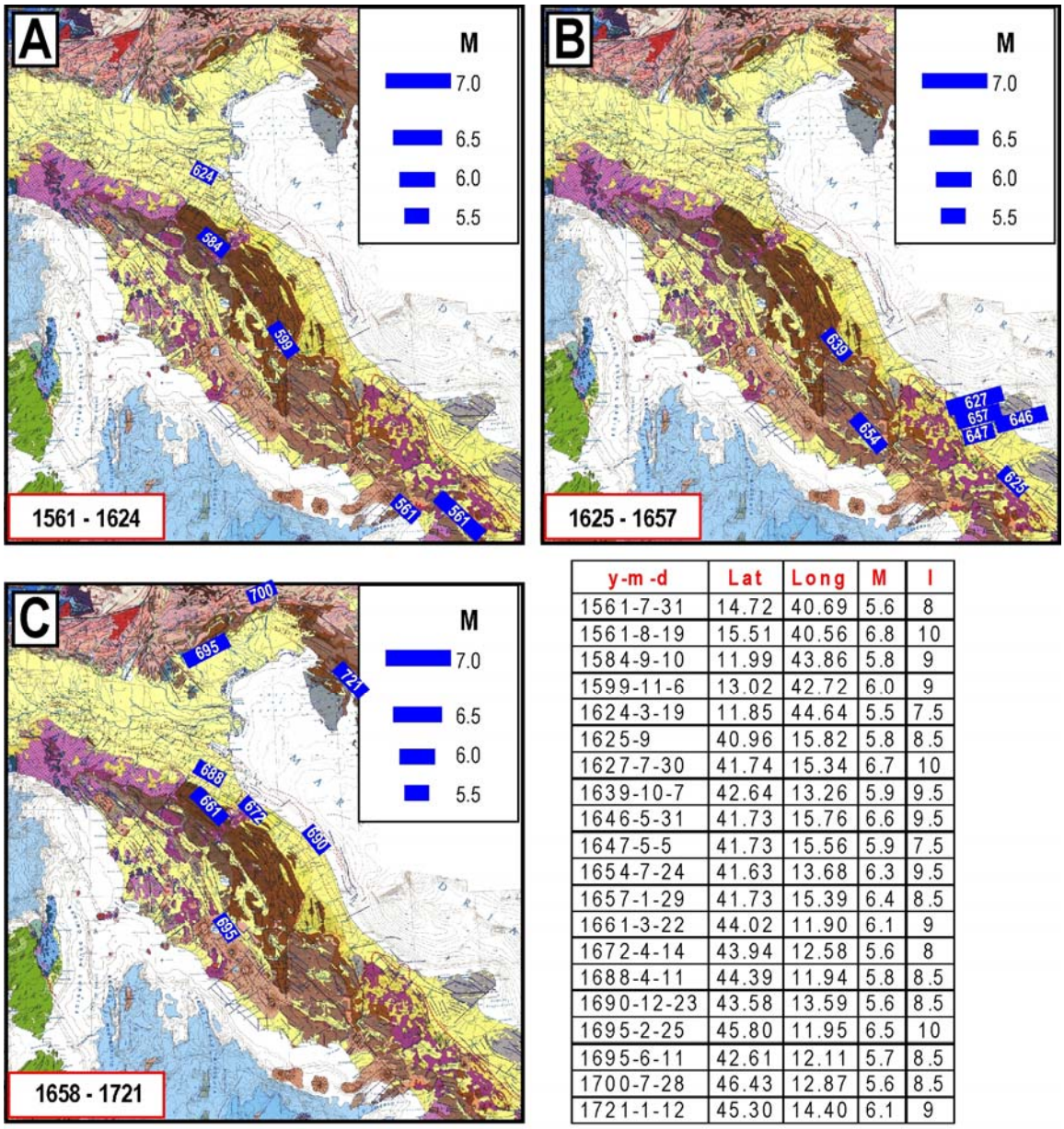

y-m-d	Lat	Long	M	I
1561-7-31	14.72	40.69	5.6	8
1561-8-19	15.51	40.56	6.8	10
1584-9-10	11.99	43.86	5.8	9
1599-11-6	13.02	42.72	6.0	9
1624-3-19	11.85	44.64	5.5	7.5
1625-9	40.96	15.82	5.8	8.5
1627-7-30	41.74	15.34	6.7	10
1639-10-7	42.64	13.26	5.9	9.5
1646-5-31	41.73	15.76	6.6	9.5
1647-5-5	41.73	15.56	5.9	7.5
1654-7-24	41.63	13.68	6.3	9.5
1657-1-29	41.73	15.39	6.4	8.5
1661-3-22	44.02	11.90	6.1	9
1672-4-14	43.94	12.58	5.6	8
1688-4-11	44.39	11.94	5.8	8.5
1690-12-23	43.58	13.59	5.6	8.5
1695-2-25	45.80	11.95	6.5	10
1695-6-11	42.61	12.11	5.7	8.5
1700-7-28	46.43	12.87	5.6	8.5
1721-1-12	45.30	14.40	6.1	9

Fig.25*. Distribution of the major earthquakes (M≥5.5) that occurred in the Apennine belt during the second sequence (orange in Fig. 13). Two sub-sequences could be tentatively recognized. The first may concern the time interval 1561-1624 (A) and the second the two phases shown in B (1625-1657) and C (1658-1721) respectively. Seismicity data in the table. See caption of figure 24.*

During the third sequence (green in figure 13), seismic activity in the Apennines underwent a clear migration from South to North (Fig. 26). In the first phase (Fig. 26A), lasting about 15 years, strong seismicity only occurred in the Southern Apennines (first) and Central Apennines (then). In the second phase (Fig. 26B), seismicity mostly involved the Marche-Umbria sector (Northern Apennines), while some activity continued in the Southern Apennines (1732). In the third phase (Figure 26C), seismicity first occurred in the Central Apennines (1762) and then, from 1768 to 1799, a number of major earthquakes activated most sectors of the inner extensional boundary of the Marche-Umbria wedge (Colfiorito, Upper Tiber Valley, Cagli, Romagna Apennines, Forlì zone) and of the outer compressional border of the same wedge (Marche Apennines, Rimini zone and Ferrara buried folds).

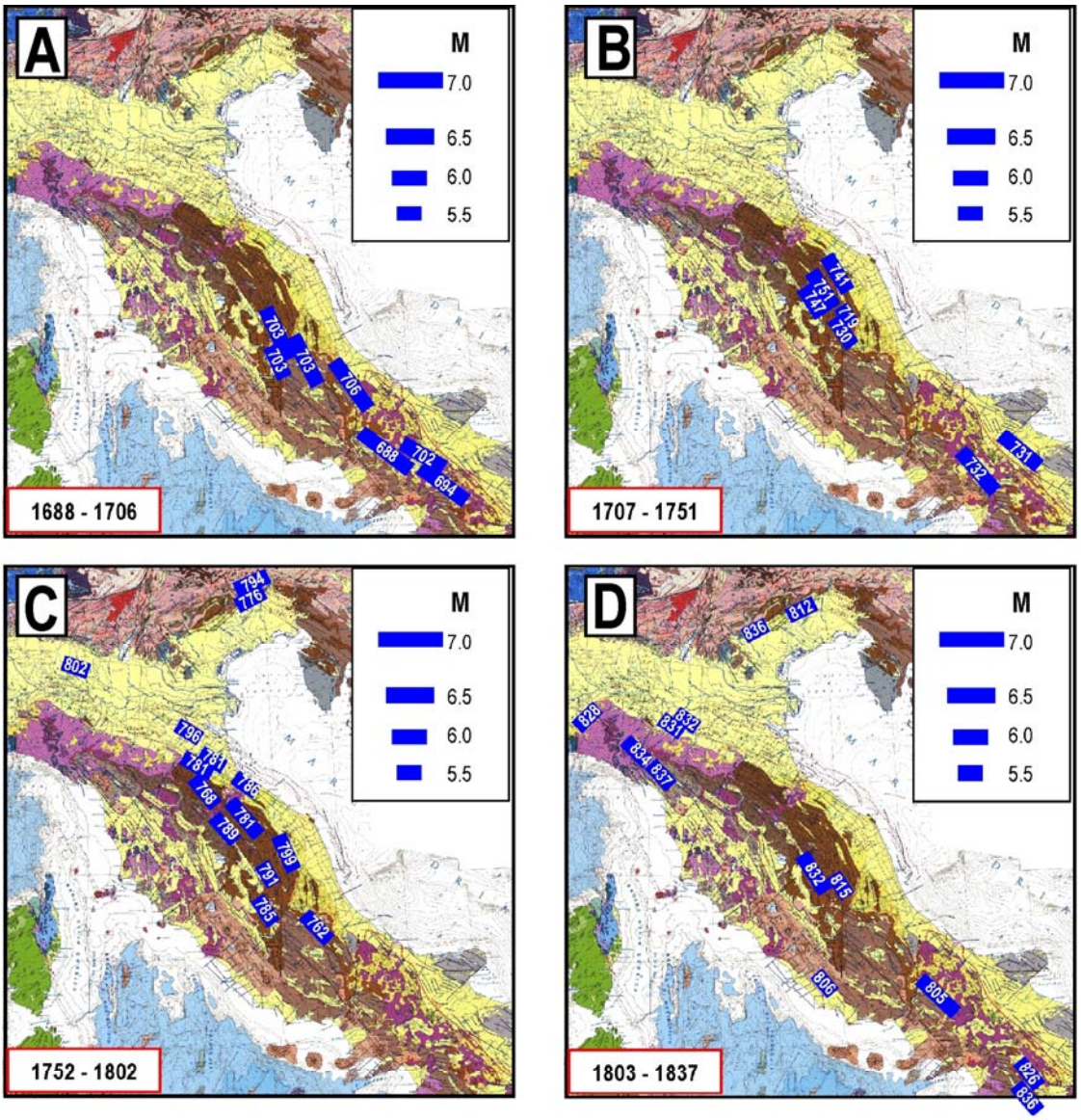

y-m-d	Lat	Long	M	I
1688-6-5	41.28	14.56	7.0	11
1694-9-8	40.86	15.41	6.8	10
1702-3-14	41.12	14.99	6.5	10
1703-1-14	42.71	13.07	6.7	11
1703-1-16	42.62	13.10	5.9	8
1703-2-2	42.43	13.29	6.7	10
1706-11-3	42.08	14.08	6.8	10.5
1719-6-27	42.88	13.05	5.5	8
1730-5-12	42.75	13.12	5.9	9
1731-3-20	41.27	15.76	6.5	9
1732-1-29	41.06	15.06	6.6	10.5

y-m-d	Lat	Long	M	I
1741-4-24	43.42	13.01	6.2	9
1747-4-17	43.20	12.77	5.9	9
1751-7-27	43.22	12.74	6.3	10
1762-10-6	42.31	13.59	6.0	9
1768-10-19	43.94	11.90	5.9	9
1776-7-10	46.23	12.71	5.8	8.5
1781-4-4	44.25	11.80	5.9	9.5
1781-6-3	43.60	12.51	6.4	10
1781-7-17	44.27	11.99	5.6	8
1785-10-9	42.54	12.79	5.7	8.5
1786-12-25	43.99	12.56	5.6	8

y-m-d	Lat	Long	M	I
1789-9-30	43.51	12.22	5.8	9
1791-10-11	42.95	12.86	5.5	8
1794-6-7	46.31	12.82	6.0	8.5
1796-10-22	44.62	11.67	5.6	7
1799-7-28	43.19	13.15	6.1	9
1802-5-12	45.42	9.84	5.6	8
1805-7-26	41.50	14.47	6.6	10
1806-8-26	41.72	12.72	5.5	8
1812-10-25	46.03	12.59	5.7	7.5
1815-9-3	42.83	13.02	5.5	8
1826-2-1	40.52	15.73	5.8	8

y-m-d	Lat	Long	M	I
1828-10-9	44.82	9.05	5.8	8
1831-9-11	44.75	10.54	5.5	7.5
1832-1-13	42.98	12.60	6.3	10
1832-3-13	44.76	10.49	5.5	7.5
1834-2-14	44.43	9.85	5.8	9
1836-6-12	45.81	11.82	5.5	8
1836-11-20	40.14	15.78	6.0	8
1837-4-11	44.17	10.18	5.8	9

Fig.26. *Distribution of major earthquakes (M≥5.5) that occurred in the Apennine belt during the third periAdriatic sequence (green in Fig. 13). The seismicity pattern in the Apennine belt is divided in 4 phases, in order to point out the progressive northward migration of seismicity in the Apennine belt. See the caption of figure 24.*

In the last phase (Fig. 26D), seismicity mostly affected the inner (Garfagnana-Lunigiana) and outer (Padanian) borders of the Toscana-Emilia units, in the northernmost sector of the Apennine

belt. In the same period, two events continued to activate the Marche-Umbria Apennines (1815, 1832). A peculiar feature of this sequence is the long time (about 150 years) it took to migrate from the Southern Apennines to the northernmost zones of the belt.

During the fourth periAdriatic sequence (yellow in figure 13), strong seismicity in the Apennines may be divided in 3 phases (Fig. 27). In the first phase (Fig. 27A), seismicity mainly took place in the Southern Apennines. In the second phase (Fig. 27B) seismicity mostly affected the Northern Apennines and Eastern Alps, by-passing the Central Apennines, where only few moderate shocks occurred in marginal zones. In this regard, it must be pointed out that strong seismicity in the Central Apennines underwent a very long quiescence (1762-1904), the longest in the known history. Thus, the fact that this long quiescence ended up with the strongest shock ever occurred in the Central Apennines (1915, M=7.0) might be not casual. Furthermore, one must consider that the above event involved the Fucino fault system, which, as far as we know, was never activated with such a magnitude (Rovida et al., 2011).

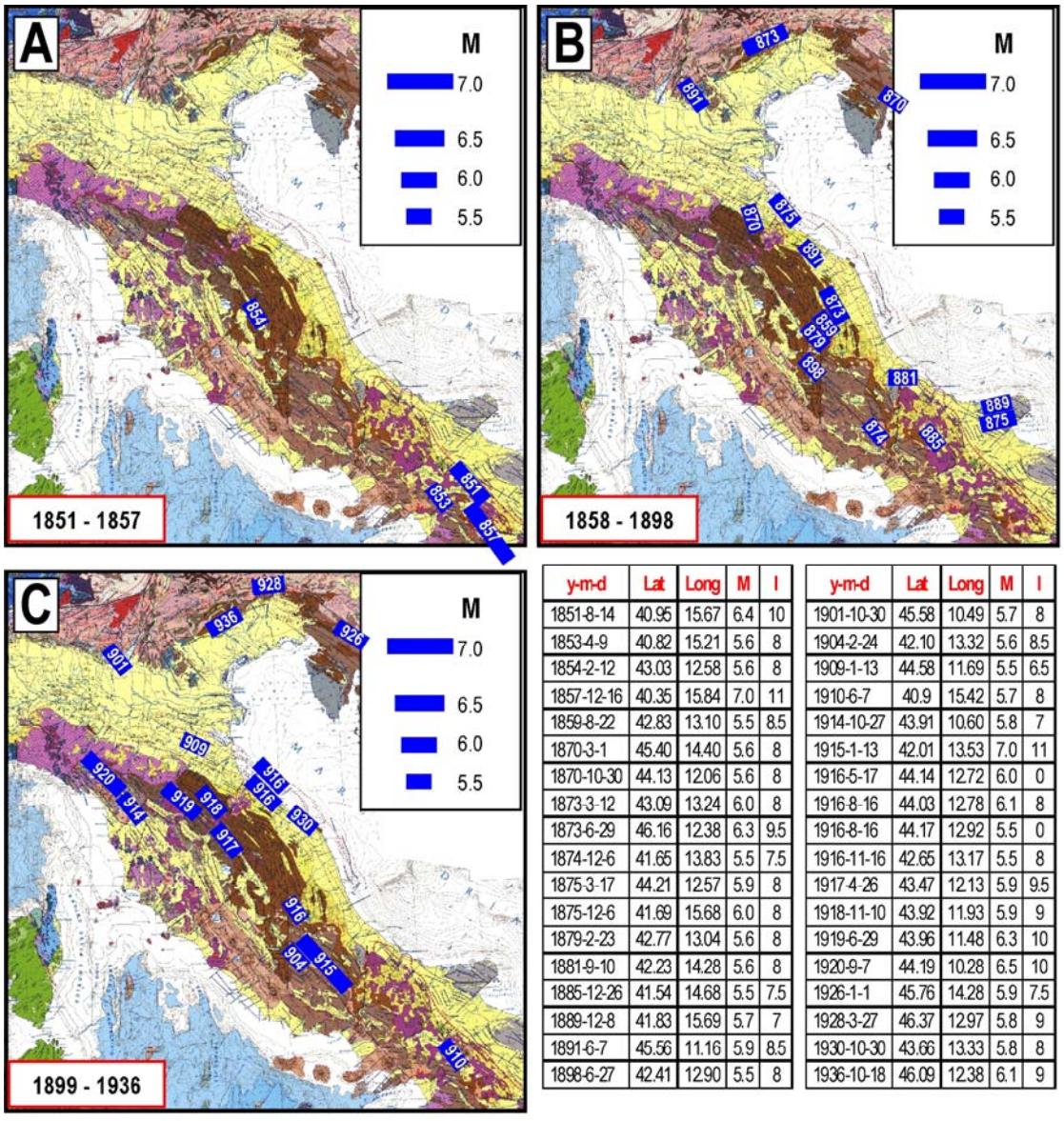

y-m-d	Lat	Long	M	I
1851-8-14	40.95	15.67	6.4	10
1853-4-9	40.82	15.21	5.6	8
1854-2-12	43.03	12.58	5.6	8
1857-12-16	40.35	15.84	7.0	11
1859-8-22	42.83	13.10	5.5	8.5
1870-3-1	45.40	14.40	5.6	8
1870-10-30	44.13	12.06	5.6	8
1873-3-12	43.09	13.24	6.0	8
1873-6-29	46.16	12.38	6.3	9.5
1874-12-6	41.65	13.83	5.5	7.5
1875-3-17	44.21	12.57	5.9	8
1875-12-6	41.69	15.68	6.0	8
1879-2-23	42.77	13.04	5.6	8
1881-9-10	42.23	14.28	5.6	8
1885-12-26	41.54	14.68	5.5	7.5
1889-12-8	41.83	15.69	5.7	7
1891-6-7	45.56	11.16	5.9	8.5
1898-6-27	42.41	12.90	5.5	8

y-m-d	Lat	Long	M	I
1901-10-30	45.58	10.49	5.7	8
1904-2-24	42.10	13.32	5.6	8.5
1909-1-13	44.58	11.69	5.5	6.5
1910-6-7	40.9	15.42	5.7	8
1914-10-27	43.91	10.60	5.8	7
1915-1-13	42.01	13.53	7.0	11
1916-5-17	44.14	12.72	6.0	0
1916-8-16	44.03	12.78	6.1	8
1916-8-16	44.17	12.92	5.5	0
1916-11-16	42.65	13.17	5.5	8
1917-4-26	43.47	12.13	5.9	9.5
1918-11-10	43.92	11.93	5.9	9
1919-6-29	43.96	11.48	6.3	10
1920-9-7	44.19	10.28	6.5	10
1926-1-1	45.76	14.28	5.9	7.5
1928-3-27	46.37	12.97	5.8	9
1930-10-30	43.66	13.33	5.8	8
1936-10-18	46.09	12.38	6.1	9

Fig.27. *Distribution of major earthquakes (M≥5.5) that occurred in the Apennine belt during the fourth periAdriatic sequence (Fig.13). The seismicity pattern in the Apennine belt is divided in 3 phases, in order to point out the progressive northward migration of seismicity. See caption of figure 24.*

As discussed in previous works (e.g., Mantovani et al., 2012), the tectonic implications of the 1915 Fucino earthquake may explain the exceptional seismic activity that occurred in the Northern Apennines (Fig. 27C), with 8 major earthquakes (M≥5.5), in the subsequent 5 years (1916-20). Furthermore, the numerical quantification of the post seismic relaxation triggered by the above earthquake (Viti et al., 2012, 2013) has provided plausible explanation for the occurrence times of the shocks occurred in the period 1916-20. Another evidence in support of the proposed tectonic interpretation is the fact that the seismicity pattern which followed the 1915 Fucino shock did not involve the activation of the No-Cf-GT-Gu fault system. In fact, the sector of the LA wedge which was decoupled by the 1915 Fucino shock did not strengthen shear stress in the above fault system. The activity in the Northern Apennines was then followed by major shocks in the Eastern Southern Alps.

In the last sequence (blue in figure 13), major seismicity in the Apennine belt has so far occurred in the Southern and Central Apennines and in the Marche-Umbria sector of the Northern Apennines (Fig. 28A,B). Only few earthquakes have involved the zones lying more to the north (Parma,1971; Po Valley, 2012; Eastern Southern Alps 1976, 1998; Rovida et al., 2011). As discussed earlier, this pattern suggests that the development of this sequence will most probably involve the tectonic sectors not yet activated of the Northern Apennines.

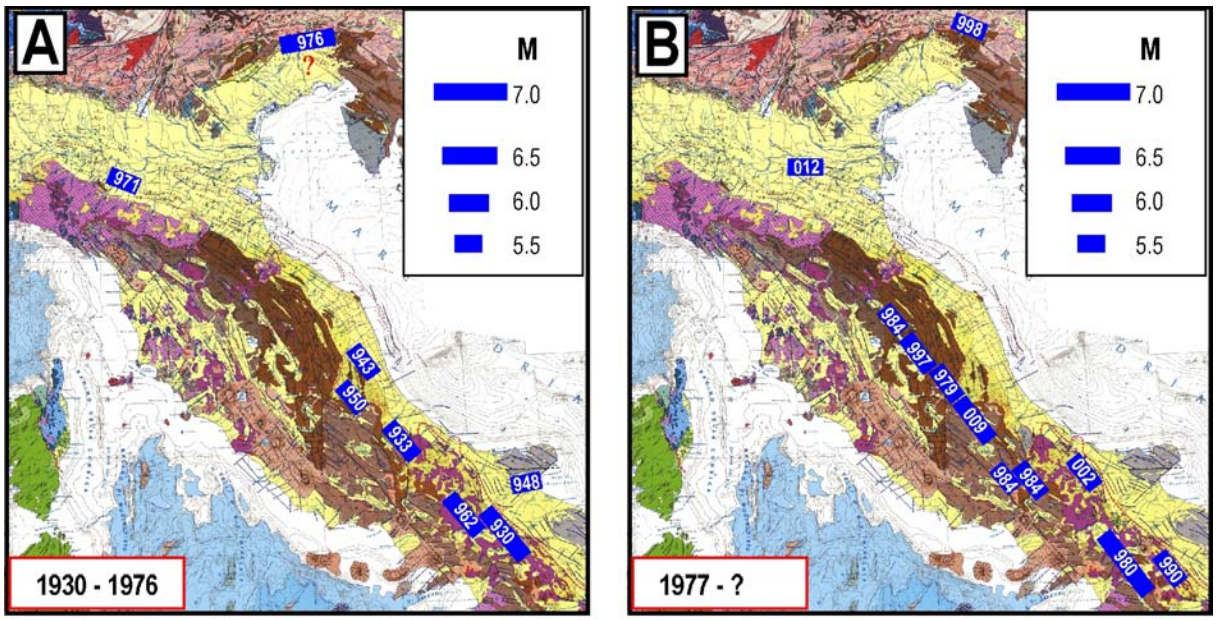

y-m-d	Lat	Long	M	I
1930-7-23	41.07	15.32	6.6	10
1933-9-26	42.08	14.09	6.0	9
1943-10-3	42.91	13.65	5.8	8.5
1948-8-18	41.58	15.75	5.6	7.5
1950-9-5	42.55	13.46	5.7	8
1962-8-21	41.23	14.93	5.7	8.5
1962-8-21	41.23	14.95	6.1	9
1971-7-15	44.81	10.35	5.6	8
1976-5-6	46.24	13.12	6.5	9.5
1976-9-11	46.26	13.23	5.6	7.5
1976-9-15	46.28	13.20	5.9	0
1976-9-15	46.30	13.17	6.0	8.5
1979-9-19	42.71	13.07	5.9	8.5
1980-11-23	40.84	15.28	6.9	10

y-m-d	Lat	Long	M	I
1984-4-29	43.26	12.52	5.7	7
1984-5-7	41.67	14.06	5.9	8
1984-5-11	41.71	13.89	5.5	7
1990-5-5	40.65	15.88	5.8	7
1997-9-26	43.02	12.89	5.7	7.5
1997-9-26	43.01	12.85	6.0	8.5
1997-10-6	43.03	12.85	5.5	7.5
1997-10-14	42.90	12.90	5.7	7.5
1998-4-12	46.31	13.63	5.7	6
2002-10-31	41.72	14.89	5.7	7.5
2002-11-1	41.74	14.84	5.7	7
2009-4-6	42.34	13.38	6.3	9
2012-5-20	44.89	11.23	5.9	0
2012-5-29	44.85	11.09	5.8	0

Fig. 28*. Distribution of major earthquakes in the Apennine belt during the last periAdriatic sequence (blue in figure 13). In the first phase (A), major seismicity has mainly involved the Southern and Central Apennines, increasing tectonic load in the Northern Apennines. In this last zone, seismicity has then affected the Umbrian Apennines (B). More recently, major earthquakes have occurred at the L'Aquila fault system (increasing the mobility of the Gran Sasso wedge) and at the Ferrara buried folds. See caption of figure 24.*

Another migration of seismicity in the previous history, involving major shocks in the Southern, Central and Northern Apennines, has developed around the middle of the XIV century

(Fig. 29). One can note a substantial similarity between this seismic sequence and the one shown in figure 24, concerning in particular the short time elapsed between the activation of the various Apennine sectors (few years) and the fact that, as far as we know, the reaction of the Northern Apennines has only involved the Upper Tiber Valley zone.

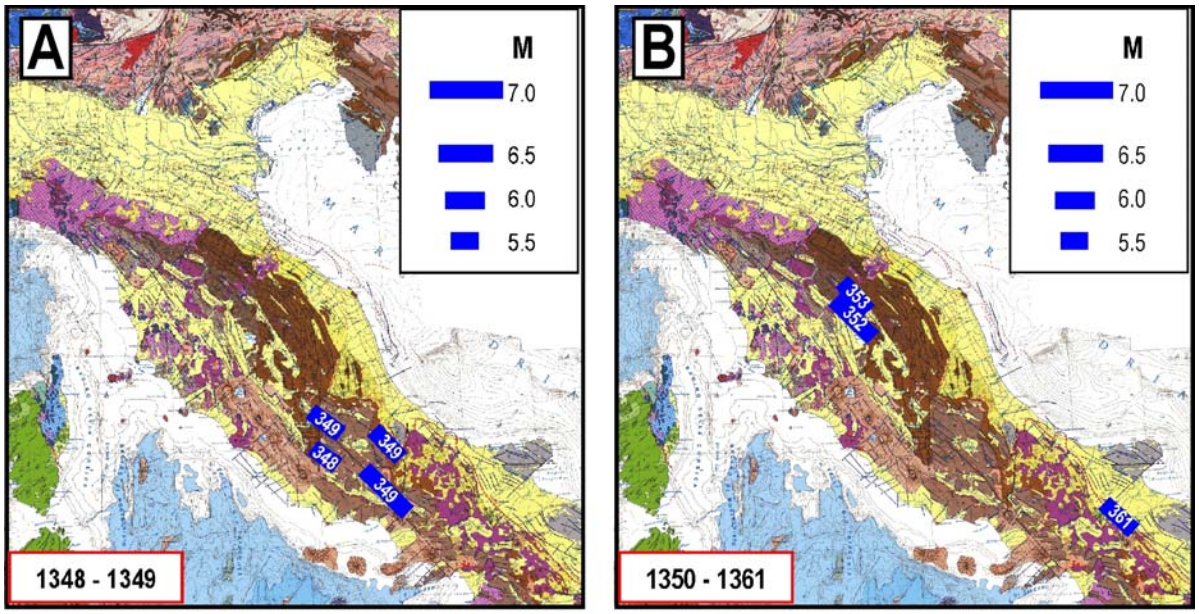

y-m-d	Lat	Long	M	I
1348-9-13	41.92	13.10	5.6	8
1349-9-9	42.27	13.12	5.9	9
1349-9-9	42.02	13.97	6.0	9
1349-9-9	41.56	13.90	5.9	8.5
1349-9-9	41.56	13.90	6.6	10
1352-12-25	43.47	12.13	6.4	9
1353-1-1	43.57	12.13	6.0	9
1361-7-17	41.20	15.56	6.0	9

Fig. 29*. Distribution of major earthquakes (M≥5.5) that occurred in the Apennine belt during another possible migrating sequence that developed around the middle of the XIV century (Table). See caption of figure 24.*

7. Priority seismic zones in the Apennine belt and Eastern Southern Alps

Apennine belt

The arguments and evidence described in the previous sections can tentatively be used for recognizing the Apennine zones where favourable conditions for the occurrence of major earthquakes are developing. For instance, considering what happened in the Apennine belt during the first 4 seismic sequences (Figs. 24-29), one could try to predict the most probable prosecution of the ongoing sequence (Fig. 28b). Above all, one must take into account that the sector of the LA platform that has been mainly mobilized in the present sequence is the Gran Sasso wedge, as indicated by the occurrence of strong shocks at the outer compressional border of that wedge (1933 M=5.7, 1943 M=5.8 and 1950, M=5.7) and its inner transtensional boundary (the L'Aquila fault system, 2009). This implies that the sector of the RMU wedge that is expected to accelerate, in response to the above seismic decouplings, is the ORMU wedge (Fig. 3), delimited to the West by the Norcia-Colfiorito-Gualdo Tadino-Gubbio and Upper Tiber Valley fault systems. This hypothesis is compatible with the fact that the southernmost segments of such system (Norcia and Colfiorito) have been already activated by major events (1979 M= 5.9 and 1997-1998 M= 5.7, 6.0, 5.5, 5.7). After these seismic decouplings, one could expect that the ORMU wedge has accelerated

causing an increase of tectonic load at its northern boundaries (UTV and RoFo fault systems), which can thus be considered zones most prone to the next strong earthquakes.

Among the previous seismic sequences, the one that shows the most evident similarities with the present one is the third one (Figs. 13 and 26), which was characterized by the mobilization of the outer LA sector in the Central Apennines (Gran Sasso wedge) and then by the seismic activation of the zones bordering the southern part of the ORMU wedge (1719-1751, Fig. 26B). Since the above phase was followed by the occurrence of major shocks in the zones lying around the northern boundaries of the ORMU wedge (1768-1796, Fig. 26C), one could suppose that such behaviour may also characterize the prosecution of the present sequence. The earthquakes that have occurred in the Padanian zone in 2012 (M=5.9, 5.8) might represent an effect of the above context.

Taking into account the previous seismic history, one could expect that the boundary sectors of the ORMU wedge that may be most prone to the next strongest events (M≥5.5) are the UTV and Ro-Fo fault systems (Fig. 3). This conviction is based on the following remarks.

- The geodetic velocity field (Fig. 9) suggests that the relative motion rate between the ORMU wedge and the inner belt is about 3-4 mm/y. Since the last major earthquake in the UTV fault system occurred about 100 years ago (1917, M=5.9), one can estimate that the relative extensional deformation so far accumulated at such fault system is about 20-30 cm, which may be associated with a earthquake magnitude of about 5.5-6.0, following the relation reported in the caption of figure 13. Instead, at the outer borders of the ORMU wedges one may expect a lower deformation, since such compressional strain is driven by the slow convergence between the ORMU wedge and Adria, which rate is most probably lower (1-2mm/year) than the extensional rate at the inner ORMU boundaries (UTV and Ro-Fo).
- It is reasonable to expect that, at the light of numerical experiments carried out for other earthquakes in the Apennine belt (Viti et al., 2012, 2013), the effects of the post-seismic relaxation induced by the 1979 and 1997 major shocks in the Norcia and Colfiorito sources are being most intense at the UTV and Ro-Fo zones.
- The UTV and Ro-Fo zones have been the site of several major historical earthquakes (Rovida et al., 2011). One could object that this condition also holds for other boundaries of the ORMU wedge, such as the Rimini-Ancona and Marche ridge zones, but it must be considered that the outer fronts of the ORMU wedge are presumably undergoing a lower strain rate with respect to the inner ones, since the Adria-ORMU convergence rate (1-2 mm/y) is lower than the divergence rate (3-4 mm/y) between the ORMU wedge and the inner belt (Figs. 3 and 9).
- The main seismic zones located in the northernmost Apennine sector (TE wedge, mainly the Lunigiana-Garfagnana zones) experienced major earthquakes (1481 M=5.6, 1497 M=5.4, 1834 M=5.6, 1837 M=5.7, 1920 M=6.5) during the grey, green and yellow sequences of figure 13, i.e. the ones that were preceded by very strong shocks in the Southern and Central Apennines. Only moderate earthquakes instead occurred in the northern TE wedge during the orange sequence, which was not characterized by very strong seismicity in the Central and Southern Apennines. The above cases could imply that the seismic activation of the Lunigiana and Garfagnana fault systems requires the occurrence of large decoupling shocks in the southern sectors of the mobile belt. When this condition is not fulfilled, the migrating deformation is not apparently sufficient to induce significant seismicity in the northernmost sector of the TE wedge. The present sequence has so far involved three major earthquakes in the Southern Apennines (1930, 1962, 1980) and a number of moderate shocks in the Central Apennines (1933 M=5.7, 1943 M=5.8, 1950 M=5.7, 1984 M=5.9, 5.5, 2009 M=6.3). However, the fact that such events were separated by relatively long time intervals suggests that their effect in the Northern Apennines may be weaker than the ones that were induced during some of the previous sequences in response to very strong shocks concentrated in time (Fig. 13). In fact, it is known that the brittle behaviour of rocks enhances as strain rate increases (Toda et al., 2002; Kato et al., 2003; Niemeijer and Spiers, 2007; Savage and Marone, 2007). The arguments described above suggest that at present the probability of major earthquakes at the boundaries of the northernmost sector of the TE wedge is lower than that at the boundaries of the ORMU wedge.

- Once tentatively identified the UTV and Ro-Fo fault systems as priority seismogenetic structures in the study area (Fig.30), it is opportune to take into account their previous seismic behaviour (Tab. 1), in order to gain orientative insights into the seismic potentiality of such fault systems, in terms of maximum macroseismic intensity (Imax, MCS scale) and average recurrence time (Tr) for major events.

For the UTV fault system zone, the known seismic history since 1000 (Rovida et al., 2011) provides a value of IX-X for Imax. Tr is 53 years for I≥VII, 145 years for for I≥VIII and 203 years for I≥IX. The last events with I=VII and I=IX occurred 68 years ago (1948) and 99 years ago (1917) respectively. The minimum and maximum inter-event time intervals are 1 and 134 years for I=VII, and 1 and 400 years for I=IX, respectively. These data suggest that predicting the occurrence time of the next major shock in this zone is rather problematic.

For the Ro-Fo fault system Imax is X, Tr is 44 years for I≥VII, 113 years for I≥VIII and 169 years for I≥IX. The last events with I=VII and I=IX occurred 60 years ago (1956) and 98 years ago (1918) respectively. The minimum and maximum inter-event time intervals are 4 and 104 years for I≥VII and 13 and 137 years for I≥IX. Of course, one must be aware that the above estimates can considerably be influenced by likely incompleteness of the oldest parts of seismic catalogues.

UPPER TIBER VALLEY	ROMAGNA – FORLI'
	1194 (VI)
1269 (VII-VIII)	
1270 (VII-VIII)	1279 (VI-VIII)
1352 (IX)	
1353 (IX)	
	1383 (VI-VIII)
1389 (IX)	1393 (VI)
	1428 (VII)
1458 (VIII-IX, VII)	
1484 (VII)	1483 (VII-IX)
1489 (VII)	
	1509 (VI)
1558 (VII-VIII)	
1559 (VIII)	
	1584 (IX)

UPPER TIBER VALLEY	ROMAGNA – FORLI'
	1661 (X)
1693 (VII)	**1688 (IX, VII)**
1694 (VII-VIII)	
1731 (VII-VIII)	
	1768 (IX)
1789 (IX)	**1781 (IX-X, VIII)**
	1813 (VII)
1865 (VII-VIII)	1861 (VII)
	1870 (VIII)
	1881 (VII)
1897 (VII-VIII)	1895 (VII-VIII)
	1911 (VII)
1917 (IX-X)	**1918 (IX)**
1948 (VII)	1952 (VII)
	1956 (VII)

Tab.1. *Earthquakes with I≥VII that occurred in the UTV and Ro-Fo zones since 1000 A.D (Rovida et al., 2011). Events with I≥IX are evidenced in red.*

Eastern Southern Alps

In sections 5, 6 and 7 we have pointed out evidence and arguments which suggest that at present the probability of major earthquakes in the Nnorthern Apennines and Southern Eastern Alps is higher than the one in the Central-Southern Apennines and Calabrian Arc. Here we point out other evidence and arguments that may help us to recognize which of the two zones cited above (Northern Apennines and Southern Eastern Alps) can be considered more prone to next strong shocks:

- In the periAdriatic sequences shown in figures 13 and 22-29, the activation of major fault systems in the Northern Apennines has mostly preceded the occurrence of major shocks in the Eastern Southern Alps.
- The fact that a couple of strong shocks (M= 6.4, 5.9) occurred in the Eastern Southern Alps in 1976 may imply that the strain/stress so far accumulated in that north Adriatic front has been at least partially released. This could delay the next seismic activation of such thrust zone.
- The northward motion of Adria and the consequent accumulation of strain/stress in the Eastern Southern Alps is favoured by the occurrence of major decoupling shocks in the left lateral

transpressional fault system recognized in the Northern Dinarides. This hypothesis is supported by the spatio-temporal distribution of major earthquakes since 1400 (Fig. 13). The above evidence suggests that the very scarce seismic activity that has so far occurred in the Northern Dinarides during the ongoing sequence (Fig. 15) may imply that the seismogenetic zones in the Southern Alps are not close to activate.

- The complex of evidence and arguments described above suggest that the next seismic activation in the Eastern Southern Alps will follow in time the next major shock in the Northern Apennines.

8. Priority seismic zones in Calabria and Sicily

As shown in the figures 1, 5 and 19 long term tectonic activity in southern Italy is mainly accommodated by the opposite escapes of the Calabrian and Hyblean wedges, driven by the convergence of the confining blocks (Mantovani et al., 2009, 2014). In Calabria, longitudinal compression causes the uplift of the belt, favouring its gravitational sliding towards the Ionian oceanic lithosphere. However, as argued earlier, this process may have encountered higher resistance since the middle of the previous century, when the effects of the post 1939 large westward displacement of the Anatolian-Aegean-Balkan system reached the Adriatic and Ionian zones. In response to this event, the seismotectonic processes that accompany the outward sliding of Calabria have slowed down. This hypothesis might explain why since 1947 seismic activity in Calabria has undergone a drastic reduction (Fig. 18). On the other hand, the above tectonic context may have important consequences on seismic hazard in Sicily, since the slowdown of Calabria's escape could be compensated by an acceleration of the roughly North to NNW ward displacement of the Hyblean wedge. This hypothesis is consistent with the fact that since 1948 the considerable slowdown of seismic activity in Calabria has been accompanied by an increase of activity along the boundaries of the Hyblean wedge (Fig.21).

The tectonic zones where the above interpretation would predict the highest seismic risk are related with the fault systems which allow the decoupling of the Hyblean wedge from Calabria, i.e. the Vulcano and Syracuse faults (Fig. 5). Since such decoupling also involves the divergence between the Peloritani block (stressed by the Hyblean wedge) and southernmost Calabria, accommodated by extension in the Messina trough, the fault systems bordering such trough may be included in the seismic zones where the probability of seismic activation has increased during the present tectonic context.

The fact that some major earthquakes have occurred in the Cephalonia fault system in January and February 2014 (M=6.1, 6.1) and November 2015 (M=6.5), deserves some remarks, since such seismic source belongs to the Hellenic zone where possible precursors of Calabrian earthquakes may be generated (Fig. 18). In particular, it would be useful to get insights into how such recent seismicity in the Cephalonia fault may influence the probability of major earthquakes in Calabria. To this regard, we report the following considerations:

- Most of the Calabrian events given in figure 18 have been preceded by Hellenic shocks with magnitude greater than 6.5, whereas the 2014 and 2015 Cephalonia earthquakes only reached a maximum magnitude of 6.5. So, it seems unlikely that such shocks may have significant effects on the activation of Calabrian faults in the next years.
- The seismic correlation shown in the table of figure 18 suggests that the influence of major shocks in the Cephalonia fault zone on the probability of a seismic activation of Calabrian faults has drastically decreased after the large westward displacement of the Anatolia-Aegea-Balkan system (Fig.18). Since it can hardly be recognized if the above condition still holds that zone, any attempt at predicting the next seismic behaviour of Calabria is affected by noticeable uncertainty. Considering the tectonic context in the southern Adriatic zone (Fig. 18) and the seismicity patterns given in the related table, we suppose that major earthquakes in the Epirus zone of the Northern Hellenides can more efficiently influence the probability of major shocks in Calabria.

9. Italian seismic zones where no prediction can be provided at present

In the previous sections, it has been recognized that in some Italian zones the probability of major shocks is higher than in other zones. However, this relative evaluation should be integrated by a more precise identification of the zones that cannot be involved in the prediction. To this regard, some considerations are given in the following about the parts of Italy where the proposed approach cannot provide reliable indications on the expected seismic activity.

Central/Western Alps, Ligurian Alps, western Po Valley

Most of the seismic zones of this area have been so far affected by earthquakes of moderate intensity (lower or equal to VIII), except the tectonic zone located offshore western Liguria, where strong shocks (Imax= X) have occurred (Fig. 30).

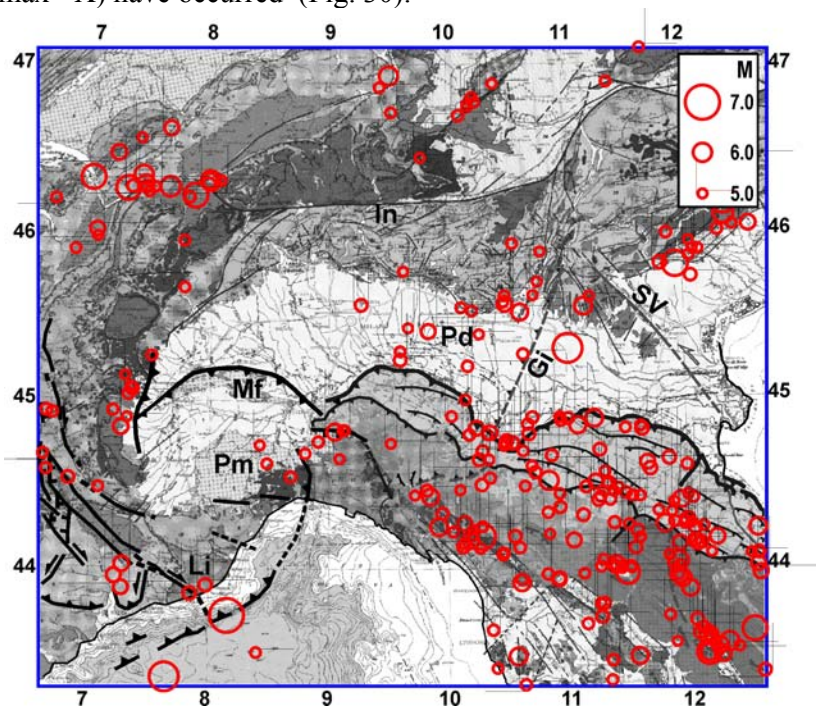

Fig.30. *Major earthquakes (M≥5) that have occurred since 1000 A.D. (Rovida et al., 2011) and main tectonic features in Northwestern Italy (e.g., Larroque et al., 2011; Bauve et al., 2014). Gi=Giudicarie fault system, In=Insubric line, Li=Ligurian Alps, Mf,Pm=Monferrato and Piemonte Apennine sectors, Pd=Padania, SV=Schio-Vicenza fault system.*

These zones are located in the sector of the Adriatic domain that is not supposed to behave as a part of the main Adria plate, being located to the west of the decoupling Schio-Vicenza and Giudicarie fault systems. Thus, it is not easy to understand what connection may exist between the seismotectonic activity of these zones and the one that is related with the migration of the Adria plate. Consequently no reliable prediction may be tried about the location of the next major shocks in this area.

Inner (Tyrrhenian) side of the Apennine belt

As discussed earlier, the tectonic activity and the relative seismicity that develop in this area (Fig. 4) are not related to the stresses induced by the Adriatic motion. The main compressional driving force that acts in the inner Apennine chain is the African push transmitted by the Calabrian wedge (Viti et al., 2015b). This suggests that understanding the connection between the seismicity of this area and that of the periAdriatic zones considered in the previous chapter is not easy.

Consequently, any attempt at recognizing the fault systems that will undergo seismic activation in the near future would be affected by considerable uncertainty.

Apulia

The seismicity of this zone (Fig. 31) is mostly associated with the activation of a fault system (Mattinata-Gondola) located in the Gargano area, belonging to the bulge of the southern Adriatic platform (e.g., Piccardi, 2005; Scisciani and Calamita, 2009; Di Bucci et al., 2011). The location of this feature implies that tectonic activity in this seismic zone is not related with the decoupling of the Adria Plate from the surrounding belts, but rather results from deformation that develops inside that platform. As a consequence, it is not simple to recognize how such activity is related with the spatio-temporal distribution of seismicity in the periAdriatic zones.

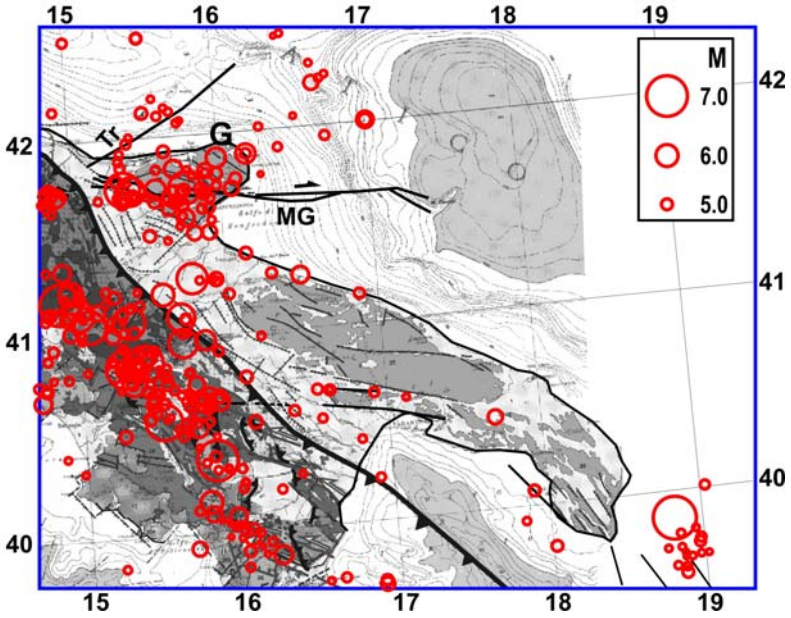

Fig. 31 *Major earthquakes (M≥5) since 1000 A.D. (Rovida et al., 2011) and main tectonic features in the Apulia zone. MG=Mattinata-Gondola fault system, G=Gargano, Tr=Tremiti fault system.*

10. Spatio-temporal distribution of minor seismicity

The attempt at identifying a connection between tectonic processes and the spatio-temporal distribution of earthquakes has so far taken into account major seismicity (M≥5.5), in line with the well-known concept that tectonic processes and plate motions are mostly controlled by strong shocks, involving long decoupling faults and significant values of seismic slip. However, it is reasonable to suppose that the ongoing deformation pattern also influences the spatio-temporal distribution of minor events (e.g., Marsan, 2005) , even if the underlying relation is not clear yet.

In order to get insights into this problem, we have taken into account the most complete and reliable data set now available about minor seismicity in the Italian area, reported in the CSI catalogue (Castello et al., 2006), for the period 1981-2015.

The distribution of such activity and the geometry of the seismic zones that we have taken into account are shown in figure 32. The time patterns of the annual number of events in the zones considered (Fig. 33) suggest the following remarks:

- The relatively low number of earthquakes that occurred in the Eastern Southern Alps (zone A) in the whole period considered could indicate that in such zone the ongoing tectonic load is not high. This interpretation would corroborate the hypothesis (discussed earlier) that the probability of major

earthquakes in that zone is actually lower than the one in the Northern Apennines. An analogous consideration could be made for the central Southern Alps.

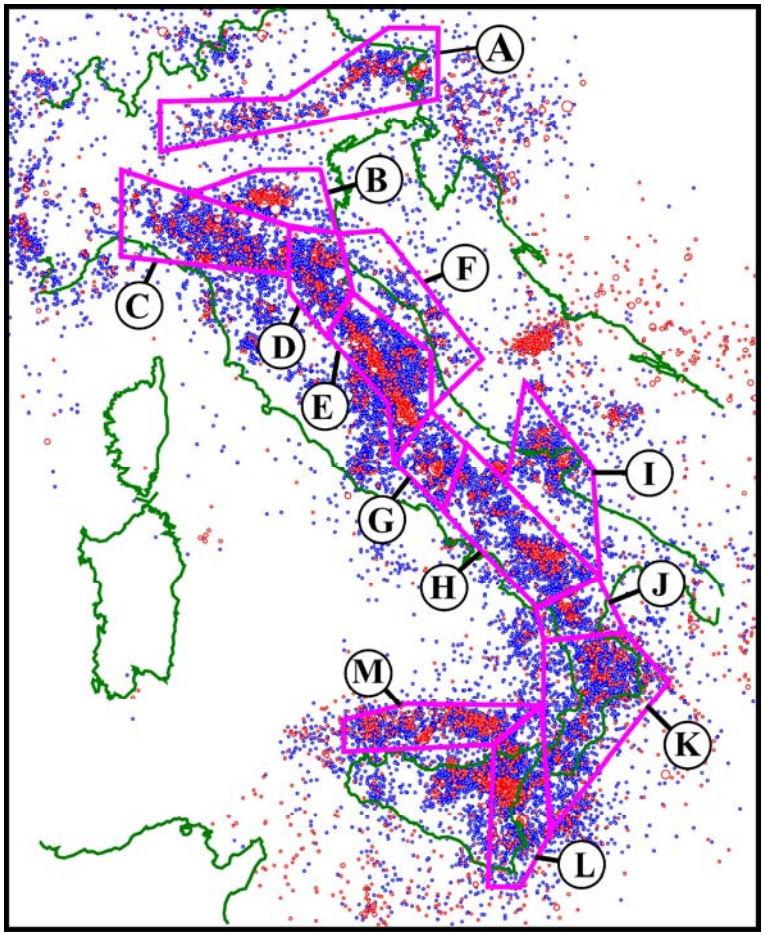

Fig.32. *Distribution of minor seismicity in the Italian area (1981-2015) and geometries of the zones here considered. Seismicity data from ISIDe Working Group (INGV, 2010). Letters correspond to the zones and relative diagrams shown in figure 33. Red circles= M ≥ 3, Blue circles= 2 ≤ M < 3.*

- It can be noted that, among the zones here considered (Fig. 32), the highest number of earthquakes has occurred in some sectors of the northern Apennines (zones C, D and E). This is mainly evident in the zone E (No-Cf-GT-Gu fault system) for period following the 1997 Colfiorito earthquake (M=6.1). To this regard, one could remark that seismic energy release in the Aq-No-Cf-GT-Gu decoupling fault system (Figs.3 and 9) may indicate an accelerated motion of the southern part of ORMU wedge with respect to the inner belt, a process that enhances tectonic load on the northern part of the same wedge. In this context, it is reasonable to expect that stress increases at the boundaries of the northern ORMU wedge (mainly related with the UTV and Ro-Fo fault systems). These considerations corroborate the hypothesis that such fault systems are actually the most prone to next seismic activations. In this regard, one could note that in the period considered no major shocks (M>5.5) have occurred in the above faults (Fig.33).

The fact that in the period considered the UTV and RoFo fault systems (zone D) have not been activated by earthquakes with M>5 indicates that those decoupling features are still blocked. This means that the mobility of the ORMU wedge is stressing the structures which lie north of those decoupling zones, i.e. the northern sector of the RMU wedge and the TE wedge (Fig.3). This hypothesis

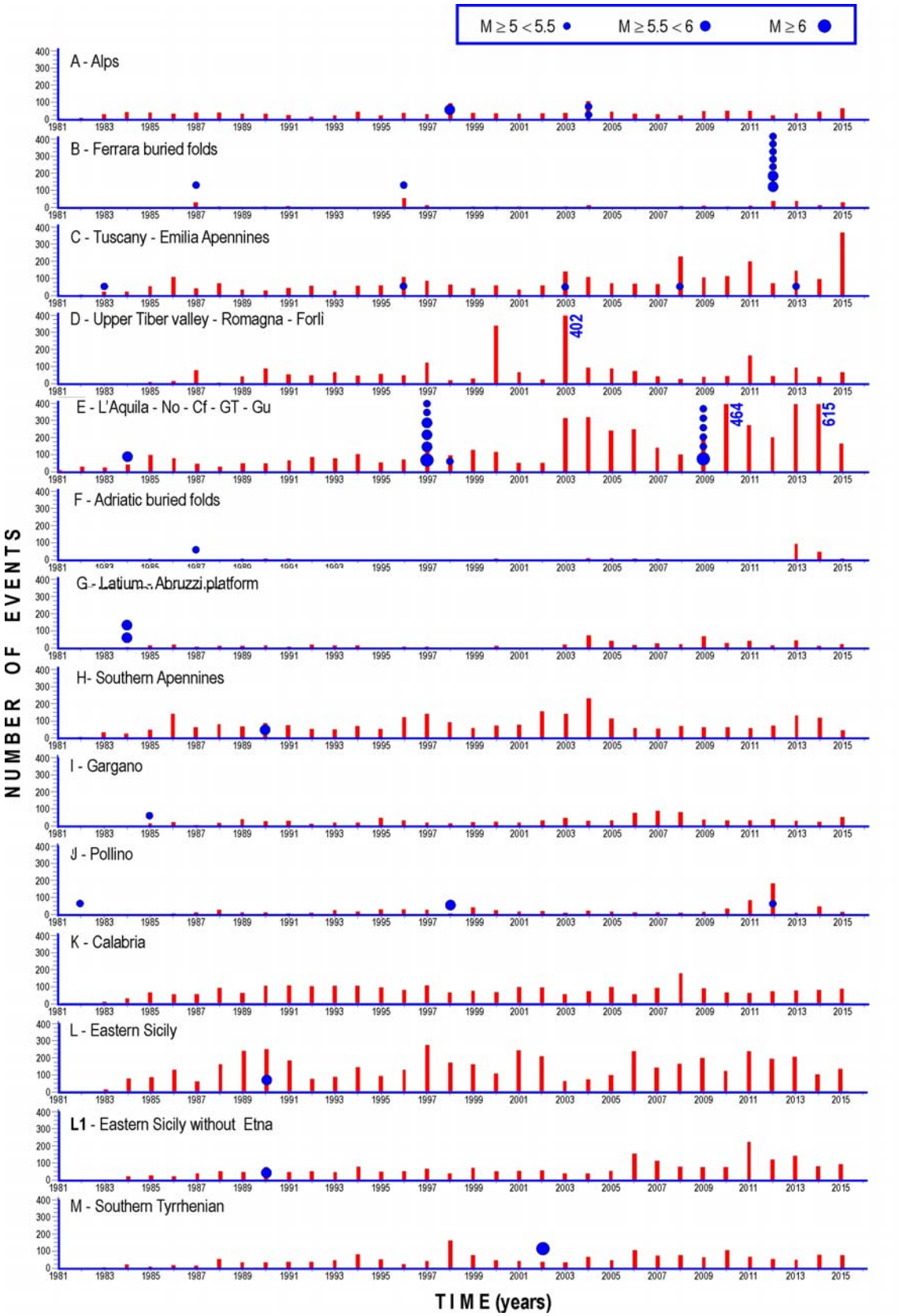

Fig.33. *Time patterns of instrumental seismicity in the period 1981-2015. See caption of figure 32. In the years in which the number of events overcomes 400, the total number is written besides the respective bar. Circles along the bars indicate the occurrence in the respective year of one or more earthquakes with M ≥ 5.*

may explain the slight increase of seismicity that occurred at the boundaries of the above wedge (zones B and C).
- Another zone where seismic activity shows a slightly higher, and almost continuous level with respect to most of the other zones, is Eastern Sicily (zone L). It is interesting to note that in such zone seismic activity undergoes a considerable reduction if the Etna area is not considered (L1 histogram).

11. Geodetic strain rate

The horizontal strain rate field has been derived by the geodetic velocity field shown in figure 8 by applying a weighted least square method (Cenni et al., 2015). In particular, the horizontal strain rate tensor has been evaluated on a regular grid (0.25° x 0.25°), applying the algorithm developed by Shen et al. (1996). The contribution of each velocity vector to the strain rate computed on a given node of the grid is weighted by using the associated uncertainties and the exponential scaling function $\exp(-d_{ik}/Df)$, where d_{ik} is the distance between the i-th node of the grid and the k-th GPS station and Df is the distance decay factor. In order to improve the reliability of the results, we have integrated the weighted least square method with two geometric criteria, as suggested for instance by Teza et al. (2008, 2012) and Cenni et al. (2012). In particular, the strain rate values are taken as acceptable only when at least three GPS sites are located at a distance lower than Df from the node considered and are uniformly distributed in the surrounding region (one in each 120° angular sector). In the computation, Df has been assumed equal to 50 km, that is about three times the average spacing of the network. The result obtained is shown in figure 34.

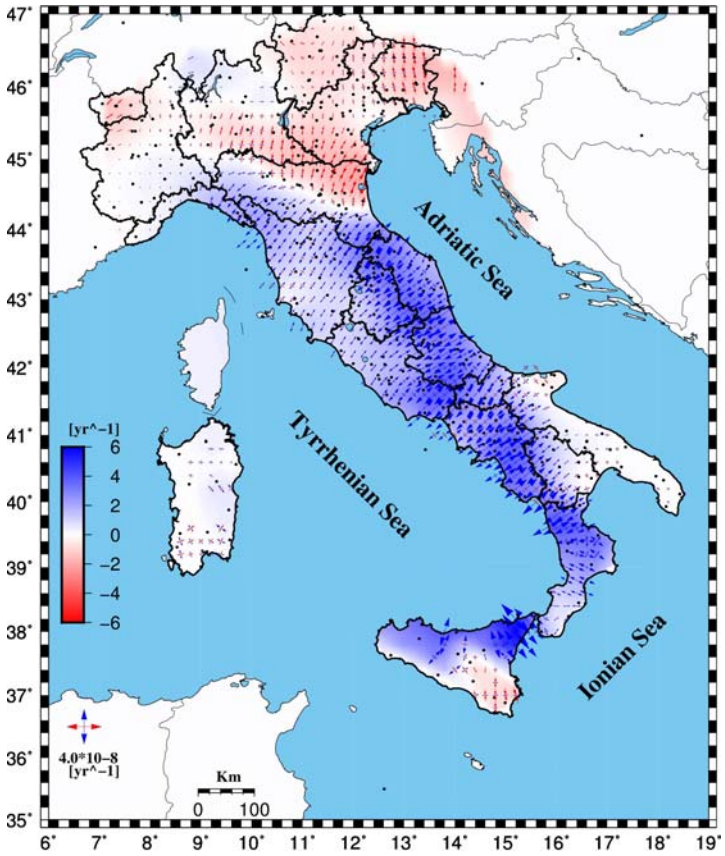

Fig.34. *Horizontal strain rate field inferred from the velocity field shown in figure 8. See text for explanations. Red converging and blue diverging arrows indicate principal axes of shortening and lengthening, respectively. The prevalence of extensional (blue) and shortening strain (red) is also evidenced in the figure, following the chromatic scale given on the left side.*

In order to estimate the amplitude of the strain rate, independently from the deformation style, we have calculated the parameter TSR (Total Strain Rate), which is defined by the following relation:

$$TSR = \sqrt{\left(\dot{\varepsilon}_{11}^2 + \dot{\varepsilon}_{22}^2 + 2\dot{\varepsilon}_{12}^2\right)}$$

where $\dot{\varepsilon}_{11}$, $\dot{\varepsilon}_{22}$ and $\dot{\varepsilon}_{12}$ are the horizontal components of the strain rate tensor (e.g., Kreemer et al., 2003; Riguzzi et al., 2012) given in figure 34.

The spatial distribution of the normalized TSR in the Italian area, is shown in figure 35.

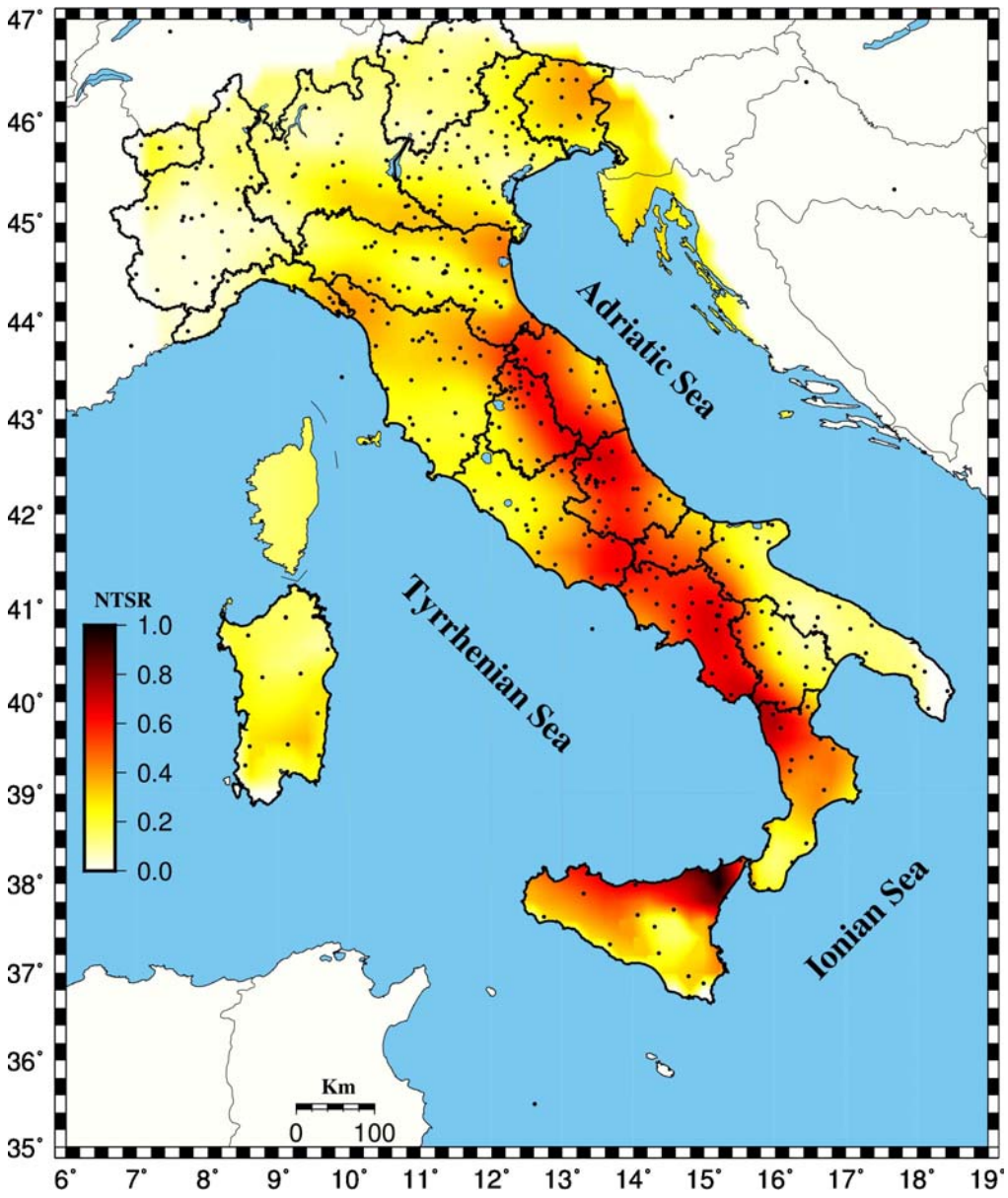

Fig.35. *Pattern of the Total Strain Rate, derived by the strain rate field given in figure 34, normalized (NTSR) by using the maximum computed amplitude ($4.1*10^{-8}$ yr^{-1}). The black dots indicate the GPS sites.*

It is worth noting that the zones here recognized as most prone to next major shocks (Umbria-Romagna Apennines and Eastern-Northeastern Sicily) are mostly located within the zones of highest strain rate values (Fig. 35).

In figure 36, the distribution of the normalized TSR values is superimposed to the of seismicity pattern that occurred from April 2005 to January 2016. Gasperini et al. (2013) indicate the magnitude M=1.9 as a reasonable completeness threshold for the above catalog. Instead, Schorlemmer *et al.* (2010a) suggest the value M=2.5. Anyway, to avoid possible bias due to data incompleteness, we have considered the seismic events with $M \geq 3.0$ only.

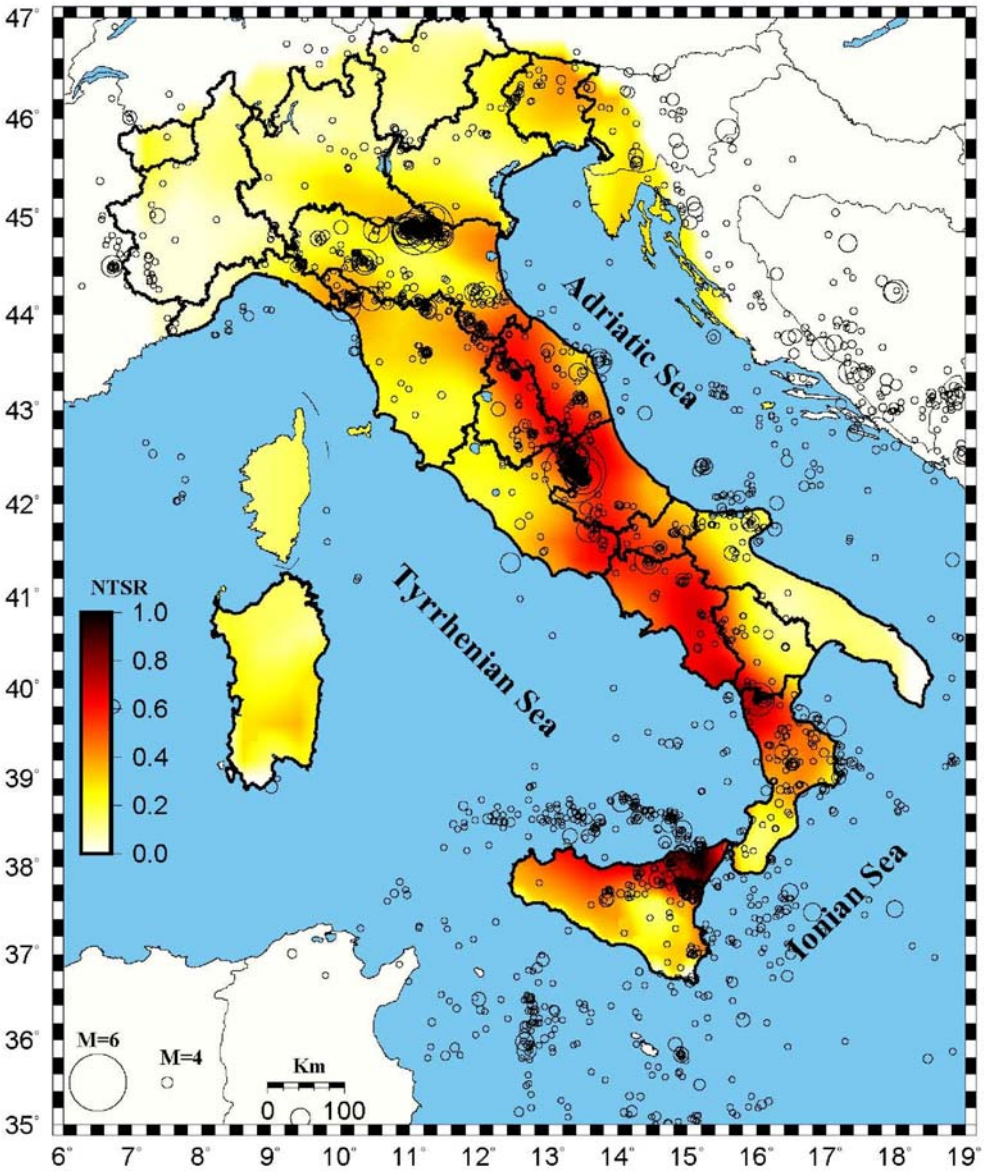

Fig. 36. *Pattern of the normalized Total Strain Rate (Fig. 35), superimposed to recent seismicity (circles) with magnitude M ≥ 3 and depth lower than 40 Km, that occurred in the Italian area from April 2005 to January 2016 (ISIDe Working Group, INGV, 2010).*

The comparison between the NTSR pattern and the seismicity distribution (Fig. 36) suggests a weak correlation between local maxima of geodetic strain rate and the location of recent earthquakes. To better explain this result, it may be useful to plot the NTSR versus earthquakes magnitude (Fig. 37). To this purpose, we have estimated the NTSR at the epicentral coordinates of each seismic event, only considering the values for which the geometrical criteria described above

are fulfilled. Figure 37 points out that for most magnitude values, the values of NTRS present a considerable spreading. This effect attenuates for magnitudes higher than 4.

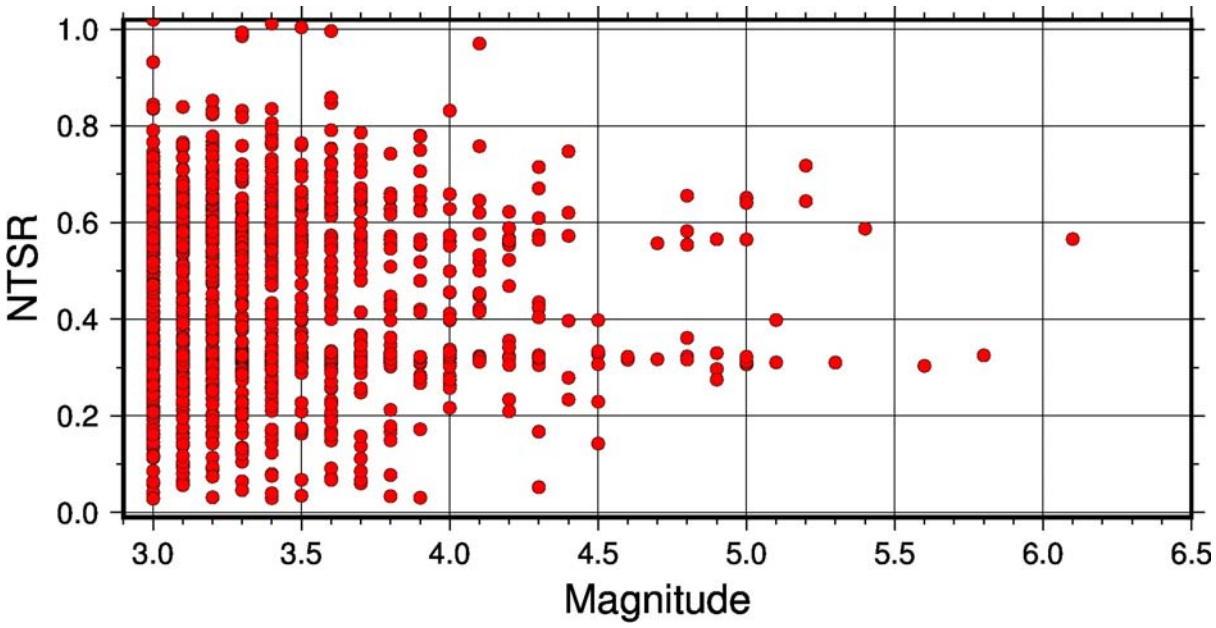

Fig.37. *Pattern of NTSR versus earthquake magnitude. See text for explanation.*

The evidence reported in this section suggests that the interpretation of the ongoing strain rate pattern in Italy for the recognition of the zones most prone to next strong shocks may be affected by significant uncertainties, which might be reduced by further investigations. As concerns geodetic observations, it has been argued that at present the best chance to gain information about future seismicity by the help of this kind of data is related with the monitoring of post seismic relaxation triggered by a strong earthquake (Cenni et al., 2015). This analysis may allow the reconstruction of the spatio-temporal development of the perturbation triggered by a strong earthquake, aimed at recognizing when the highest values of the induced strain and strain rate are expected to arrive in the seismic zones of interest. The possibility of applying the above procedure for middle-term earthquake prediction is supported by several examples of interaction between seismic sources in the central Mediterranean area (Viti et al., 2003, 2012, 2013; Mantovani et al., 2008, 2010, 2012).

12. Reliability of the proposed predictions and alternative approaches

As discussed earlier, an efficient mitigation of seismic risk in Italy can hardly be realized without a tentative recognition of few priority zones, where the very limited resources now available can be concentrated. The only doubts about the feasibility of such strategy are due to the possibility that the proposed recognition is unreliable. So, it is opportune to make some considerations about the possible uncertainties that may affect the results of the procedure here adopted.

First of all, it must be pointed out that such procedure is based on the most reliable approach, i.e. the one that takes into account the deterministic nature of earthquakes and hinges on the concept that the spatio-temporal distribution of major shocks is closely related with the short-term development of tectonic processes. The geodynamic/tectonic context here adopted s the one that best accounts for the huge amount of evidence now available about the recent evolution of the central Mediterranean area, as described in several publications (cited above). Furthermore, the reliability of such model is supported by the fact that its implications can provide plausible and coherent explanations for the distribution of the strong earthquakes that have occurred in the peri-

Adriatic regions since 1400 A.D. This important result encourages to think that the approach here adopted is plausible, but the limited length of the seismic history which can be taken as complete and reliable does not allow to remove all doubts about the validity of the proposed predictions.

Notwithstanding this uncertainty, we think that an attempt at using the proposed predictions may anyway be convenient. In case of successful recognition, the concentration of resources in the expected priority zones would have allowed a significant reduction of casualties and damages. In case of failed prediction, the resources employed in the priority zones would not be wasted, since they would have allowed a significant improvement of safety in zones which can plausibly be considered as most prone to next shocks in the Italian area. On the other hand, if a *blind* strategy (no priority zones) was alternatively adopted, each of the numerous seismic areas of Italy would only benefit from a very limited improvement of its safety.

Attempts at identifying the Italian seismic zones where the probability of earthquakes is highest have also been made by adopting alternative approaches, mainly based on statistical analysis of the seismic history (e.g., Boschi et al., 1995; Valensise and Pantosti, 2001; Valensise et al., 2003; Marzocchi, 2008; Schorlemmer et al., 2010b; Lombardi and Marzocchi, 2010; Stucchi et al., 2011). However, as discussed in detail by Mantovani et al. (2012), this kind of approach can hardly provide reliable predictions, being based on the assumption that earthquakes are casual and independent events, which is clearly incompatible with the nature of earthquakes and the recognized interaction of seismic sources. Furthermore, statistical analysis requires that seismic activity is a stationary phenomenon over time, which evidently contrasts with the spatio-temporal distribution of major earthquakes, as discussed in the previous sections.

Objections may also be raised against the deterministic approach. For instance one could deny the reliability of the tectonic setting here adopted. We think that this problem can easily be overcome by a careful reading of the numerous publications (e.g., Mantovani, 2005; Mantovani et al., 2006, 2007a,b, 2009, 2014, 2015a,b; Viti et al., 2006, 2009, 2011), which point out the compatibility of such model with the available evidence and the fact that the alternative geodynamic interpretations so far proposed in literature can hardly be reconciled with several major features of the observed deformation pattern. Anyway, to avoid that the above problem may become an obstacle towards the adoption of a very convenient strategy for the mitigation of seismic risk in Italy, the Civil Protection authorities could promote a public discussion about the reliability of the geodynamic interpretations so far presented, in order to allow the various authors to exhaustively explain the evidence and arguments in support of their view and to point out the presumed limitations of the alternative interpretations.

Appendix 1: Geodetic data

Velocities (mm/yr) of the 527 GPS sites considered in this study (Fig.8). Code = international alphanumeric code of the site. Lon (°E), Lat (°N) = station coordinates, T = observation time interval (yr). V= station velocities (mm/yr) and respective uncertainties of the North, East and Vertical components in the ITRF2008 reference frame (Altamimi et. al., 2012). Vn, Ve= horizontal velocity components (North and East) and resulting velocity (Vh) with respect to the adopted Eurasian frame (Euler pole at 54.23°N, 98.83°W, ω = 0.257°/Myr, Altamimi et al., 2012). Vv= absolute vertical velocities.

Code	Lon.	Lat.	T (yr)	V_N (mm/yr)	V_E (mm/yr)	V_h (mm/yr)	V_V (mm/yr)
ACCA	15.33	41.16	8.19	4.0 ± 0.1	1.9 ± 0.1	4.5 ± 0.1	0.2 ± 0.3
ACCE	6.99	44.48	5.69	-0.2 ± 0.1	0.9 ± 0.1	1.0 ± 0.1	-0.6 ± 0.6
ACER	15.94	40.79	8.02	4.4 ± 0.1	1.0 ± 0.1	4.5 ± 0.1	0.4 ± 0.2
ACOM	13.51	46.55	12.04	0.9 ± 0.1	0.5 ± 0.1	1.1 ± 0.1	1.4 ± 0.1
AFAL	12.17	46.53	12.07	0.7 ± 0.1	-0.3 ± 0.1	0.8 ± 0.1	1.0 ± 0.1
AGNE	7.14	45.47	7.24	0.6 ± 0.4	1.4 ± 0.5	1.5 ± 0.5	2.0 ± 1.4
AJAC	8.76	41.93	14.55	0.0 ± 0.1	-0.0 ± 0.1	0.0 ± 0.1	0.4 ± 0.2
ALAT	13.38	41.67	6.32	1.6 ± 0.5	-0.1 ± 0.4	1.6 ± 0.5	0.2 ± 1.1
ALBI	16.46	39.95	3.19	5.9 ± 1.0	-0.1 ± 0.5	5.9 ± 1.0	0.5 ± 1.6
ALIF	14.33	41.33	6.26	2.6 ± 0.1	0.5 ± 0.1	2.6 ± 0.1	-3.2 ± 0.4
ALIN	8.62	44.92	5.58	0.1 ± 0.1	0.7 ± 0.1	0.7 ± 0.1	-0.6 ± 0.5
ALRA	14.03	41.73	8.44	1.4 ± 0.4	3.0 ± 0.4	3.3 ± 0.4	1.9 ± 0.9
ALSN	8.62	44.92	4.4	0.5 ± 0.1	0.1 ± 0.1	0.5 ± 0.1	-1.9 ± 0.5
ALTA	16.56	40.82	4.13	4.8 ± 0.2	1.4 ± 0.2	5.0 ± 0.2	-0.7 ± 0.7
AMAN	16.08	39.12	3.08	4.1 ± 0.4	0.6 ± 0.5	4.1 ± 0.5	0.3 ± 1.8
AMPE	12.8	46.41	6.94	0.5 ± 0.1	0.7 ± 0.1	0.9 ± 0.1	-0.7 ± 0.4
AMUR	16.6	40.91	8.93	4.4 ± 0.1	1.3 ± 0.1	4.6 ± 0.1	0.0 ± 0.2
ANCG	13.5	43.6	7.5	3.7 ± 0.1	0.2 ± 0.1	3.7 ± 0.1	1.6 ± 0.2
ANCN	13.53	43.61	3.96	5.8 ± 0.4	1.4 ± 0.2	6.0 ± 0.3	-0.5 ± 0.5
ANGE	15.18	40.93	7.04	2.9 ± 0.1	0.5 ± 0.1	2.9 ± 0.1	0.1 ± 0.3
AO01	7.32	45.74	6.51	-0.2 ± 0.1	0.6 ± 0.1	0.6 ± 0.1	-0.0 ± 0.4
AOST	7.34	45.74	3.51	-0.2 ± 1.2	1.5 ± 0.9	1.6 ± 1.0	2.9 ± 2.8
APRI	12.66	41.6	7.23	-0.1 ± 0.1	-0.4 ± 0.3	0.4 ± 0.3	0.2 ± 0.5
AQRA	13.37	42.37	9.07	1.7 ± 0.1	-0.3 ± 0.2	1.7 ± 0.2	-0.9 ± 0.6
AQSA	16.08	39.72	2.9	3.3 ± 0.7	-0.1 ± 0.8	3.3 ± 0.7	0.1 ± 2.0
AQUI	13.35	42.37	14.55	2.2 ± 0.1	0.5 ± 0.1	2.2 ± 0.1	-0.2 ± 0.2
AQUM	13.47	42.33	4.02	2.1 ± 0.4	0.0 ± 0.4	2.1 ± 0.4	-3.6 ± 0.9
ARBU	8.59	39.52	5.66	1.6 ± 0.4	0.7 ± 0.9	1.8 ± 0.5	-2.3 ± 2.0
ARCA	16.23	39.37	7.05	3.6 ± 0.1	1.8 ± 0.1	4.0 ± 0.1	-1.3 ± 0.3
ASCC	13.59	42.86	6.63	2.8 ± 0.3	1.8 ± 0.3	3.4 ± 0.3	0.3 ± 0.8
ASCG	13.61	42.85	3.52	4.2 ± 1.1	2.4 ± 0.9	4.8 ± 1.0	0.4 ± 3.2
ASIA	11.53	45.87	6.9	0.8 ± 0.2	0.2 ± 0.2	0.8 ± 0.2	0.6 ± 0.7
ASTI	8.2	44.91	5.29	0.4 ± 0.2	0.8 ± 0.2	0.9 ± 0.3	-2.1 ± 0.8
ATBU	12.55	43.48	5.22	2.9 ± 0.1	0.7 ± 0.1	3.0 ± 0.1	0.7 ± 0.4
ATFO	12.57	43.37	6.03	3.5 ± 0.5	2.1 ± 0.4	4.1 ± 0.5	1.7 ± 0.7
ATLO	12.41	43.32	5.32	1.7 ± 0.1	-0.1 ± 0.1	1.7 ± 0.1	0.6 ± 0.4
ATMI	12.27	43.33	3.48	1.4 ± 0.8	0.8 ± 0.8	1.6 ± 0.8	3.5 ± 1.8
ATTE	12.35	43.2	5.32	1.4 ± 0.1	0.1 ± 0.2	1.4 ± 0.2	0.9 ± 0.5
AV04	15.44	40.9	5.56	4.4 ± 0.1	1.1 ± 0.1	4.5 ± 0.1	0.5 ± 0.4
AVEL	14.78	40.91	6.54	1.9 ± 0.3	-0.1 ± 0.2	1.9 ± 0.3	-2.3 ± 1.4
AVZZ	13.45	42.03	3.52	4.0 ± 0.9	0.2 ± 0.9	4.0 ± 0.9	-0.8 ± 3.6
BAJA	7.72	43.9	4.71	0.8 ± 0.1	1.6 ± 0.1	1.8 ± 0.1	-2.5 ± 0.4
BARC	12.56	46.19	6.94	2.2 ± 0.2	0.9 ± 0.2	2.4 ± 0.2	-1.2 ± 0.8
BARS	13.58	42.34	4.81	2.3 ± 0.2	-0.3 ± 0.2	2.3 ± 0.2	1.1 ± 0.7
BART	15.02	41.41	3.11	3.7 ± 0.4	1.0 ± 0.4	3.9 ± 0.5	-0.0 ± 1.8
BATE	12.19	43.71	12.06	1.9 ± 0.1	0.7 ± 0.1	2.0 ± 0.1	1.1 ± 0.1

Code	Lon.	Lat.	T (yr)	V_N (mm/yr)	V_E (mm/yr)	V_h (mm/yr)	V_V (mm/yr)
BERT	12.13	44.15	5.81	3.6 ± 0.1	1.8 ± 0.1	4.0 ± 0.1	-1.2 ± 0.3
BEVA	13.07	45.67	6.94	2.6 ± 0.2	-0.0 ± 0.2	2.6 ± 0.2	-2.0 ± 0.9
BEVE	9.77	44.19	5.62	0.0 ± 0.1	0.5 ± 0.1	0.5 ± 0.1	-1.6 ± 0.4
BGDR	11.89	43.89	2.98	2.6 ± 0.8	0.4 ± 1.1	2.6 ± 0.8	2.3 ± 3.2
BIEL	8.05	45.56	11.43	0.0 ± 0.1	0.4 ± 0.1	0.4 ± 0.1	-1.0 ± 1.3
BL01	12.2	46.14	7.28	1.5 ± 0.4	0.2 ± 0.2	1.5 ± 0.3	1.4 ± 0.6
BLGN	11.35	44.51	6.92	2.3 ± 0.2	2.0 ± 0.2	3.1 ± 0.2	-2.7 ± 0.8
BLRA	13.56	41.81	8.53	1.3 ± 0.4	-0.8 ± 0.7	1.5 ± 0.5	0.7 ± 0.9
BO01	11.32	44.49	9.22	1.9 ± 0.2	1.3 ± 0.2	2.3 ± 0.2	-2.0 ± 0.7
BOBB	9.38	44.77	6.51	1.2 ± 0.3	0.6 ± 0.2	1.3 ± 0.3	0.1 ± 0.7
BOLG	11.36	44.5	10.55	4.4 ± 0.2	0.5 ± 0.2	4.4 ± 0.2	-3.1 ± 0.9
BOLO	11.33	44.49	7.49	2.7 ± 0.3	1.7 ± 0.2	3.2 ± 0.3	0.3 ± 0.7
BOLZ	11.37	46.5	3.52	0.7 ± 0.3	0.2 ± 0.4	0.7 ± 0.3	2.0 ± 1.1
BORC	12.22	46.44	6.32	0.7 ± 0.1	0.2 ± 0.1	0.7 ± 0.1	0.6 ± 0.4
BORR	10.7	44.31	7.08	1.1 ± 0.2	1.7 ± 0.2	2.1 ± 0.2	1.2 ± 0.9
BOSC	11.03	45.6	6.07	0.4 ± 0.2	0.5 ± 0.2	0.6 ± 0.2	-0.3 ± 0.5
BOVA	15.91	37.94	3.08	3.4 ± 1.1	-0.5 ± 0.5	3.5 ± 1.1	-1.3 ± 1.7
BRAS	11.11	44.12	14.55	1.6 ± 0.1	0.6 ± 0.1	1.7 ± 0.1	0.8 ± 0.1
BRBZ	11.94	46.8	4.54	0.6 ± 0.2	0.1 ± 0.1	0.6 ± 0.2	0.4 ± 0.6
BRIS	11.77	44.22	5.14	4.1 ± 0.2	0.8 ± 0.2	4.2 ± 0.2	-1.2 ± 0.7
BRSE	12.08	46.1	4.02	1.8 ± 0.4	-1.3 ± 0.3	2.2 ± 0.3	1.3 ± 0.8
BRU1	9.72	44.24	4.12	0.4 ± 0.2	0.4 ± 0.2	0.6 ± 0.2	-0.8 ± 0.9
BSSO	14.59	41.55	9.51	3.1 ± 0.1	1.0 ± 0.1	3.3 ± 0.1	-0.6 ± 0.2
BTAC	11.28	45.26	7.04	2.1 ± 0.2	0.5 ± 0.1	2.2 ± 0.2	-6.1 ± 0.6
BUCU	26.13	44.46	14.55	-1.1 ± 0.1	-0.3 ± 0.1	1.2 ± 0.1	2.4 ± 0.1
BULG	15.38	40.08	8.59	2.5 ± 0.1	-0.1 ± 0.1	2.5 ± 0.1	0.3 ± 0.1
BUSL	7.15	45.14	4.4	-0.5 ± 0.3	0.4 ± 0.2	0.6 ± 0.3	-0.7 ± 0.8
BUTE	19.06	47.48	7.55	-0.4 ± 0.1	0.8 ± 0.2	0.9 ± 0.2	1.4 ± 0.8
BZRG	11.34	46.5	13.04	0.6 ± 0.1	-0.1 ± 0.1	0.6 ± 0.1	0.9 ± 0.2
CA02	9	39.01	6.49	0.4 ± 0.1	0.3 ± 0.1	0.5 ± 0.1	-1.9 ± 0.4
CA04	9.13	39.54	5.81	0.4 ± 0.1	0.2 ± 0.1	0.5 ± 0.1	-1.6 ± 0.4
CA05	9.12	39.24	4.39	0.7 ± 0.2	0.2 ± 0.2	0.7 ± 0.2	-0.9 ± 0.5
CAFE	15.24	41.03	9.55	3.3 ± 0.1	0.2 ± 0.1	3.3 ± 0.1	1.2 ± 0.1
CAFI	11.97	43.33	7.78	2.0 ± 0.1	0.4 ± 0.1	2.1 ± 0.1	0.2 ± 0.2
CAFV	11.94	45.67	3.36	1.9 ± 0.3	0.7 ± 0.3	2.0 ± 0.3	-0.2 ± 0.8
CAKO	16.44	46.39	3.81	1.0 ± 0.2	1.3 ± 0.3	1.7 ± 0.3	-0.0 ± 0.7
CALA	11.16	43.87	7.55	1.7 ± 0.1	1.4 ± 0.1	2.2 ± 0.2	-0.1 ± 0.9
CAMN	8.28	44.41	5.6	-0.2 ± 0.1	0.7 ± 0.1	0.7 ± 0.1	-0.7 ± 0.4
CAMP	12.74	37.63	3.55	3.9 ± 0.4	-1.4 ± 0.4	4.1 ± 0.3	0.1 ± 1.1
CAMU	11.98	43.26	6.95	1.8 ± 0.2	0.4 ± 0.3	1.8 ± 0.2	-0.5 ± 0.6
CANL	8.29	44.72	4.4	0.1 ± 0.2	0.6 ± 0.1	0.7 ± 0.2	-1.2 ± 0.6
CANV	12.44	46.01	11.16	1.4 ± 0.4	0.3 ± 0.3	1.5 ± 0.3	-0.1 ± 0.2
CAOC	13.48	42.29	4.8	1.1 ± 0.2	-1.4 ± 0.2	1.7 ± 0.2	-1.3 ± 0.6
CAR1	16.21	39.25	6.07	3.5 ± 0.1	0.6 ± 0.1	3.6 ± 0.1	0.4 ± 0.4
CARG	10.32	44.11	11.56	0.7 ± 0.1	0.5 ± 0.1	0.9 ± 0.1	-0.4 ± 0.3
CARI	13.97	41.19	6.52	2.2 ± 0.1	-0.7 ± 0.1	2.3 ± 0.1	-0.6 ± 0.4
CARP	10.43	45.37	7.53	0.4 ± 0.2	0.3 ± 0.2	0.5 ± 0.3	-0.1 ± 0.8
CARZ	8.68	46.04	7.27	0.2 ± 0.1	0.2 ± 0.1	0.3 ± 0.1	0.1 ± 0.2
CASG	14.94	40.27	6.04	2.0 ± 0.1	-0.1 ± 0.1	2.0 ± 0.1	-1.6 ± 0.4
CASP	10.87	42.79	8.1	1.2 ± 0.1	-0.6 ± 0.1	1.4 ± 0.1	0.3 ± 0.3
CAST	10.41	44.43	8.33	2.4 ± 0.2	0.8 ± 0.2	2.6 ± 0.2	-0.1 ± 0.7
CATU	9.12	45.74	3.52	0.5 ± 0.3	0.1 ± 0.3	0.5 ± 0.3	1.0 ± 1.1
CCAS	14.94	40.27	6.04	1.6 ± 0.5	-0.6 ± 0.2	1.8 ± 0.5	-0.3 ± 1.2
CDRA	13.72	42.37	8.62	3.7 ± 0.4	0.1 ± 0.4	3.7 ± 0.4	-2.0 ± 1.4
CDRU	15.3	40.49	8.88	1.7 ± 0.1	-1.2 ± 0.1	2.1 ± 0.1	0.1 ± 0.2
CECI	10.53	43.31	5.57	1.0 ± 0.2	0.3 ± 0.2	1.0 ± 0.2	-0.2 ± 0.8
CELI	16.51	39.4	3.75	3.9 ± 0.3	0.8 ± 0.3	4.0 ± 0.3	1.0 ± 1.0
CERA	14.02	41.6	9	3.5 ± 0.1	1.6 ± 0.1	3.9 ± 0.1	1.1 ± 0.1
CERT	12.98	41.95	9.29	1.4 ± 0.1	-0.6 ± 0.1	1.5 ± 0.1	0.1 ± 0.2

Code	Lon.	Lat.	T (yr)	V_N (mm/yr)	V_E (mm/yr)	V_h (mm/yr)	V_V (mm/yr)
CESI	12.9	43.01	8.4	2.5 ± 0.3	0.4 ± 0.2	2.5 ± 0.3	1.3 ± 0.8
CGIA	12.27	45.21	4.55	1.2 ± 0.2	-0.7 ± 0.2	1.4 ± 0.2	-5.9 ± 0.6
CHAT	7.62	45.75	3.52	-1.0 ± 0.6	-0.2 ± 0.4	1.0 ± 0.5	2.1 ± 1.2
CHIA	9.4	46.32	7.62	0.5 ± 0.2	0.4 ± 0.1	0.7 ± 0.2	1.3 ± 0.5
CHIG	11.28	45.54	3.52	0.2 ± 0.4	0.4 ± 0.4	0.4 ± 0.4	-1.8 ± 1.1
CHIV	9.32	44.32	5.59	0.1 ± 0.1	0.5 ± 0.1	0.5 ± 0.1	-2.1 ± 0.4
CIPV	12.01	42.95	4.4	1.3 ± 0.3	0.3 ± 0.2	1.3 ± 0.3	0.2 ± 0.9
CIT1	12.25	43.47	5.32	1.9 ± 0.2	0.1 ± 0.2	1.9 ± 0.2	-0.3 ± 0.9
CITT	11.79	45.64	6.39	1.7 ± 0.3	-0.2 ± 0.3	1.7 ± 0.3	-0.6 ± 0.9
CIUF	11.63	43.58	3.47	2.5 ± 0.4	0.2 ± 0.5	2.5 ± 0.5	-1.7 ± 1.4
CODD	12.11	44.84	3.81	2.0 ± 0.2	0.0 ± 0.1	2.0 ± 0.2	-6.1 ± 0.6
CODI	12.11	44.84	7.91	2.0 ± 0.1	1.0 ± 0.1	2.3 ± 0.1	-2.5 ± 0.4
CODR	12.98	45.96	8.05	2.1 ± 0.1	0.4 ± 0.1	2.1 ± 0.1	0.7 ± 0.3
COLI	9.38	46.14	7.55	0.7 ± 0.2	0.3 ± 0.2	0.8 ± 0.2	-1.2 ± 0.7
COLL	10.22	44.75	7.93	2.6 ± 0.1	1.3 ± 0.1	2.9 ± 0.1	-0.5 ± 0.3
COLR	16.42	40.19	3.84	5.1 ± 0.2	1.0 ± 0.2	5.2 ± 0.2	0.3 ± 0.8
COMO	9.1	45.8	13.25	0.2 ± 0.1	0.3 ± 0.1	0.3 ± 0.1	0.2 ± 0.2
CONC	11.01	44.92	3.52	3.5 ± 0.8	0.8 ± 0.4	3.6 ± 0.8	0.3 ± 1.6
CONI	13.39	42.41	6.22	0.7 ± 0.1	0.8 ± 0.1	1.1 ± 0.1	-1.4 ± 0.4
CONS	11.83	44.52	7.1	3.2 ± 0.1	1.3 ± 0.1	3.4 ± 0.1	-7.1 ± 0.4
CORL	13.3	37.89	9.05	3.8 ± 0.1	-1.1 ± 0.1	4.0 ± 0.1	0.7 ± 0.1
CRAC	16.44	40.38	9.55	4.3 ± 0.1	1.1 ± 0.1	4.5 ± 0.1	1.1 ± 0.1
CREA	9.69	45.35	9.44	0.8 ± 0.1	0.5 ± 0.1	1.0 ± 0.1	-0.9 ± 0.2
CREM	10	45.15	9.54	1.1 ± 0.1	0.6 ± 0.1	1.2 ± 0.1	-0.3 ± 0.1
CRMI	10.98	43.8	8.76	1.8 ± 0.1	1.2 ± 0.1	2.1 ± 0.1	-0.3 ± 0.2
CRSN	8.11	45.19	4.4	0.4 ± 0.1	-0.1 ± 0.1	0.4 ± 0.1	-0.2 ± 0.6
CSSB	12.25	43.21	9.06	1.7 ± 0.1	0.4 ± 0.1	1.8 ± 0.1	0.8 ± 0.2
CTMG	11.38	44.57	5.81	3.2 ± 0.4	3.7 ± 0.4	4.9 ± 0.4	-3.1 ± 1.4
CUOR	7.65	45.39	4.4	-0.0 ± 0.2	0.2 ± 0.2	0.2 ± 0.2	-0.1 ± 0.6
DEMN	7.29	44.32	4.4	-0.5 ± 0.4	0.8 ± 0.3	0.9 ± 0.3	-0.2 ± 1.4
DEVE	8.26	46.31	7.29	0.2 ± 0.1	0.4 ± 0.1	0.4 ± 0.1	1.2 ± 0.4
DOMS	8.29	46.12	4.4	-0.4 ± 0.2	-0.3 ± 0.2	0.5 ± 0.2	0.4 ± 0.8
DUB2	18.11	42.65	3.57	2.4 ± 0.7	1.0 ± 0.6	2.6 ± 0.6	0.8 ± 1.8
EDEN	14.3	37.52	4.2	4.9 ± 0.5	0.5 ± 0.5	4.9 ± 0.5	-0.4 ± 1.4
EIIV	15.08	37.51	9.54	2.5 ± 0.2	0.0 ± 0.1	2.5 ± 0.2	1.4 ± 0.4
ELBA	10.21	42.75	14.55	0.5 ± 0.1	-0.3 ± 0.1	0.6 ± 0.1	-0.1 ± 0.1
FAEZ	11.86	44.3	7.11	3.8 ± 0.3	1.2 ± 0.2	4.0 ± 0.3	-3.9 ± 0.7
FASA	17.36	40.83	8.33	4.2 ± 0.1	1.4 ± 0.1	4.4 ± 0.1	-0.7 ± 0.4
FDOS	11.72	46.3	4.75	0.3 ± 0.2	0.1 ± 0.1	0.3 ± 0.2	-0.5 ± 0.6
FERA	11.63	44.81	7.55	2.2 ± 0.1	0.9 ± 0.1	2.4 ± 0.1	0.1 ± 0.5
FERR	11.6	44.83	7.98	1.8 ± 0.1	1.0 ± 0.1	2.1 ± 0.1	0.4 ± 0.4
FIAN	12.59	42.16	3.45	1.7 ± 0.4	-0.7 ± 0.3	1.8 ± 0.3	-0.5 ± 0.9
FIGL	11.47	43.62	7.55	2.2 ± 0.1	0.6 ± 0.1	2.3 ± 0.1	-0.3 ± 0.2
FIOR	11.59	42.83	3.52	2.0 ± 0.6	-0.3 ± 0.6	2.0 ± 0.6	-1.6 ± 1.7
FIRE	11.38	44.12	7.55	2.6 ± 0.2	-0.0 ± 0.2	2.6 ± 0.2	1.0 ± 0.6
FISC	14.79	40.77	4.06	1.7 ± 0.4	-1.1 ± 0.4	2.1 ± 0.4	-1.4 ± 0.9
FOGG	15.53	41.45	8.09	4.0 ± 0.1	1.7 ± 0.1	4.3 ± 0.1	-0.3 ± 0.4
FOL1	12.7	42.95	7.55	2.6 ± 0.1	0.3 ± 0.2	2.6 ± 0.1	-0.2 ± 0.4
FOND	13.41	41.33	3.51	0.3 ± 0.7	-1.1 ± 0.5	1.1 ± 0.5	1.2 ± 1.1
FORL	12.07	44.2	4.45	3.9 ± 0.3	2.2 ± 0.4	4.5 ± 0.3	-4.2 ± 0.9
FOSS	12.81	43.69	7.55	3.2 ± 0.2	2.0 ± 0.3	3.8 ± 0.2	0.7 ± 1.1
FRES	14.67	41.97	8.84	3.1 ± 0.1	1.6 ± 0.1	3.5 ± 0.1	0.6 ± 0.4
FRMO	13.73	43.17	5.83	3.6 ± 0.5	1.6 ± 0.3	3.9 ± 0.5	0.2 ± 0.9
FRRA	14.29	42.42	8.71	3.9 ± 0.2	1.5 ± 0.1	4.2 ± 0.2	-1.5 ± 0.5
FUSE	13	46.41	7.85	1.1 ± 0.1	0.5 ± 0.1	1.2 ± 0.1	-0.5 ± 0.2
FVRA	13.67	37.32	5.77	3.2 ± 0.2	-1.6 ± 0.2	3.6 ± 0.2	0.3 ± 0.7
GALF	14.57	37.71	8.63	4.1 ± 0.1	-2.3 ± 0.1	4.6 ± 0.1	0.9 ± 0.1
GARI	12.25	44.68	6	1.6 ± 0.1	1.4 ± 0.1	2.2 ± 0.1	-4.9 ± 0.4
GATE	14.91	41.51	6.05	3.6 ± 0.1	0.8 ± 0.1	3.7 ± 0.1	0.7 ± 0.4

Code	Lon.	Lat.	T (yr)	V_N (mm/yr)	V_E (mm/yr)	V_h (mm/yr)	V_V (mm/yr)
GAVO	10.89	42.94	6.66	1.7 ± 0.4	-0.2 ± 0.2	1.8 ± 0.4	0.9 ± 1.2
GAZZ	9.83	45.79	6.66	0.1 ± 0.2	0.1 ± 0.2	0.2 ± 0.2	-0.0 ± 0.8
GBLM	14.03	37.99	10.45	5.3 ± 0.2	-0.3 ± 0.1	5.3 ± 0.2	0.6 ± 0.4
GENO	8.92	44.42	14.55	-0.0 ± 0.1	0.6 ± 0.1	0.6 ± 0.1	-0.4 ± 0.1
GENU	8.96	44.4	5.6	0.2 ± 0.1	0.6 ± 0.1	0.7 ± 0.1	-2.2 ± 0.4
GEOT	13.51	43.57	3.52	3.4 ± 0.5	1.4 ± 0.4	3.6 ± 0.5	1.8 ± 1.2
GINE	13.38	43.12	3.52	4.0 ± 0.4	2.2 ± 0.4	4.6 ± 0.4	-2.1 ± 1.3
GINO	16.76	40.58	7.47	4.3 ± 0.1	1.8 ± 0.1	4.7 ± 0.1	0.4 ± 0.4
GIOI	15.89	38.42	7.05	3.5 ± 0.2	1.5 ± 0.2	3.8 ± 0.2	-0.2 ± 0.7
GIUR	18.43	40.12	7.47	3.7 ± 0.1	1.1 ± 0.1	3.9 ± 0.1	-1.2 ± 0.4
GNAL	13.52	42.58	4.55	2.3 ± 0.2	1.2 ± 0.2	2.6 ± 0.2	0.7 ± 0.6
GODE	12.38	45.93	3.52	1.0 ± 0.4	0.0 ± 0.3	1.0 ± 0.3	-3.0 ± 0.9
GORI	13.62	45.94	6.94	2.8 ± 0.3	0.0 ± 0.3	2.8 ± 0.3	-0.6 ± 1.1
GOZZ	8.43	45.75	4.4	0.3 ± 0.1	-0.0 ± 0.1	0.3 ± 0.1	-0.3 ± 0.5
GRAM	13.87	42.98	7.04	2.3 ± 0.3	1.6 ± 0.2	2.8 ± 0.3	0.2 ± 0.7
GRAS	6.92	43.75	14.55	-0.1 ± 0.1	1.0 ± 0.1	1.0 ± 0.1	-0.9 ± 0.2
GRAZ	15.49	47.07	14.52	0.5 ± 0.1	0.8 ± 0.1	1.0 ± 0.1	0.2 ± 0.2
GRO1	15.1	41.07	6.73	2.9 ± 0.3	0.2 ± 0.1	2.9 ± 0.3	1.0 ± 0.9
GROA	11.11	42.78	6.64	0.5 ± 0.1	-0.2 ± 0.1	0.6 ± 0.1	0.8 ± 0.5
GROG	9.89	43.43	8.99	0.6 ± 0.1	0.5 ± 0.1	0.8 ± 0.1	-0.9 ± 0.1
GROT	15.06	41.07	10.15	2.9 ± 0.1	0.3 ± 0.1	2.9 ± 0.2	1.1 ± 0.5
GRZM	11.15	44.26	7.23	2.6 ± 0.2	1.1 ± 0.2	2.8 ± 0.2	1.1 ± 0.9
GSR1	14.54	46.05	14.48	2.1 ± 0.1	0.0 ± 0.1	2.1 ± 0.1	-0.1 ± 0.1
GUAR	13.31	41.79	9.13	2.1 ± 0.2	0.9 ± 0.2	2.2 ± 0.2	2.7 ± 0.7
GUB2	12.58	43.35	7.55	2.0 ± 0.1	0.5 ± 0.1	2.1 ± 0.1	-0.4 ± 0.4
GUMA	13.34	43.06	7.27	3.9 ± 0.2	2.0 ± 0.2	4.4 ± 0.2	0.8 ± 0.7
HELM	12.38	46.72	3.26	0.7 ± 0.4	-0.6 ± 0.4	0.9 ± 0.4	-1.2 ± 1.0
HMDC	14.78	36.96	9.05	4.5 ± 0.1	-1.3 ± 0.2	4.6 ± 0.2	-1.2 ± 0.6
IENG	7.64	45.02	11.62	-0.4 ± 0.1	0.6 ± 0.1	0.7 ± 0.1	0.2 ± 0.1
IGLE	8.53	39.31	7.05	0.7 ± 0.4	1.0 ± 0.2	1.2 ± 0.3	1.3 ± 0.8
IGMI	11.21	43.8	8.61	2.3 ± 0.1	0.9 ± 0.1	2.5 ± 0.1	-1.2 ± 0.2
IMOL	11.71	44.35	3.14	4.3 ± 0.3	1.2 ± 0.3	4.5 ± 0.3	-2.2 ± 0.9
IMP3	8.01	43.87	5	-0.8 ± 0.3	0.5 ± 0.2	0.9 ± 0.3	-0.1 ± 0.7
INGR	12.51	41.83	13.47	1.3 ± 0.1	-0.5 ± 0.1	1.4 ± 0.1	-0.7 ± 0.2
ISCH	15.9	41.9	7.98	3.6 ± 0.1	1.5 ± 0.1	3.9 ± 0.1	-0.3 ± 0.6
ISER	14.24	41.6	6.99	2.9 ± 0.2	0.4 ± 0.3	2.9 ± 0.3	1.2 ± 0.9
ITGT	12.78	43.23	8.15	3.4 ± 0.1	1.5 ± 0.1	3.7 ± 0.1	-0.1 ± 0.3
ITIM	11.72	44.35	8.37	3.1 ± 0.2	2.1 ± 0.1	3.8 ± 0.2	-1.3 ± 0.5
ITRA	14	42.66	5.8	4.3 ± 0.1	2.0 ± 0.1	4.8 ± 0.1	-2.0 ± 0.4
ITRN	12.58	44.05	7.32	3.7 ± 0.1	1.3 ± 0.3	3.9 ± 0.2	-0.9 ± 0.4
JOAN	13.42	46.18	8.06	1.8 ± 0.1	0.2 ± 0.1	1.8 ± 0.1	-0.8 ± 0.1
JOPP	15.89	38.61	8.86	3.3 ± 0.1	1.4 ± 0.1	3.6 ± 0.1	0.7 ± 0.2
KNJA	22.26	43.57	3.18	-1.8 ± 0.7	0.8 ± 0.7	2.0 ± 0.7	1.6 ± 2.0
LAGA	10.95	44.08	8.39	1.5 ± 0.1	0.6 ± 0.1	1.6 ± 0.1	-1.4 ± 0.2
LAME	16.23	38.88	3.08	3.9 ± 0.5	0.6 ± 0.4	4.0 ± 0.5	2.1 ± 1.8
LAMP	12.61	35.5	14.55	2.9 ± 0.1	-2.7 ± 0.1	4.0 ± 0.1	0.2 ± 0.1
LANC	14.38	42.2	3.51	3.7 ± 0.4	1.2 ± 0.4	3.9 ± 0.4	-0.0 ± 1.3
LANU	9.55	39.88	7.29	-0.4 ± 0.2	0.0 ± 0.2	0.4 ± 0.2	-0.2 ± 0.7
LARI	14.92	41.81	7.53	3.8 ± 0.1	1.8 ± 0.1	4.2 ± 0.1	-1.0 ± 0.4
LASP	9.84	44.07	9.07	0.7 ± 0.1	0.7 ± 0.1	0.9 ± 0.1	-0.3 ± 0.2
LAT1	12.9	41.47	7.54	0.5 ± 0.1	-1.4 ± 0.1	1.5 ± 0.1	-1.0 ± 0.9
LDNS	10.83	45.17	3.14	0.8 ± 0.8	0.5 ± 0.7	1.0 ± 0.8	0.0 ± 1.8
LEGN	11.27	45.18	6.47	1.8 ± 0.2	0.8 ± 0.2	2.0 ± 0.2	0.3 ± 0.6
LERO	11.96	45.35	5.72	0.7 ± 0.1	1.0 ± 0.1	1.2 ± 0.1	-1.8 ± 0.4
LINZ	14.28	48.31	7.55	0.2 ± 0.1	0.3 ± 0.1	0.4 ± 0.1	-0.3 ± 0.4
LMPR	10.89	43.81	3.46	2.2 ± 0.4	0.5 ± 0.4	2.3 ± 0.4	-0.2 ± 1.2
LNSS	13.04	42.6	9.14	2.0 ± 0.1	0.1 ± 0.1	2.0 ± 0.1	-0.5 ± 0.4
LOAN	8.25	44.12	5.6	-0.1 ± 0.1	0.5 ± 0.1	0.5 ± 0.1	-1.7 ± 0.4
LOCR	16.24	38.24	2.84	3.9 ± 0.7	0.5 ± 0.7	3.9 ± 0.7	0.4 ± 1.9

Code	Lon.	Lat.	T (yr)	V_N (mm/yr)	V_E (mm/yr)	V_h (mm/yr)	V_V (mm/yr)
LPEL	14.18	42.05	7.26	3.8 ± 0.2	3.7 ± 0.4	5.3 ± 0.3	-1.4 ± 0.8
LUCE	15.34	41.51	4.13	3.9 ± 0.2	1.0 ± 0.2	4.1 ± 0.2	-0.6 ± 0.7
M0SE	12.49	41.89	10.76	1.1 ± 0.1	-0.8 ± 0.1	1.4 ± 0.1	-1.2 ± 0.5
MABZ	10.55	46.69	4.55	0.3 ± 0.2	0.6 ± 0.2	0.7 ± 0.2	2.0 ± 0.6
MACE	13.45	43.29	7.55	3.1 ± 0.2	2.0 ± 0.2	3.7 ± 0.2	-0.5 ± 0.6
MACO	8.77	40.27	7.55	1.0 ± 0.1	0.2 ± 0.1	1.0 ± 0.1	-0.4 ± 0.2
MADA	10.37	43.75	6.39	0.6 ± 0.2	0.3 ± 0.1	0.7 ± 0.2	-0.2 ± 0.7
MAGL	13.59	43.14	3.52	3.7 ± 0.4	2.5 ± 0.4	4.5 ± 0.4	-2.3 ± 1.3
MANO	14.06	42.27	3.1	4.2 ± 0.4	0.1 ± 0.4	4.2 ± 0.4	-4.8 ± 1.8
MANT	10.79	45.16	9.54	0.9 ± 0.1	0.6 ± 0.1	1.0 ± 0.1	0.0 ± 0.2
MAON	11.13	42.43	9.22	0.6 ± 0.1	-0.3 ± 0.1	0.7 ± 0.1	-0.2 ± 0.4
MARG	9.77	45.57	3.4	-0.3 ± 0.3	-0.5 ± 0.3	0.6 ± 0.3	2.0 ± 1.1
MARI	11.87	42.04	3.52	1.4 ± 0.3	-0.8 ± 0.4	1.7 ± 0.3	-0.2 ± 1.7
MARO	11.67	45.75	3.52	0.7 ± 0.2	-0.3 ± 0.3	0.7 ± 0.3	-0.8 ± 1.0
MARS	5.35	43.28	14.55	-0.3 ± 0.1	0.4 ± 0.1	0.5 ± 0.1	-0.9 ± 0.4
MAT1	16.7	40.65	14.2	3.7 ± 0.1	1.1 ± 0.1	3.9 ± 0.1	0.4 ± 0.2
MATE	16.7	40.65	14.55	4.1 ± 0.1	0.8 ± 0.1	4.2 ± 0.1	0.4 ± 0.1
MATG	16.7	40.65	3.46	5.4 ± 0.3	0.6 ± 0.2	5.4 ± 0.3	-1.0 ± 0.8
MCEL	15.8	40.33	8.59	4.5 ± 0.1	0.7 ± 0.1	4.6 ± 0.1	0.7 ± 0.2
MCIN	11.49	43.06	5.24	1.5 ± 0.3	0.0 ± 0.2	1.5 ± 0.3	-0.9 ± 0.9
MCRV	15.17	40.78	9.99	2.8 ± 0.1	0.2 ± 0.1	2.8 ± 0.1	1.5 ± 0.2
MDEA	13.44	45.92	12.48	2.4 ± 0.1	0.1 ± 0.1	2.4 ± 0.1	0.5 ± 0.4
MEDI	11.65	44.52	14.55	1.9 ± 0.1	1.7 ± 0.3	2.5 ± 0.2	-1.6 ± 0.3
MELA	15.13	41.71	7.52	3.3 ± 0.1	0.6 ± 0.1	3.4 ± 0.1	0.0 ± 0.2
MFUS	14.83	41.06	3.67	3.2 ± 0.4	-1.2 ± 0.2	3.4 ± 0.3	-1.8 ± 1.0
MGAB	12.11	42.91	7.29	1.6 ± 0.1	-0.5 ± 0.1	1.6 ± 0.1	1.1 ± 0.2
MILA	9.23	45.48	9.55	0.6 ± 0.1	0.4 ± 0.1	0.7 ± 0.1	-0.1 ± 0.2
MITT	11.29	46.69	2.94	1.6 ± 0.8	-0.3 ± 0.6	1.6 ± 0.7	0.3 ± 2.0
MLAG	12.78	43.43	2.91	5.2 ± 0.6	2.8 ± 0.8	5.9 ± 0.6	2.1 ± 1.6
MLFT	16.6	41.2	4.47	4.1 ± 0.2	0.7 ± 0.2	4.2 ± 0.2	-1.3 ± 0.6
MMNO	15.97	39.87	3.83	2.9 ± 1.0	-1.3 ± 1.2	3.2 ± 1.0	2.2 ± 1.8
MNIA	16.69	40.36	2.9	4.4 ± 0.4	0.4 ± 0.4	4.4 ± 0.4	-0.1 ± 1.4
MO01	10.9	44.64	9.21	2.7 ± 0.1	1.6 ± 0.1	3.1 ± 0.1	-3.4 ± 0.4
MO02	10.83	44.34	12.3	2.9 ± 0.1	1.8 ± 0.1	3.4 ± 0.1	0.6 ± 0.2
MO03	10.62	44.36	9.22	3.3 ± 0.1	1.4 ± 0.1	3.6 ± 0.1	0.4 ± 0.4
MO05	11.29	44.84	9.01	1.7 ± 0.1	0.4 ± 0.1	1.7 ± 0.1	-0.3 ± 0.3
MOCA	11.14	46.1	3.36	1.4 ± 0.4	1.3 ± 0.4	1.9 ± 0.5	0.6 ± 1.6
MOCO	15.16	41.37	8.75	4.0 ± 0.1	0.9 ± 0.1	4.1 ± 0.1	0.4 ± 0.4
MODE	10.95	44.63	8.62	3.2 ± 0.1	0.9 ± 0.1	3.3 ± 0.1	-3.2 ± 0.2
MODR	13.88	41.15	8.93	1.7 ± 0.1	-1.1 ± 0.1	2.0 ± 0.1	0.5 ± 0.1
MOGG	13.2	46.41	6.93	1.1 ± 0.1	0.5 ± 0.1	1.2 ± 0.1	-0.7 ± 0.4
MOIE	13.12	43.5	8.5	3.5 ± 0.5	2.1 ± 0.2	4.1 ± 0.4	-1.7 ± 1.0
MONC	7.93	45.07	9.24	0.0 ± 0.1	0.8 ± 0.1	0.8 ± 0.1	-1.0 ± 0.1
MONF	8.45	45.13	3.52	0.8 ± 0.4	0.7 ± 0.3	1.0 ± 0.4	-0.6 ± 1.2
MONT	7.71	45.39	3.52	0.0 ± 0.3	-0.4 ± 0.4	0.4 ± 0.4	0.8 ± 0.9
MONV	7.83	44.39	4.4	-0.1 ± 0.2	0.9 ± 0.2	0.9 ± 0.2	-1.5 ± 0.6
MONZ	9.27	45.58	4.8	0.1 ± 0.1	0.9 ± 0.1	0.9 ± 0.1	-1.1 ± 0.5
MOPI	17.27	48.37	7.53	0.1 ± 0.1	0.5 ± 0.1	0.5 ± 0.1	1.2 ± 0.4
MOPS	10.95	44.63	8.29	3.1 ± 0.1	1.1 ± 0.1	3.3 ± 0.1	-1.3 ± 0.4
MORB	9.57	46.13	7.55	0.1 ± 0.3	0.7 ± 0.1	0.7 ± 0.2	0.8 ± 0.6
MORO	12.62	42.05	7.1	0.9 ± 0.1	0.4 ± 0.1	1.0 ± 0.1	0.9 ± 0.3
MOST	16.57	38.44	2.87	3.7 ± 0.6	1.5 ± 0.6	4.0 ± 0.6	1.3 ± 1.6
MOZ2	10.54	43.98	5.87	2.8 ± 0.4	2.4 ± 0.4	3.7 ± 0.4	-0.9 ± 1.3
MPRA	12.99	46.24	12.53	1.2 ± 0.1	-0.2 ± 0.1	1.2 ± 0.1	0.1 ± 0.1
MRGE	7.06	45.77	8.86	-0.6 ± 0.1	-0.1 ± 0.1	0.6 ± 0.1	0.3 ± 0.2
MRLC	15.49	40.76	9.65	5.0 ± 0.1	1.8 ± 0.1	5.3 ± 0.1	0.5 ± 0.2
MRRA	13.92	42.89	8.67	3.6 ± 0.2	2.2 ± 0.1	4.2 ± 0.2	-1.7 ± 0.5
MRVN	16.2	41.06	9.17	4.5 ± 0.1	1.1 ± 0.1	4.6 ± 0.1	0.3 ± 0.1
MSAG	15.91	41.71	9.15	3.9 ± 0.1	1.2 ± 0.1	4.1 ± 0.1	0.4 ± 0.1

Code	Lon.	Lat.	T (yr)	V_N (mm/yr)	V_E (mm/yr)	V_h (mm/yr)	V_V (mm/yr)
MSEL	11.65	44.52	10.86	2.7 ± 0.1	1.3 ± 0.1	3.0 ± 0.1	-1.5 ± 0.2
MSRU	15.51	38.26	8.48	4.7 ± 0.1	0.8 ± 0.1	4.8 ± 0.1	-1.3 ± 0.4
MT01	12.2	45.75	6.33	2.3 ± 0.2	-0.3 ± 0.2	2.3 ± 0.2	-0.4 ± 0.7
MTRA	13.24	42.53	8.71	4.4 ± 0.4	1.8 ± 0.4	4.7 ± 0.4	0.2 ± 1.1
MTSN	15.75	40.27	8.59	3.9 ± 0.1	1.0 ± 0.1	4.0 ± 0.1	1.3 ± 0.2
MTTG	15.7	38	9.52	2.9 ± 0.1	1.0 ± 0.1	3.0 ± 0.1	0.9 ± 0.2
MTTO	12.99	42.46	8.62	1.8 ± 0.1	-0.9 ± 0.2	2.0 ± 0.2	1.1 ± 0.4
MUR1	12.52	43.26	2.91	2.2 ± 0.7	-0.5 ± 0.6	2.2 ± 0.7	3.1 ± 1.8
MURA	9.57	39.42	4.03	-0.2 ± 1.4	1.2 ± 1.2	1.2 ± 1.3	1.8 ± 2.0
MVAL	12.41	43.38	9.06	1.8 ± 0.1	0.4 ± 0.1	1.9 ± 0.1	1.3 ± 0.1
NAPO	14.28	40.87	6.54	2.8 ± 0.2	1.4 ± 0.4	3.2 ± 0.3	1.9 ± 0.8
NERO	8.45	45.71	3.52	-0.2 ± 0.3	0.1 ± 0.4	0.2 ± 0.3	-0.1 ± 1.9
NETT	12.65	41.46	3.48	1.5 ± 0.3	-0.5 ± 0.3	1.5 ± 0.3	-1.1 ± 0.8
NICO	14.33	41.05	5.34	2.2 ± 0.1	0.0 ± 0.1	2.2 ± 0.1	-1.1 ± 0.4
NOCI	17.06	40.79	9.98	4.2 ± 0.1	1.6 ± 0.1	4.5 ± 0.1	1.0 ± 0.1
NOT1	14.99	36.88	14.55	4.7 ± 0.1	-1.4 ± 0.1	4.9 ± 0.1	-0.4 ± 0.1
NOVE	12.59	45.67	5.64	2.0 ± 0.3	0.9 ± 0.4	2.2 ± 0.3	-3.4 ± 1.2
NOVR	8.61	45.45	4.4	0.8 ± 0.2	0.5 ± 0.2	1.0 ± 0.2	-0.8 ± 0.6
NPAZ	20.52	43.14	3.86	-0.3 ± 0.2	0.7 ± 0.2	0.8 ± 0.2	0.6 ± 0.7
NU01	9.31	40.31	7.14	0.9 ± 0.1	0.4 ± 0.1	0.9 ± 0.1	-0.8 ± 0.3
OATO	7.77	45.04	7.24	-0.7 ± 0.1	0.6 ± 0.1	0.9 ± 0.1	0.6 ± 0.4
OBE4	11.28	48.08	2.66	1.5 ± 0.4	-0.6 ± 0.5	1.7 ± 0.5	1.8 ± 2.5
OCRA	13.04	42.05	8.57	1.6 ± 0.3	-0.7 ± 0.4	1.8 ± 0.3	0.7 ± 0.7
ODEZ	12.49	45.79	4.38	2.0 ± 0.1	0.2 ± 0.1	2.1 ± 0.1	-1.8 ± 0.5
OLB2	9.49	40.92	2.54	0.3 ± 0.9	1.1 ± 0.9	1.2 ± 0.9	3.6 ± 2.0
OLGI	12.36	42.05	7.3	1.1 ± 0.1	-1.1 ± 0.2	1.5 ± 0.2	-0.1 ± 0.7
OMBR	11.56	43.73	12.06	1.8 ± 0.1	0.6 ± 0.1	1.9 ± 0.1	-0.2 ± 0.1
ORID	20.79	41.13	14.55	-2.9 ± 0.1	1.0 ± 0.1	3.1 ± 0.1	-0.0 ± 0.2
ORZI	9.92	45.41	3.52	0.2 ± 0.4	0.7 ± 0.4	0.7 ± 0.4	-1.1 ± 1.0
OSIM	13.48	43.48	3.48	3.5 ± 0.4	1.8 ± 0.3	4.0 ± 0.4	0.5 ± 1.3
OTRA	13.65	41.95	6.58	4.6 ± 0.2	-0.1 ± 0.1	4.6 ± 0.2	1.3 ± 0.4
OVRA	13.52	42.14	8.67	2.4 ± 0.4	0.6 ± 0.5	2.5 ± 0.5	0.3 ± 1.0
PACA	14.56	40.87	12.21	1.6 ± 0.1	-0.9 ± 0.1	1.8 ± 0.1	-2.0 ± 0.1
PADO	11.9	45.41	13.64	1.3 ± 0.1	0.3 ± 0.1	1.3 ± 0.1	-0.8 ± 0.1
PAGA	13.47	42.36	3.52	2.2 ± 1.6	0.4 ± 0.9	2.2 ± 1.6	0.6 ± 2.2
PAGL	14.5	42.16	5.27	3.8 ± 0.2	0.7 ± 0.2	3.9 ± 0.2	-1.0 ± 0.7
PALA	9.9	45.6	7.07	0.5 ± 0.3	-0.0 ± 0.6	0.5 ± 0.3	2.0 ± 1.1
PALE	13.35	38.11	3.55	5.0 ± 0.4	-0.7 ± 0.4	5.0 ± 0.4	0.6 ± 1.1
PALZ	15.96	40.94	8.59	4.4 ± 0.1	1.0 ± 0.1	4.5 ± 0.1	0.8 ± 0.1
PAMA	10.36	44.8	2.71	0.2 ± 0.6	1.3 ± 0.5	1.3 ± 0.5	3.2 ± 2.0
PAOL	14.57	41.03	5.58	2.1 ± 0.4	-0.5 ± 0.6	2.1 ± 0.4	0.4 ± 0.8
PARM	10.31	44.76	8.76	1.8 ± 0.2	1.0 ± 0.1	2.0 ± 0.2	-0.4 ± 0.8
PARO	8.08	44.45	7.28	0.1 ± 0.2	1.0 ± 0.1	1.1 ± 0.2	0.2 ± 0.6
PARR	11.12	45.78	6.54	1.0 ± 0.1	0.3 ± 0.1	1.0 ± 0.1	-0.4 ± 0.4
PASS	11.9	46.19	6.05	0.7 ± 0.1	-0.2 ± 0.1	0.7 ± 0.1	-0.1 ± 0.4
PATT	14.97	38.14	4.18	7.5 ± 0.4	-1.5 ± 0.6	7.6 ± 0.5	0.0 ± 1.6
PAUN	13.35	38.11	3.55	5.0 ± 0.4	-0.7 ± 0.4	5.0 ± 0.4	0.6 ± 1.1
PAVI	9.14	45.2	14.04	0.8 ± 0.1	-0.1 ± 0.1	0.8 ± 0.1	-0.7 ± 0.2
PAZO	13.05	45.81	7.55	2.1 ± 0.1	0.3 ± 0.1	2.1 ± 0.1	0.1 ± 0.4
PBRA	14.23	42.12	8.52	4.5 ± 0.3	1.4 ± 0.4	4.7 ± 0.3	-1.0 ± 0.7
PE2N	19.28	47.79	2.54	-1.0 ± 1.2	-0.4 ± 1.4	1.1 ± 1.2	-4.8 ± 2.8
PEJO	10.68	46.36	6.54	-0.0 ± 0.2	0.5 ± 0.2	0.5 ± 0.2	1.6 ± 0.7
PENC	19.28	47.79	14.54	0.2 ± 0.1	0.5 ± 0.1	0.5 ± 0.1	0.1 ± 0.3
PES2	12.89	43.89	5.87	3.3 ± 0.2	1.0 ± 0.2	3.4 ± 0.2	1.0 ± 0.8
PESA	12.92	43.9	3.52	3.8 ± 0.3	1.6 ± 0.2	4.1 ± 0.3	-0.0 ± 0.9
PESC	14.2	42.47	3.46	3.8 ± 0.4	1.0 ± 0.3	4.0 ± 0.3	-1.1 ± 1.1
PESR	12.84	43.94	3.96	5.5 ± 0.3	2.7 ± 0.3	6.1 ± 0.3	-0.6 ± 0.7
PFA2	9.78	47.52	7.24	0.4 ± 0.1	0.1 ± 0.1	0.4 ± 0.1	0.6 ± 0.3
PFER	10.29	42.79	4.54	0.3 ± 0.7	0.3 ± 0.4	0.5 ± 0.6	-2.2 ± 1.6

Code	Lon.	Lat.	T (yr)	V_N (mm/yr)	V_E (mm/yr)	V_h (mm/yr)	V_V (mm/yr)
PIAC	9.69	45.04	7.93	1.8 ± 0.1	0.7 ± 0.1	1.9 ± 0.1	-0.1 ± 0.4
PIBI	12.45	43.13	3.39	1.4 ± 0.4	-1.0 ± 0.4	1.7 ± 0.4	-0.6 ± 1.2
PIC1	9.69	45.04	7.55	1.2 ± 0.1	0.8 ± 0.1	1.5 ± 0.1	-0.4 ± 0.4
PIET	12.4	43.45	9.05	2.0 ± 0.1	0.3 ± 0.1	2.0 ± 0.1	1.1 ± 0.1
PIGN	14.18	41.2	3.93	2.5 ± 0.2	-0.7 ± 0.2	2.6 ± 0.2	-1.4 ± 0.7
PILA	11.91	46.57	4.55	-0.8 ± 0.3	0.6 ± 0.3	1.0 ± 0.3	0.7 ± 0.7
PIOB	12.48	43.61	3.52	3.4 ± 0.5	1.5 ± 0.4	3.7 ± 0.5	-0.5 ± 1.4
PIPA	16.82	39.49	8.25	3.6 ± 0.1	1.3 ± 0.1	3.9 ± 0.1	1.1 ± 0.2
PITI	11.67	42.63	4.25	1.3 ± 0.3	-0.4 ± 0.4	1.3 ± 0.3	-0.1 ± 0.9
PLAC	16.44	38.45	9.84	2.9 ± 0.1	1.6 ± 0.1	3.3 ± 0.1	1.2 ± 0.2
PLND	21.12	45.23	3.86	-0.9 ± 0.2	0.7 ± 0.3	1.2 ± 0.3	-0.1 ± 0.9
POFI	13.71	41.72	8.31	1.7 ± 0.3	-0.2 ± 0.2	1.7 ± 0.3	1.4 ± 0.7
POGG	16.25	40.92	8.15	4.3 ± 0.2	1.6 ± 0.2	4.6 ± 0.2	2.0 ± 0.4
POMP	14.49	40.75	2.82	2.6 ± 0.9	-2.2 ± 0.6	3.4 ± 0.8	2.8 ± 1.7
PORD	12.66	45.96	6.94	2.1 ± 0.3	-0.2 ± 0.3	2.1 ± 0.3	-0.5 ± 0.8
PORE	13.6	45.23	3.81	2.6 ± 0.6	0.4 ± 0.6	2.7 ± 0.6	-0.7 ± 1.7
POZE	17.68	45.33	3.81	1.0 ± 0.4	1.0 ± 0.3	1.4 ± 0.4	-0.6 ± 0.9
POZL	14.79	36.73	3.51	5.2 ± 0.3	-1.3 ± 0.4	5.3 ± 0.3	-0.0 ± 0.9
POZZ	11.68	46.42	6.54	0.8 ± 0.1	0.1 ± 0.1	0.8 ± 0.1	0.4 ± 0.3
PRAI	15.78	39.9	2.99	3.0 ± 0.5	-2.9 ± 0.7	4.2 ± 0.6	-0.6 ± 2.0
PRAT	11.1	43.89	14.55	1.7 ± 0.1	0.7 ± 0.1	1.8 ± 0.1	0.2 ± 0.1
PREM	9.88	45.87	6.76	0.6 ± 0.2	0.1 ± 0.3	0.6 ± 0.2	0.5 ± 0.6
PRET	12.07	47.03	4.55	-0.9 ± 0.4	1.6 ± 0.3	1.8 ± 0.3	2.3 ± 0.8
PRIG	15.11	40.31	4.74	2.3 ± 1.0	0.6 ± 0.9	2.3 ± 1.0	0.5 ± 2.8
PROV	9.2	45.46	9.31	0.4 ± 0.1	0.5 ± 0.1	0.6 ± 0.1	-0.3 ± 0.1
PRTG	12.83	45.77	6.89	2.6 ± 0.2	-0.1 ± 0.2	2.6 ± 0.2	-4.8 ± 0.8
PSAN	14.14	42.52	6.61	2.8 ± 0.5	2.3 ± 0.4	3.6 ± 0.5	-1.4 ± 1.6
PSB1	14.81	41.22	9.31	2.6 ± 0.1	0.2 ± 0.1	2.6 ± 0.1	0.6 ± 0.1
PSST	11.12	42.43	3.52	1.0 ± 0.4	-0.7 ± 0.4	1.2 ± 0.4	-2.9 ± 1.2
PSTE	11.12	42.43	7.55	0.5 ± 0.2	0.0 ± 0.2	0.5 ± 0.2	-0.0 ± 0.9
PTNZ	15.82	40.63	4.13	5.2 ± 0.4	0.9 ± 0.4	5.3 ± 0.4	-0.1 ± 1.2
PTO1	12.33	44.95	4.99	1.5 ± 0.2	0.1 ± 0.1	1.5 ± 0.2	-5.4 ± 0.6
PTRJ	14.53	41.36	9	2.2 ± 0.1	0.6 ± 0.1	2.3 ± 0.1	0.9 ± 0.2
PTRP	16.06	40.53	8.04	4.3 ± 0.1	0.7 ± 0.1	4.3 ± 0.1	1.0 ± 0.4
RAFF	14.36	37.22	9.52	4.7 ± 0.1	-1.7 ± 0.1	5.0 ± 0.1	-0.5 ± 0.1
RAMS	10.28	44.41	5.38	1.9 ± 0.3	0.8 ± 0.2	2.1 ± 0.3	-0.5 ± 0.6
RAPA	9.22	44.36	3.41	0.1 ± 0.4	0.9 ± 0.4	0.9 ± 0.4	-1.0 ± 1.2
RASS	11.84	43.65	9.22	1.7 ± 0.1	-0.1 ± 0.1	1.7 ± 0.2	0.1 ± 0.4
RAVE	12.2	44.41	10.19	3.0 ± 0.1	2.2 ± 0.1	3.7 ± 0.1	-3.8 ± 0.2
RAVS	12.19	44.41	8.44	2.8 ± 0.1	2.3 ± 0.1	3.6 ± 0.1	-4.2 ± 0.4
RDPI	12.71	41.76	8.85	1.3 ± 0.1	-1.2 ± 0.1	1.8 ± 0.1	0.9 ± 0.4
RE01	10.64	44.89	9.22	0.6 ± 0.1	1.9 ± 0.1	2.0 ± 0.1	-2.6 ± 0.4
REAM	12.41	42.56	5.35	2.5 ± 0.2	0.5 ± 0.2	2.6 ± 0.2	1.1 ± 0.6
REBO	12.03	45.2	5.16	1.4 ± 0.1	0.4 ± 0.1	1.5 ± 0.1	-1.8 ± 0.3
REFO	12.7	42.96	8.08	2.3 ± 0.1	0.1 ± 0.1	2.3 ± 0.1	0.5 ± 0.2
REGG	10.64	44.71	7.29	2.9 ± 0.1	2.4 ± 0.1	3.8 ± 0.1	-1.7 ± 0.3
REPI	12	42.95	8.15	2.0 ± 0.1	0.0 ± 0.1	2.0 ± 0.1	-0.8 ± 0.3
RESU	14.06	37.65	7.35	2.6 ± 0.1	-0.4 ± 0.1	2.6 ± 0.1	0.5 ± 0.2
RETO	12.41	42.78	8.15	2.2 ± 0.2	0.0 ± 0.1	2.2 ± 0.2	-0.4 ± 0.5
RIET	12.86	42.41	7.55	1.2 ± 0.2	-0.9 ± 0.2	1.5 ± 0.2	-0.1 ± 0.9
RMPO	12.7	41.81	9.06	1.4 ± 0.1	-0.7 ± 0.1	1.5 ± 0.1	0.4 ± 0.3
RNI2	14.15	41.7	10.94	2.8 ± 0.1	0.8 ± 0.1	2.9 ± 0.1	1.3 ± 0.4
ROGA	10.34	44.21	11.89	0.9 ± 0.1	0.4 ± 0.1	1.0 ± 0.1	-1.0 ± 0.1
RONC	10.67	45.98	6.55	0.6 ± 0.1	0.4 ± 0.1	0.7 ± 0.1	0.3 ± 0.2
ROPI	13.34	42.33	6.28	0.4 ± 0.1	-0.9 ± 0.1	1.0 ± 0.1	-2.6 ± 0.5
ROSS	16.64	39.6	3.08	5.4 ± 0.6	1.6 ± 0.5	5.7 ± 0.6	-1.1 ± 1.6
ROVE	11.04	45.89	9.38	1.4 ± 0.1	0.2 ± 0.1	1.4 ± 0.1	0.9 ± 0.2
ROVI	11.78	45.09	6.89	2.3 ± 0.1	0.8 ± 0.2	2.5 ± 0.2	-0.5 ± 0.5
ROVR	11.07	45.65	6.77	1.0 ± 0.1	0.1 ± 0.1	1.0 ± 0.1	0.5 ± 0.2

Code	Lon.	Lat.	T (yr)	V_N (mm/yr)	V_E (mm/yr)	V_h (mm/yr)	V_V (mm/yr)
RSMN	12.45	43.93	9.64	3.1 ± 0.1	1.8 ± 0.1	3.5 ± 0.1	0.1 ± 0.4
RSPX	7.27	45.15	9.17	-0.2 ± 0.1	0.7 ± 0.1	0.8 ± 0.1	1.0 ± 0.1
RSTO	14	42.66	12.55	2.9 ± 0.1	1.3 ± 0.1	3.2 ± 0.1	-0.3 ± 0.2
SABA	19.7	44.76	3.86	0.0 ± 0.3	1.4 ± 0.2	1.4 ± 0.3	1.5 ± 0.9
SACR	14.71	41.4	10.53	1.8 ± 0.1	-0.1 ± 0.1	1.8 ± 0.1	1.3 ± 0.2
SALA	15.56	40.42	5.25	3.7 ± 0.4	1.9 ± 0.6	4.2 ± 0.5	1.6 ± 1.3
SALB	16.35	39.88	6.05	4.4 ± 0.1	1.1 ± 0.1	4.5 ± 0.1	1.1 ± 0.4
SALO	10.52	45.62	9.69	0.1 ± 0.2	1.0 ± 0.1	1.0 ± 0.2	-1.1 ± 0.6
SAPP	12.69	46.57	6.41	1.1 ± 0.4	-0.0 ± 0.2	1.1 ± 0.4	1.7 ± 0.6
SAPR	15.63	40.07	7.31	2.9 ± 0.2	0.3 ± 0.1	2.9 ± 0.2	-1.5 ± 0.7
SAQU	8.4	44.29	6.18	0.2 ± 0.4	0.5 ± 0.6	0.5 ± 0.5	-1.6 ± 1.0
SARN	11.14	46.42	6.54	0.9 ± 0.1	0.2 ± 0.1	0.9 ± 0.1	0.3 ± 0.3
SASA	17.96	40.39	8.17	3.7 ± 0.2	1.3 ± 0.1	3.9 ± 0.2	-1.6 ± 0.4
SASO	11.82	43.93	4.94	4.3 ± 0.4	1.2 ± 0.7	4.4 ± 0.5	-1.0 ± 1.4
SASS	8.57	40.72	7.55	0.6 ± 0.1	0.3 ± 0.1	0.6 ± 0.1	-0.5 ± 0.3
SAVI	7.66	44.65	5.29	0.1 ± 0.1	0.5 ± 0.1	0.5 ± 0.1	-1.1 ± 0.4
SBG2	13.11	47.8	7.46	0.5 ± 0.1	0.3 ± 0.1	0.6 ± 0.1	0.7 ± 0.4
SBPO	10.92	45.05	9.15	1.3 ± 0.1	0.2 ± 0.1	1.3 ± 0.1	0.0 ± 0.2
SCHI	11.36	45.72	7.15	1.3 ± 0.2	0.2 ± 0.1	1.3 ± 0.2	0.2 ± 0.7
SCHR	16.09	40.19	9.84	3.8 ± 0.1	1.0 ± 0.1	4.0 ± 0.1	1.2 ± 0.2
SCRA	14	42.27	8.65	3.6 ± 0.2	1.4 ± 0.3	3.8 ± 0.2	-1.6 ± 0.8
SCTE	18.47	40.07	9.46	3.8 ± 0.1	1.2 ± 0.1	4.0 ± 0.1	-0.0 ± 0.1
SDNA	12.56	45.63	6.89	1.9 ± 0.1	0.3 ± 0.1	2.0 ± 0.1	-1.2 ± 0.2
SEAN	11.03	43.83	3.42	1.8 ± 0.8	1.0 ± 0.7	2.0 ± 0.8	-1.6 ± 2.5
SENI	13.21	43.71	3.52	3.6 ± 0.3	1.4 ± 0.3	3.9 ± 0.3	-0.0 ± 0.9
SERM	11.3	45.01	7.54	1.7 ± 0.1	2.3 ± 0.1	2.9 ± 0.1	-0.2 ± 0.3
SERR	8.85	44.73	4.4	1.2 ± 0.2	0.7 ± 0.3	1.4 ± 0.3	-0.5 ± 0.8
SERS	16.69	39.04	8.84	3.0 ± 0.1	1.7 ± 0.1	3.4 ± 0.1	-0.3 ± 0.2
SEVI	7.84	45.54	5.18	-0.6 ± 0.3	0.1 ± 0.3	0.7 ± 0.3	1.3 ± 0.9
SFER	353.79	36.46	14.55	0.1 ± 0.1	-4.5 ± 0.1	4.5 ± 0.1	1.3 ± 0.2
SGIO	11.8	45.6	3.52	0.9 ± 0.7	-0.2 ± 0.6	1.0 ± 0.7	-0.4 ± 1.4
SGIP	11.18	44.64	10.36	1.5 ± 0.1	2.0 ± 0.1	2.5 ± 0.1	-6.2 ± 0.1
SGL1	13.77	41.41	6.02	1.2 ± 0.1	0.7 ± 0.1	1.4 ± 0.1	0.1 ± 0.4
SGRE	13.5	42.34	6.18	3.2 ± 0.5	-0.6 ± 0.4	3.3 ± 0.5	-2.7 ± 0.9
SGRT	15.74	41.75	9.15	3.9 ± 0.2	0.9 ± 0.1	4.0 ± 0.2	-0.2 ± 0.3
SGTA	15.37	41.14	8.53	4.3 ± 0.1	0.7 ± 0.1	4.3 ± 0.1	1.0 ± 0.2
SIEN	11.34	43.31	11.6	1.1 ± 0.1	-0.2 ± 0.1	1.1 ± 0.1	0.4 ± 0.2
SILA	10.79	46.63	3.52	0.1 ± 1.5	1.2 ± 1.4	1.2 ± 1.4	6.1 ± 5.2
SIN2	9.69	40.57	5.62	0.1 ± 0.4	0.2 ± 0.5	0.2 ± 0.5	-0.1 ± 0.9
SIRC	15.28	37.08	5.64	4.8 ± 0.2	-1.1 ± 0.2	4.9 ± 0.2	-2.2 ± 0.8
SIRI	15.87	40.18	8.59	4.2 ± 0.1	1.8 ± 0.1	4.6 ± 0.1	-0.1 ± 0.2
SLCN	15.63	40.39	10.13	2.7 ± 0.1	1.1 ± 0.1	3.0 ± 0.1	1.0 ± 0.2
SMRA	13.92	42.05	9.07	3.9 ± 0.4	1.8 ± 0.3	4.3 ± 0.3	-1.7 ± 1.4
SNAL	15.21	40.93	10.55	2.7 ± 0.1	0.3 ± 0.1	2.7 ± 0.1	1.3 ± 0.1
SOFI	23.39	42.56	14.36	-1.9 ± 0.1	0.6 ± 0.1	2.0 ± 0.1	-0.6 ± 0.1
SONA	10.83	45.45	3.52	1.1 ± 0.4	0.6 ± 0.6	1.2 ± 0.4	-2.2 ± 1.2
SORR	14.4	40.63	4	2.2 ± 0.4	-0.6 ± 0.3	2.3 ± 0.3	-1.4 ± 0.9
SOV1	16.55	38.68	4.1	3.1 ± 0.3	1.6 ± 0.3	3.5 ± 0.3	-0.1 ± 0.9
SPCI	15.26	41.74	8.19	3.6 ± 0.1	1.9 ± 0.1	4.0 ± 0.1	-0.4 ± 0.2
SPER	11.51	46.07	6.55	0.8 ± 0.1	0.2 ± 0.1	0.8 ± 0.1	0.3 ± 0.2
SPRN	16.58	47.68	7.55	0.6 ± 0.1	1.1 ± 0.1	1.3 ± 0.1	0.0 ± 0.4
STBZ	11.43	46.9	4.55	0.3 ± 0.2	0.6 ± 0.2	0.7 ± 0.2	1.8 ± 0.6
SUSE	12.21	45.86	4.08	0.9 ± 0.2	0.8 ± 0.2	1.2 ± 0.2	-1.3 ± 1.1
SVTO	16.44	40.6	8.59	4.1 ± 0.1	1.1 ± 0.1	4.2 ± 0.1	1.0 ± 0.1
TAMB	12.4	46.06	3.87	0.3 ± 0.3	0.5 ± 0.2	0.6 ± 0.3	0.9 ± 0.8
TAOR	15.29	37.85	7.05	4.9 ± 0.2	-1.0 ± 0.4	5.0 ± 0.3	0.8 ± 0.8
TARA	17.28	40.53	4.57	4.8 ± 0.2	0.9 ± 0.1	4.9 ± 0.2	-1.4 ± 0.6
TARO	9.77	44.49	8	1.4 ± 0.1	0.9 ± 0.1	1.7 ± 0.1	-0.7 ± 0.4
TARQ	11.76	42.25	5.38	0.2 ± 0.3	-0.7 ± 0.3	0.8 ± 0.3	2.2 ± 1.2

Code	Lon.	Lat.	T (yr)	V_N (mm/yr)	V_E (mm/yr)	V_h (mm/yr)	V_V (mm/yr)
TARV	13.59	46.5	6.94	1.5 ± 0.2	0.5 ± 0.2	1.6 ± 0.2	2.2 ± 0.8
TELI	15.01	41.97	3.47	3.3 ± 0.4	2.9 ± 0.3	4.4 ± 0.3	-10.8 ± 1.1
TEMP	9.1	40.91	7.05	0.5 ± 0.3	0.5 ± 0.2	0.7 ± 0.3	0.6 ± 0.7
TEOL	11.68	45.34	10.27	2.0 ± 0.1	0.0 ± 0.1	2.0 ± 0.1	-0.2 ± 0.1
TERA	13.7	42.66	6.48	4.9 ± 0.2	1.7 ± 0.2	5.2 ± 0.2	-1.3 ± 1.2
TERI	12.65	42.57	7.46	1.1 ± 0.4	-0.9 ± 0.4	1.4 ± 0.4	0.4 ± 0.8
TGPO	12.23	45	6.89	1.7 ± 0.1	0.5 ± 0.1	1.8 ± 0.1	-7.0 ± 0.2
TGRC	15.65	38.11	3.08	4.2 ± 0.6	0.3 ± 0.5	4.3 ± 0.5	1.7 ± 1.7
TITO	15.72	40.6	6.54	3.3 ± 0.4	1.1 ± 0.4	3.5 ± 0.4	1.6 ± 1.4
TLSE	1.48	43.56	14.53	-0.0 ± 0.1	0.7 ± 0.1	0.7 ± 0.1	-0.1 ± 0.1
TOIR	8.21	44.12	5.78	0.1 ± 0.4	1.2 ± 0.4	1.2 ± 0.4	-0.9 ± 1.3
TOLF	12	42.06	10.34	1.1 ± 0.1	-0.5 ± 0.1	1.2 ± 0.1	-1.7 ± 0.2
TORC	7.64	45.02	3.52	0.0 ± 0.3	0.5 ± 0.3	0.5 ± 0.3	1.3 ± 1.1
TORI	7.66	45.06	14.55	-0.1 ± 0.1	0.2 ± 0.1	0.2 ± 0.1	0.8 ± 0.1
TREB	16.53	39.87	3.08	4.9 ± 0.5	1.1 ± 0.5	5.1 ± 0.5	1.6 ± 1.4
TREC	10.02	44.34	11.7	1.1 ± 0.1	0.5 ± 0.1	1.2 ± 0.1	-0.5 ± 0.1
TREN	11.12	46.09	6.54	0.8 ± 0.1	0.5 ± 0.1	0.9 ± 0.1	-0.8 ± 0.2
TREV	12.22	45.68	6.27	1.7 ± 0.2	0.1 ± 0.1	1.7 ± 0.2	-0.4 ± 0.4
TRI0	13.79	45.66	6.94	2.7 ± 0.1	0.9 ± 0.1	2.8 ± 0.1	-1.3 ± 0.4
TRIE	13.76	45.71	12.44	2.4 ± 0.1	-0.0 ± 0.1	2.4 ± 0.1	-0.3 ± 0.1
TRIV	14.55	41.77	10.35	3.4 ± 0.1	1.7 ± 0.1	3.8 ± 0.1	0.4 ± 0.1
TRLU	11.27	43.61	12.3	1.9 ± 0.1	0.9 ± 0.1	2.1 ± 0.1	-0.1 ± 0.1
UDI1	13.25	46.04	9.19	2.1 ± 0.1	0.1 ± 0.1	2.1 ± 0.1	-1.0 ± 0.1
UDIN	13.23	46.06	6.94	2.8 ± 0.3	0.8 ± 0.2	2.9 ± 0.3	-0.9 ± 0.6
UGEN	18.16	39.93	8.18	3.9 ± 0.1	1.2 ± 0.1	4.0 ± 0.1	-0.7 ± 0.4
UMBE	12.33	43.31	9.48	1.8 ± 0.1	0.2 ± 0.1	1.8 ± 0.1	0.5 ± 0.6
UNPA	13.35	38.11	3.28	4.2 ± 0.6	-0.6 ± 0.6	4.2 ± 0.6	2.3 ± 1.7
UNPG	12.36	43.12	14.55	1.8 ± 0.1	1.0 ± 0.1	2.1 ± 0.1	-1.0 ± 0.1
UNTR	12.67	42.56	8.55	2.6 ± 0.1	-1.2 ± 0.1	2.9 ± 0.1	0.6 ± 0.2
USAL	18.11	40.33	5.39	4.1 ± 0.1	1.1 ± 0.1	4.3 ± 0.1	-0.2 ± 0.3
VAGA	14.23	41.42	9.35	1.0 ± 0.2	-0.4 ± 0.1	1.0 ± 0.2	0.7 ± 0.4
VALC	12.28	43.28	8.29	1.9 ± 0.1	-0.1 ± 0.1	1.9 ± 0.1	0.6 ± 0.1
VALD	12	45.9	4.38	0.5 ± 0.3	-0.1 ± 0.2	0.5 ± 0.3	-1.1 ± 0.7
VALE	16.9	41.02	8	4.2 ± 0.1	1.5 ± 0.1	4.4 ± 0.1	-0.7 ± 0.3
VARE	8.83	45.81	4.84	0.2 ± 0.1	0.2 ± 0.1	0.3 ± 0.1	-0.2 ± 0.6
VELO	11.37	45.79	6.19	0.6 ± 0.4	0.2 ± 0.2	0.7 ± 0.4	-1.1 ± 1.1
VEN1	12.35	45.43	7.07	0.8 ± 0.1	0.1 ± 0.1	0.8 ± 0.1	-1.2 ± 0.5
VENO	15.81	40.97	5.26	4.8 ± 0.3	1.3 ± 0.2	4.9 ± 0.3	-0.8 ± 0.8
VENT	13.42	40.79	9.46	1.6 ± 0.1	-0.6 ± 0.1	1.7 ± 0.1	-0.7 ± 0.1
VERB	8.57	45.94	3.52	-0.2 ± 0.4	0.2 ± 0.4	0.2 ± 0.4	2.9 ± 1.1
VERG	11.11	44.29	7.86	2.0 ± 0.2	2.6 ± 0.1	3.2 ± 0.2	1.0 ± 0.4
VERL	8.42	45.33	4.25	0.1 ± 0.2	0.4 ± 0.2	0.4 ± 0.2	-1.3 ± 0.8
VERO	11	45.44	7.55	0.7 ± 0.3	0.5 ± 0.2	0.9 ± 0.3	0.0 ± 0.8
VGAR	15.96	41.89	4.46	4.2 ± 0.2	1.4 ± 0.2	4.4 ± 0.2	-1.5 ± 0.8
VICE	11.56	45.56	6.89	1.7 ± 0.2	0.5 ± 0.2	1.7 ± 0.2	0.2 ± 0.9
VIGE	8.86	45.31	9.55	0.8 ± 0.1	0.8 ± 0.1	1.1 ± 0.1	-0.2 ± 0.2
VIGG	16.12	39.99	3.84	4.7 ± 0.9	1.4 ± 0.7	4.9 ± 0.9	1.9 ± 2.3
VILL	356.05	40.44	14.55	0.1 ± 0.1	0.6 ± 0.1	0.6 ± 0.1	-1.2 ± 0.1
VILS	9.52	39.14	7.24	0.7 ± 0.1	0.3 ± 0.1	0.8 ± 0.1	-1.4 ± 0.4
VINC	14.56	41.47	3.47	3.4 ± 0.7	1.4 ± 0.6	3.7 ± 0.6	-0.8 ± 2.1
VIT1	12.1	42.43	5.38	1.2 ± 0.1	-0.5 ± 0.1	1.3 ± 0.2	0.5 ± 0.8
VITE	12.11	42.42	3.52	1.3 ± 0.7	-1.5 ± 0.4	1.9 ± 0.5	-0.0 ± 1.1
VITT	12.3	45.99	3.4	1.4 ± 0.4	0.4 ± 0.3	1.5 ± 0.4	-0.6 ± 0.9
VLPN	10.85	43.01	3.52	1.3 ± 0.6	0.0 ± 0.4	1.3 ± 0.6	-0.2 ± 1.1
VLSG	15.64	38.22	9.54	3.1 ± 0.1	0.4 ± 0.1	3.2 ± 0.1	0.4 ± 0.2
VMIG	7.65	43.79	3.12	-0.3 ± 0.5	-0.1 ± 0.7	0.3 ± 0.5	-0.5 ± 1.2
VR02	10.99	45.44	7.14	0.4 ± 0.3	0.8 ± 0.2	0.9 ± 0.2	0.9 ± 1.0
VRRA	10.87	43.4	6.11	0.2 ± 0.2	1.0 ± 0.1	1.0 ± 0.2	-0.1 ± 0.7
VTRA	14.71	42.11	8.62	3.4 ± 0.2	1.6 ± 0.2	3.7 ± 0.2	-2.0 ± 0.7

Code	Lon.	Lat.	T (yr)	V_N (mm/yr)	V_E (mm/yr)	V_h (mm/yr)	V_V (mm/yr)
VULT	15.62	40.95	9.91	4.3 ± 0.1	1.2 ± 0.1	4.4 ± 0.1	0.5 ± 0.1
VVLO	13.62	41.87	14.54	2.3 ± 0.1	-0.2 ± 0.1	2.3 ± 0.1	1.2 ± 0.4
WTZR	12.88	49.14	14.54	0.1 ± 0.1	0.1 ± 0.1	0.2 ± 0.1	-0.2 ± 0.1
YEBE	356.91	40.52	14.55	-0.2 ± 0.1	-0.1 ± 0.1	0.3 ± 0.1	0.8 ± 0.1
ZADA	15.23	44.11	3.81	2.8 ± 0.2	-0.7 ± 0.2	2.9 ± 0.2	-0.8 ± 0.7
ZAGA	12.75	41.86	3.52	1.9 ± 0.4	-0.9 ± 0.4	2.1 ± 0.4	-0.8 ± 1.0
ZERI	9.75	44.39	9.48	0.4 ± 0.1	0.7 ± 0.1	0.8 ± 0.1	-1.0 ± 0.2
ZIMM	7.47	46.88	14.55	0.4 ± 0.1	0.2 ± 0.1	0.5 ± 0.1	1.1 ± 0.1
ZOUF	12.97	46.56	12.18	0.7 ± 0.1	0.4 ± 0.1	0.8 ± 0.1	2.4 ± 0.2

Appendix 2: Seismicity data

List of earthquakes used for the diagrams of figure 9. M= magnitude, Cat = reference to seismic catalogues listed as follows: **1)** Albini P (2004) **2)** Ambraseys (1990) **3)** Global CMT Catalog (www.globalcmt.org) **4)** Working Group CPTI (2004) **5)** Rovida et al (2011) **6)** Guidoboni and Comastri (2005) **7)** ISIDe Working Group (INGV, 2010) **8)** Karnik (1971) **9)** Mariotti and Guidoboni (2006) **10)** Seismological Catalogues of Greece, at http://www.geophysics.geol.uoa.gr/ **11)** Makropoulos et al (2012) **12)** Margottini et al (1993) **13)** Comninakis and Papazachos (1986) **14)** Papazachos and Papazachos (1989) **15)** Ribaric (1982) **16)** Shebalin et al (1974) **17)** Stucchi et al (2012) **18)** Shebalin et al (1998) **19)** Toth et al (1988) **20)** EMSC/CSEM (*http://www.emsc-csem.org/)*.

Zone A		
Date(y–m–d)	M	Cat
1469	6.6	17
1577	6.2	17
1601 - 4 - 26	6.3	17
1612 - 5 - 26	6.3	17
1613 - 10 - 12	6.3	17
1625 - 6 - 28	6.5	17
1630 - 7 - 2	6.5	17
1636 - 9 - 20	7.2	10
1638 - 7 - 16	6.3	17
1650	6.2	14
1651 - 2 - 26	5.9	17
1658 - 8 - 24	6.7	17
1666 - 11	6.2	18
1674 - 1 - 16	6.3	17
1701 - 4 - 5	6.6	17
1704 - 11 - 22	6.4	17
1709	6.2	17
1714 - 9 - 8	6.3	17
1722 - 6 - 5	6.3	17
1723 - 2 - 22	6.3	17
1732 - 11	6.6	17
1736	6	10
1741 - 6 - 23	6.3	17
1743 - 2 - 20	6.9	10
1759 - 6 - 13	6.3	17
1766 - 7 - 24	6.6	17
1767 - 7 - 22	6.7	17
1769 - 10 - 12	6.8	14
1772 - 5 - 12	6.1	18
1773 - 5 - 23	6.5	10
1783 - 3 - 23	6.6	17
1783 - 6 - 7	6.5	10
1786 - 2 - 5	6.5	17
1815	6.3	17
1820 - 2 - 21	6.6	17
1823 - 6 - 19	6.1	17
1825 - 1 - 19	6.7	17
1826 - 1 - 26	5.8	17
1833 - 1 - 19	6.5	14
1851 - 10 - 12	6.8	17
1858 - 4 - 5	6	10
1858 - 9 - 20	6.2	17
1858 - 10 - 10	6.4	17
1859 - 9 - 12	6	18
1860 - 4 - 10	6.4	18
1862 - 3 - 14	6.4	17
1862 - 10 - 4	6.2	17
1865 - 10 - 10	6.3	17
1866 - 1 - 2	6.6	17
1866 - 3 - 2	6.3	18
1866 - 12 - 4	6.4	17
1867 - 2 - 4	7.2	17
1869 - 8 - 14	6	18
1869 - 12 - 28	6.7	17
1871 - 4 - 9	5.8	17
1872 - 2 - 11	6	18
1883 - 6 - 27	5.5	10
1883 - 8	5.5	10
1885 - 12 - 14	6	10
1889 - 4 - 1	5.9	17
1890 - 5 - 21	5.9	17
1891 - 6 - 27	5.8	17
1893 - 6 - 14	6.6	17
1895 - 5 - 13	6.2	17
1895 - 5 - 14	6.5	17
1895 - 5 - 15	6.2	17
1895 - 6 - 16	6.2	18
1896 - 2 - 10	5.5	18
1896 - 3 - 18	5.8	18
1897 - 1 - 17	6.6	17
1912 - 1 - 24	6.1	11
1914 - 11 - 27	5.9	11
1915 - 1 - 27	6.1	11
1915 - 8 - 7	6.3	11
1915 - 8 - 10	5.6	11
1915 - 8 - 10	6	11
1915 - 8 - 11	5.7	11
1915 - 8 - 19	5.9	11
1917 - 5 - 23	5.6	11
1920 - 10 - 21	5.6	11
1920 - 11 - 26	6	18
1920 - 11 - 29	5.5	18
1921 - 9 - 13	5.5	11
1930 - 11 - 21	5.8	18
1938 - 3 - 13	5.7	11
1939 - 9 - 20	5.5	11
1943 - 2 - 14	5.6	11
1948 - 4 - 22	6.5	11
1948 - 6 - 30	6.5	11
1953 - 8 - 9	5.9	11
1953 - 8 - 11	6.6	11
1953 - 8 - 12	7	11
1953 - 8 - 12	5.7	11
1953 - 8 - 12	5.9	11
1953 - 10 - 21	6.2	11
1960 - 11 - 5	5.7	11
1967 - 2 - 9	5.5	11
1970 - 7 - 2	5.8	11
1972 - 9 - 17	5.8	11
1973 - 11 - 4	5.8	11
1976 - 1 - 18	5.6	11
1979 - 11 - 6	5.6	11
1983 - 1 - 17	6.7	11
1983 - 1 - 19	5.5	11
1983 - 3 - 23	6	11
1987 - 2 - 27	5.6	3
1988 - 5 - 18	5.5	3
1990 - 6 - 16	5.8	3
1992 - 1 - 23	5.6	3
1993 - 6 - 13	5.7	3
1994 - 2 - 25	5.5	3
2000 - 5 - 26	5.6	3
2003 - 8 - 14	6.2	3
2003 - 8 - 14	5.5	3
2007 - 3 - 25	5.7	3
2014 - 1 - 26	6.1	20
2014 - 2 - 3	6.1	20
2015 – 11- 17	6.5	20

Zone B		
Date (y–m–d)	M	Cat
1509 - 2 - 25	5.6	5
1626 - 4 - 4	6	5
1638 - 3 - 27	7	5
1638 - 6 - 8	6.9	5
1659 - 11 - 5	6.6	5
1693 - 1 - 8	5.7	5
1708 - 1 - 26	5.5	5
1743 - 12 - 7	5.7	5
1744 - 3 - 21	5.7	5
1767 - 7 - 14	6	5
1783 - 2 - 5	7	5
1783 - 2 - 7	6.6	5
1783 - 3 - 28	7	5
1791 - 10 - 13	6	5
1832 - 3 - 8	6.6	5
1835 - 10 - 12	5.8	5
1836 - 4 - 25	6.2	5
1854 - 2 - 12	6.2	5
1870 - 10 - 4	6.1	5
1886 - 3 - 6	5.6	5
1887 - 12 - 3	5.5	5
1894 - 11 - 16	6.1	5
1905 - 9 - 8	7	5
1907 - 10 - 23	5.9	5
1908 - 12 - 28	7.1	5
1913 - 6 - 28	5.7	5
1928 - 3 - 7	5.8	5
1947 - 5 - 11	5.7	5

Zone C		
Date (y–m–d)	M	Cat
1444	6.4	18
1451	6.1	18
1471	6.1	18
1472	5.7	18
1473 - 1 - 20	5.5	18
1479 - 10 - 20	5.5	18
1480 - 10 - 18	5.5	18
1482 - 2 - 15	6.2	18
1520 - 5 - 17	6	17
1559 - 6 - 24	6	1
1563 - 6 - 13	6.1	18
1608 - 7 - 25	5.6	17
1617	6.2	18
1632	6	17
1639 - 7 - 28	6.4	18
1667 - 4 - 6	7.5	18
1713 - 1 - 0	6.3	17
1780 - 9 - 21	6.5	18
1816	6.3	18
1823 - 8 - 7	5.7	18
1827 - 4 - 17	6.5	18
1830	5.6	18
1833 - 1 - 19	6.5	14
1837 - 10 - 4	5.5	18
1843 - 9 - 5	6.2	17
1843 - 9 - 26	5.6	18
1848	6.4	17
1850 - 4 - 13	5.6	17
1851 - 1 - 20	6	18
1851 - 10 - 17	6.2	18
1851 - 10 - 17	6.6	17
1851 - 10 - 20	6.3	18
1851 - 12 - 29	5.5	18
1852 - 8 - 26	6.2	17
1853 - 12 - 11	5.7	18
1855 - 7 - 3	6.6	10
1855 - 7 - 5	6.8	18
1855 - 7 - 16	5.5	18
1855 - 8 - 14	5.5	18
1865 - 10 - 10	5.5	18
1869 - 1 - 10	5.6	18
1869 - 3 - 18	6	18
1869 - 4 - 14	5.5	17
1869 - 9 - 1	6.2	18
1870 - 9 - 28	6.5	17
1876 - 6 - 4	6.3	18
1876 - 6 - 5	5.6	18
1894 - 4 - 6	5.9	17
1895 - 5 - 14	5.5	18
1895 - 6 - 21	5.5	18
1895 - 8 - 6	6.2	17
1895 - 10 - 8	5.5	18
1896 - 2 - 10	5.9	17
1896 - 2 - 10	6.2	17
1905 - 6 - 1	6.6	18
1905 - 6 - 1	5.5	18
1905 - 6 - 3	5.5	18
1905 - 8 - 4	6	18
1905 - 8 - 6	5.5	18
1906 - 3 - 1	6.4	18
1907 - 8 - 1	5.7	18
1907 - 8 - 16	6.2	18
1920 - 11 - 29	5.6	13
1920 - 12 - 18	5.6	18
1921 - 3 - 30	5.6	11
1922 - 4 - 11	5.6	18
1926 - 12 - 17	5.8	18
1926 - 12 - 17	5.8	18
1927 - 2 - 14	6	18

1934 - 2 - 4	5.6	18
1935 - 3 - 31	5.6	11
1940 - 2 - 23	5.5	18
1948 - 8 - 27	5.5	18
1958 - 4 - 3	5.6	18
1959 - 8 - 17	5.9	18
1959 - 9 - 1	6.2	18
1959 - 10 - 7	5.6	18
1962 - 3 - 18	6.2	18
1968 - 11 - 3	5.5	18
1969 - 4 - 3	5.5	11
1970 - 8 - 19	5.5	18
1979 - 4 - 15	7	2
1979 - 4 - 15	5.7	11
1979 - 5 - 24	6.4	18
1982 - 11 - 16	5.7	18
1988 - 1 - 9	5.7	18
1996 - 9 - 5	6	3

Zone D		
Date (y–m–d)	M	Cat
1414 – 0 – 0	5.8	5
1456 - 12 - 5	7.2	5
1456 - 12 - 5	7	6
1456 - 12 - 5	6.3	6
1466 - 1 - 15	6.1	5
1560 – 5 - 11	5.6	5
1561 - 7 - 31	5.6	5
1561 - 8 - 19	6.8	5
1625 - 9 - 0	5.8	5
1627 – 7 - 30	6.7	5
1646 – 5 - 31	6.6	5
1647 – 5 – 5	5.9	5
1657 – 1 - 29	6.4	5
1688 - 6 - 5	7	5
1694 - 9 - 8	6.8	5
1702 - 3 - 14	6.5	5
1731 – 3 – 10	6.5	5
1732 - 11 - 29	6.6	5
1805 - 7 - 26	6.6	5
1826 - 2 - 1	5.8	5
1831 - 1 - 2	5.5	5
1836 - 11 - 20	6	5
1851 - 8 - 14	6.4	5
1853 - 4 - 9	5.6	5
1857 - 12 - 16	7	5
1875 – 12 – 6	6	5
1885 - 12 - 26	5.5	5
1889 – 12 – 8	5.7	5
1910 - 6 - 7	5.7	5
1930 - 7 - 23	6.6	5
1948 – 8 – 18	5.6	5
1962 - 8 - 21	5.7	5
1962 - 8 - 21	6.1	5
1980 - 11 - 23	6.9	5
1990 - 5 - 5	5.8	5
1990 - 5 - 5	5.5	5
1998 - 9 - 9	5.6	5
2002 - 10 - 31	5.7	5
2002 - 11 - 1	5.7	5

Zone E		
Date (y-m-d)	M	Cat
1456 - 12 - 5	5.8	6
1461 - 11 - 27	6.4	5
1599 - 11 - 6	6	5
1639 - 10 - 7	5.9	5
1654 - 7 - 24	6.3	5
1703 - 1 - 14	6.7	5
1703 - 1 - 16	5.9	17
1703 - 2 - 2	6.7	5
1706 - 11 - 3	6.8	5
1730 - 5 - 12	5.9	5
1762 - 10 - 6	6	5
1859 - 8 - 22	5.5	5
1874 - 12 - 6	5.5	5
1879 - 2 - 23	5.6	5
1881 - 9 - 10	5.6	5
1904 - 2 - 24	5.6	5
1915 - 1 - 13	7	5
1916 - 11 - 16	5.5	5
1933 - 9 - 26	6	5
1943 - 10 - 3	5.8	5
1950 - 9 - 5	5.7	5
1979 - 9 - 19	5.9	5
1984 - 5 - 7	5.9	5
1984 - 5 - 11	5.5	5
2009 - 4 - 6	6.2	5

Zone F		
Date (y-m-d)	M	Cat
1428 - 7 - 3	5.5	5
1458 - 4 - 26	5.8	5
1483 - 8 - 11	5.7	5
1584 - 9 - 10	5.8	5
1661 - 3 - 22	6.1	5
1672 - 4 - 14	5.6	5
1688 - 4 - 11	5.8	5
1690 - 12 - 23	5.6	5
1719 - 6 - 27	5.5	5
1741 - 4 - 24	6.2	5
1747 - 4 - 17	5.9	5
1751 - 7 - 27	6.3	5
1768 - 10 - 19	5.9	5
1781 - 4 - 4	5.9	5
1781 - 6 - 3	6.4	5
1781 - 7 - 17	5.6	5
1786 - 12 - 25	5.6	5
1789 - 9 - 30	5.8	5
1791 - 10 - 11	5.5	5
1799 - 7 - 28	6.1	5
1815 - 9 - 3	5.5	5
1832 - 1 - 13	6.3	5
1854 - 2 - 12	5.6	5
1870 - 10 - 30	5.6	5
1873 - 3 - 12	6	5
1875 - 3 - 17	5.9	5
1897 - 9 - 21	5.5	5
1916 - 5 - 17	6	5
1916 - 8 - 16	6.1	5
1916 - 8 - 16	5.5	5
1917 - 4 - 26	5.9	5
1918 - 11 - 10	5.9	5
1930 - 10 - 30	5.8	5
1984 - 4 - 29	5.7	5
1997 - 9 - 26	5.7	5
1997 - 9 - 26	6	5
1997 - 10 - 6	5.5	5
1997 - 10 - 14	5.7	5

Zone G		
Date (y-m-d)	M	Cat
1438 - 6 - 11	5.6	5
1470 - 4 - 11	5.6	5
1481 - 5 - 7	5.6	5
1497 - 3 - 3	5.9	6
1501 - 6 - 5	6	5
1505 - 1 - 3	5.6	5
1542 - 6 - 13	5.9	5
1570 - 11 - 17	5.5	5
1624 - 3 - 19	5.5	5
1796 - 10 - 22	5.6	5
1828 - 10 - 9	5.8	5
1831 - 9 - 11	5.5	5
1832 - 3 - 13	5.5	5
1834 - 2 - 14	5.8	5
1837 - 4 - 11	5.8	5
1909 - 1 - 13	5.5	5
1914 - 10 - 27	5.8	5
1919 - 6 - 29	6.3	5
1920 - 9 - 7	6.5	5
1971 - 7 - 15	5.6	5
2012 - 5 - 20	5.9	7
2012 - 5 - 29	5.8	7

Zone H		
Date (y-m-d)	M	Cat
1403 - 9 - 6	5.6	5
1502 - 3 - 26	5.7	18
1511 - 3 - 26	7	5
1511 - 6 - 25	5.6	17
1511 - 8 - 8	6.3	18
1551 - 3 - 26	6.3	18
1574 - 8 - 14	5.6	5
1626 - 7 - 3	6.5	18
1628 - 6 - 17	5.6	4
1640	6	4
1645	5.6	4
1648	5.7	18
1689 - 3 - 10	5.6	4
1690 - 12 - 4	6.5	5
1695 - 2 - 25	6.5	5
1697 - 3 - 15	5.6	4
1699 - 2 - 11	5.6	4
1700 - 7 - 28	5.6	5
1721 - 1 - 12	6.1	5
1750 - 12 - 17	5.9	18
1775 - 10 - 13	6.8	19
1776 - 7 - 10	5.8	5
1794 - 6 - 7	6	5
1802 - 1 - 4	5.6	18
1812 - 10 - 25	5.7	5
1836 - 6 - 12	5.5	5
1845 - 12 - 12	5.7	18
1870 - 3 - 1	6.4	18
1870 - 3 - 1	5.6	17
1873 - 6 - 29	6.3	5
1878 - 9 - 23	5.6	17
1880 - 11 - 9	6.3	18
1891 - 6 - 7	5.9	5
1895 - 4 - 14	6.2	5
1897 - 5 - 15	5.6	5
1905 - 12 - 17	5.6	18
1906 - 1 - 2	6.1	18
1916 - 3 - 12	5.6	5
1917 - 1 - 29	5.8	4
1926 - 1 - 1	5.9	5
1928 - 3 - 27	5.8	5
1936 - 10 - 18	6.1	5

1976 - 5 - 6	6.5	5
1976 - 9 - 11	5.6	5
1976 - 9 - 15	5.9	5
1976 - 9 - 15	6	18
1976 - 9 - 15	6	5
1998 - 4 - 12	5.7	3

Acknowledgments

We are very grateful to the following Institutions: A.S.I., ARPA Piemonte; Dipartimento di Fisica ed Astronomia (DIFA) dell'Università di Bologna; Dipartimento di Ingegneria Civile, Chimica, Ambientale e dei Materiale (DICAM) dell'Università di Bologna; Dipartimento della Protezione Civile della Calabria; E.U.R.E:F.; FOGER (Fondazione dei Geometri e Geometri Laureati dell'Emilia Romagna); FREDNET (O.G.S.); Italpos – Leica; Netgeo – Topcon; Provincia Autonoma di Bolzano (STPOS); Provincia Autonoma di Trento (TPOS); Regione Abruzzo; Regione Campania; Regione Friuli Venezia Giulia; Regione Liguria; Regione Lombardia; Regione Piemonte; Regione Puglia; Regione Umbria (Latopo); Regione Veneto; R.I.N.G.-I.N.G.V.; Stonex; which have kindly made available GPS recordings.

References

Albini P., 2004. A survey of past earthquakes in the Eastern Adriatic (14th to early 19th century). Ann. Geophysics, 47, 675-703.

Aliaj Sh., 2006. The Albanian orogen: convergence zone between Eurasia and the Adria microplate. In: Pinter N., Grenerczy G., Weber J., Stein S., Medak D. (Eds.), The Adria Microplate: GPS Geodesy, Tectonics and Hazard. NATO Science Series IV-Earth and Environmental Sciences, vol. 61. Springer, pp. 133-149.

Altamimi Z., Métivier L., Collilieux X., 2012. ITRF2008 plate motion model. J. Geophys. Res., 117, B07402, doi:10.1029/2011JB008930.

Ambraseys N., Finkel C.F., 1987. Seismicity of Turkey and neighbouring regions, 1899-1915. Ann. Geophysicae, 5B, 501-726.

Ambraseys N.N., 1990. Uniform magnitude re-valuation of European earthquakes associated with strong-motion records. Earthquake Eng. Struct. Dyn., 19, 1-20, doi: 10.1002/eqe.4290190103.

Ambraseys N.N., Jackson J.A., 1998. Faulting associated with historical and recent earthquakes in the eastern Mediterranean region. Geophys. J. Int., 133, 390-406.

Amoroso O., Ascione A., Mazzoli S., Virieux J., Zollo A., 2014. Seismic imaging of a fluid storage in the actively extending Apennine mountain belt, southern Italy. Geophys. Res. Lett., 41, 3802-3809.

Amoruso A., Crescentini L., Scarpa R., 1998. Inversion of source parameters from near- and far field observations: an application to the 1915 Fucino earthquake, central Apennines, Italy. J. Geophys. Res., 103, 29989-29999.

Anderson D.L., 1975. Accelerated plate tectonics. Science, 167, 1077-1079.

Anderson H., Jackson J., 1987. Active tectonics of the Adriatic region. Geophys. J.R. Astron. Soc., 91, 937-983.

Anelli L., Gorza M., Pieri M., Riva M., 1994. Subsurface well data in the northernApennines (Italy). Mem. Soc. Geol. Ital. 48, 461-471.

Argnani A., Frugoni F., Cosi R., Ligi M., Favali P., 2001. Tectonics and seismicity of the Apulian Ridge south of Salento Peninsula (Southern Italy). Ann. Geofisica., 44, 527-540.

Argnani A., Barbacini G., Bernini M., Camurri F., Ghielmi M., Papani G., Rizzini F.,Rogledi S., Torelli L., 2003. Gravity tectonics driven by Quaternary uplift in the Northern Apennines: insights from the La Spezia-Reggio Emilia geo-transect. Quaternary. Int., 101-102, 13-26.

Ascione A., Cinque A., Improta L., Villani F., 2003. Late Quaternary faulting within the Southern Apennines seismic belt: new data from Mt. Marzano area (southern Italy). Quaternary Int. 101-102, 27-41.

Ascione A., Caiazzo C., Cinque A., 2007. Recent faulting in Southern Apennines (Italy): geomorphic evidence, spatial distribution and implications for rates of activity. Boll. Soc. Geol. It. (It. J. Geosciences), 126, 293-305.

Ascione A., Cinque A., Miccadei E., Villani F., 2008. The Plio-Quaternary uplift of the Apennines Chain: new data from the analysis of topography and river valleys in Central Italy. Geomorphology, 102, 105-118, http://dx.doi.org/10.1016/j.geomorph.2007.07.022.

Barka A.A., 1996. Slip distribution along the North Anatolian Fault associated with the large earthquakes of the period 1939 to 1967. Bull. Seism. Soc. America, 86,1238-1254.

Bartolini C., 2003. When did the Northern Apennine become a mountain chain? Quaternary Int., 101-102, 75-80.

Bauve V., Plateaux R., Rolland Y., Sanchez G., Bethoux N., Delouis B., Darnault R., 2014. Long-lasting transcurrent tectonics in SW Alps evidenced by Neogene to present-day stress fields. Tectonophysics, 621, 85-100, http://dx.doi.org/10.1016/j.tecto.2014.02.006.

Benetatos C., Kiratzi A., 2006. Finite-fault slip models for the 15 April 1979 (Mw 7.1) Montenegro earthquake and its strongest aftershock of 24 May 1979 (Mw 6.2). Tectonophysics, 421, 129-143.

Ben-Menahem A., 1979. Earthquake catalogue for the Middle East (92 B.C.-1980 A.D.). Boll. Geofis. Teor. Appl., 84, 245-310.

Benouar D., 1994. Materials for the investigation of the seismicity of Algeria and adjacent regions during the twentieth century. Ann. Geofisica, 37, 4, doi:10.4401/ag-4466.

Blewitt G., Lavallée D., 2002. Effect of annual signals on geodetic velocity. J. Geophys. Res., 107, 2145, http://dx.doi.org/10.1029/2001JB000570.

Boccaletti M., Martelli L. (a cura di) 2004. Carta sismo-tettonica della Regione Emilia-Romagna, scala 1:250.000 e note illustrative. Selca, Firenze.

Boccaletti M., Corti G., Martelli L., 2010. Recent and active tectonics of the external zone of the Northern Apennines (Italy). Int. J. Earth Sci. (Geologische Rundschau), doi: 10.1007/s00531-010-0545-y.

Boncio P., Lavecchia G., 2000. A structural model for active extension in Central Italy. J. Geodynamics, 29, 233-244.

Boncio P., Bracone V., 2009. Active stress from earthquake focal mechanisms along the padan-adriatic side of the northern Apennines (Italy), with considerations on stress magnitudes and pore fluid pressures. Tectonophysics, 476, 180-194.

Bos M.S., Fernandes R.M.S., Williams S.D.P., Bastos L., 2008. Fast error analysis of continuous GPS observations. J. Geodesy, 82, 157-166, http://dx.doi.org/10.1007/s00190-007-0165-x.

Bos M.S., Bastos L., Fernandes R.M.S., 2010. The influence of seasonal signals on the estimation of the tectonic motion in short continuous GPS time-series. J. Geodynamics, 49, 205-209.

Bos M.S., Fernandes R.M.S., S.D.P. Williams and Bastos, 2013. Fast error analysis of continuous GNSS observations with missing data. J. Geod., 87, 351-360, doi: 10.1007/s00190-012-0605-0.

Boschi E., Gasperini P., Mulargia F., 1995. Forecasting where larger crustal earthquakes are likely to occur in Italy in the near future. Bull. Seismol. Soc. Am., 85, 1475-1482.

Bott M.H.P. and Dean D.S.,1973. Stress diffusion from plate boundaries. Nature, 243, 339-341.

Bressan G, Bragato P., Venturini C., 2003. Stress and strain tensors based on focal mechanisms in the seismotectonic framework of the Eastern Southern Alps. Bull. Seism. Soc. Am., 93, 1280-1297.

Brodsky E.E., 2009. The 2004-2008 Worldwide Superswarm. Eos. Trans. AGU, Fall Meet. Suppl., 90, S53B.

Brozzetti F., 2011. The Campania-Lucania Extensional Fault System, southern Italy: a suggestion for a uniform model of active extension in the Italian Apennines. Tectonics, 30, TC5009, http://dx.doi.org/10.1029/2010TC002794.

Burrato P., Poli M.E., Vannoli P., Zanferrari A., Basili R., Galadini F., 2008. Sources of Mw5+ earthquakes in northeastern Italy and western Slovenia: an updated view based on geological and seismological evidence. Tectonophysics, 453, 157-176, doi:10.1016/j.tecto.2007.07.009.

Calamita F., Coltorti M., Pieruccini P., Pizzi A., 1999. Evoluzione strutturale e morfogenesi plio-quaternaria dell'Appennino umbro-marchigiano tra il preappennino umbro e la costa adriatica. Boll. Soc. Geol. Ital., 118, 125-139.

Caputo R., Salviulo L., Bianca M., 2008. Late Quaternary activity of the Scorciabuoi Fault (southern Italy) as inferred from morphotectonic investigations and numerical modeling. Tectonics, 27, TC3004, doi:10.1029/2007TC002203.

Castellarin A., Colacicchi R., Praturlon A., Cantelli C., 1982. The Jurassic-Lower Pliocene history of the Ancona-Anzio line (Central Italy). Mem. Sot. Geol. Ital., 24, 325-336.

Castello, B., Selvaggi, G., Chiarabba, C., Amato, A., 2006. CSI Catalogo della sismicità italiana 1981-2002, versione 1.1. INGV-CNT, Roma (http://csi.rm.ingv.it/).

Catalano S., Monaco C., Tortorici L., 2004. Neogene-Quaternary tectonic evolution of the Southern Apennines. Tectonics, 23, TC2003, doi:10.1029/2003TC001512.

Cello G., Mazzoli S., Tondi E., Turco E., 1997. Active tectonics in the central Apennines and possible implications for seismic hazard analysis in peninsular Italy. Tectonophysics, 272, 43-68.

Cello G., Mazzoli S., Tondi E., 1998. The crustal fault structure responsible for the 1703 earthquake sequence of central Italy. J. Geodynamics, 26, 443-460.

Cenni N., D'Onza F., Viti M., Mantovani E., Albarello D., Babbucci D., 2002. Post seismic relaxation processes in the Aegean-Anatolian system: insights from space geodetic data (GPS) and geological/geophysical evidence. Boll. Geof. Teor. Appl., 43, 23-36.

Cenni N., Mantovani E., Baldi P., Viti M., 2012. Present kinematics of Central and Northern Italy from continuous GPS measurements. J. Geodynamics, 58, 62-72, doi:10.1016/j.jog.2012.02.004.

Cenni N., Viti M., Baldi P., Mantovani E., Bacchetti M.,Vannucchi A., 2013. Present vertical movements in central and northern Italy from GPS data: possible role of natural and anthropogenic causes. J. Geodynamics, 71, 74-85, http://dx.doi.org/10.1016/j.jog.2013.07.004.

Cenni N., Viti M., Mantovani E. 2015. Space geodetic data (GPS) and earthquake forecasting: examples from the Italian geodetic network. Boll.Geof. Teor. Appl., 56, 2,129-150.

Cerrina Feroni A., Martelli L., Martinelli P., Ottria G., Sarti G., 2001. The Romagna Apennines, Italy: an eroded duplex. Geological J., 36, 39-54.

Chilovi C., De Feyter J., Pompucci A., 2000. Wrench zone reactivation in the Adriatic block: the example of the Mattinata fault system (SE Italy). Boll. Soc. Geol. It., 119, 3-8.

Ciarapica G., Passeri L., 2002. The paleogeographic duplicity of the Apennines. Boll. Soc. Geol. Ital. Spec. Vol. 1, 67-75.

Ciarapica G., Passeri L., 2005. Late Triassic and Early Jurassic sedimentary evolution of the Northern Apennines: an overview. Boll. Soc. Geol. Ital., 124, 189-201.

Cloos M., 1993. Lithospheric buoyancy and collisional orogenesis: subduction of oceanic plateaus, continental margins, island arcs, spreading ridges, and seamounts. Geol. Soc. Am. Bull., 105, 715-737.

Comninakis P.E., Papazachos B.C., 1986. Catalogue of earthquakes in Greece and surrounding area for the period 1901-1985. Geophys. Lab. Pub. 1, University of Thessaloniki, Greece.

Costa M., 2003. The buried, Apenninic arcs of the Po Plain and Northern Adriatic Sea (Italy): a new model. Boll. Soc. Geol. It., 122, 3-23.

De Alteriis B., 1995. Different foreland basins in Italy: examples from the central and southern Adriatic Sea. Tectonophysics, 252, 349-373.

Del Ben A., Barnaba C., Taboga A.. 2008. Strike-slip systems as the main tectonic features in the Plio-Quaternary kinematics of the Calabrian Arc. Mar. Geophys. Res., 29, 1-12.

DeMets C., Gordon R.G., Argus D.F., 2010. Geologically current plate motions. Geophys. J. Int. 181, 1-80, doi: 10.1111/j.1365-246X.2009.04491.x.

De Paola N., Collettini C., Faulkner D.R., Trippetta F., 2008. Fault zone architecture and deformation processes within evaporitic rocks in the upper crust. Tectonics, 27, TC4017, http://dx.doi.org/10.1029/2007TC002230.

Devoti R., Esposito A., Pietrantonio G., Pisani A.R., Riguzzi F., 2011. Evidence of large scale deformation patterns from GPS data in the Italian subduction boundary. Earth Planet. Sci. Lett., 311, 230-241, http://dx.doi.org/10.1016/j.epsl.2011.09.034.

Di Bucci D., Mazzoli S., 2003. The October-November 2002 Molise seismic sequence (southern Italy): an expression of Adria intraplate deformation. J. Geol. Soc., 160, 503-506.

Di Bucci D., Caputo R., Mastronuzzi G., Fracassi U., Selleri G., P. Sansò P., 2011. Quantitative analysis of extensional joints in the southern Adriatic foreland (Italy), and the active tectonics of the Apulia region. Journal of Geodynamics, 51, 141–155.

Dong D., Herring T.A. and King R.W., 1998. Estimating regional deformation from a combination of space and terrestrial geodetic data. J. Geodesy, 72, 200-214.

Durand V., Bouchon M., Karabulut H., Marsan D., Schmittbuhl J., Bouin M.-P., Aktar M., Daniel G., 2010. Seismic interaction and delayed triggering along the North Anatolian Fault. Geophys. Res. Lett. 37:L18310. doi:10.1029/2010GL044688.

Elter F.M., Elter P., Eva C., Eva E., Kraus R.K., Padovano M., Solarino S., 2012. An alternative model for the recent evolution of Northern-Central Apennines (Italy). J. Geodynamics, 54, 55-63.

Ergin K., Guclu U., Uz Z,, 1967. A catalogue of earthquakes for Turkey and surrounding area (11 A.D. to 1964 A.D.). Instambul, Turkey.

Ergintav S., McClusky S., Hearn E., Reilinger R., Cakmak R., Herring T., Ozener H., Lenk O., Tari E., 2009. Seven years of postseismic deformation following the 1999, M=7.4 and M=7.2, Izmit-Duzce, Turkey earthquake sequence. J. Geophys. Res., 114, B07403, doi:10.1029/2008JB006021.

Eva C., Riuscetti M., Slejko D., 1988. Seismicity of the Black sea region. Boll. Geof. Teor. Appl. 117/118, 53-66.

Ferranti L., Santoro E., Mazzella M.E., Monaco C., Morelli D., 2009. Active transpression in the northern Calabria Apennines, southern Italy. Tectonophysics, 476, 226-251, doi:10.106/j.tecto.2008.11.010.

Ferranti L., Burrato P., Pepe F., Santoro E., Mazzella M.E., Morelli D., Passaro S., Vannucci G., 2014. An active obliquecontractional belt at the transition between the Southern Apennines and Calabrian Arc: The Amendolara Ridge, Ionian Sea, Italy. Tectonics, 33, 2169-2194, doi:10.1002/2014TC003624.

Finetti I.R., 2005. Ionian and Alpine Neotethyan Oceans opening. In: Finetti, I.R. (Ed.), Deep Seismic Exploration of the Central Mediterranean and Italy, CROP PROJECT. Elsevier, Amsterdam, pp. 103-108 (Chapter 6).

Finetti I., Del Ben A., 1986. Geophysical study of the Tyrrhenian opening. Boll. Geof. Teor. Appl., 110, 75-156.

Finetti I.R., Del Ben A., 2005. Ionian Tethys lithosphere roll-back sinking and back-arc Tyrrhenian Opening from new CROP seismic data. In: Finetti, I.R. (Ed.), Deep Seismic Exploration of the Central Mediterranean and Italy, CROP PROJECT. Elsevier, Amsterdam, pp. 483-504 (Chapter 21).

Finetti I.R., Boccaletti M., Bonini M., Del Ben A., Pipan M., Prizzon A., Sani F., 2005. Lithospheric tectono-stratigraphic setting of the Ligurian sea-Northern Apennines-Adriatic foreland from integrated CROP seismic data. In: Finetti, I.R. (Ed.), Deep Seismic Exploration of the Central Mediterranean and Italy, CROP PROJECT. Elsevier, Amsterdam, pp. 119-158 (Chapter 8).

Freed A.M., 2005. Earthquake triggering by static, dynamic, and postseismic stress transfer. Ann. Rev. Earth Planet. Sci., 33, 335-367.

Freed A.M., Ali S.T., Burgmann R., 2007. Evolution of stress in southern California for the past 200 years from coseismic, postseismic and interseismic stress changes. Geophys. J. Int., 169, 1164-1179.

Galadini F., Poli M.E., Zanferrari A., 2005. Seismogenic sources potentially responsible for earthquakes with M≥6 in the Eastern Southern Alps (Thiene-Udine sector, NE Italy). Geophys. J. Int., 161, 739-762.

Gasperini P., Lolli B., Vannucci G., 2013. Empirical calibration of local magnitude data sets versus moment magnitude in Italy. Bull. Seismol. Soc. Am., 103, 2227-2246, doi: 10.1785/0120120356.

Ghisetti F., Vezzani L., 1999. Depth and modes of Pliocene-Pleistocene crustal extension of the Apennines (Italy). Terra Nova, 11, 67-72.

Giunta G., Luzio D., Tondi E., De Luca L., Giorgianni A., D'Anna G., Renda P., Cello G., Nigro F., Vitale M., 2004. The Palermo (Sicily) seismic cluster of September 2002, in the seismotectonic framework of the Tyrrhenian Sea-Sicily border area. Ann. Geophysics, 47, 1755-1770.

Godey S., Bossu R., Guilbert J., Mazet-Roux G., 2006. The Euro-Mediterranean Bulletin: a comprehensive seismological bulletin at regional scale. Seismol. Res. Lett., 77, 460-474.

Guarnieri P., 2006. Plio-Quaternary segmentation of the south Tyrrhenian forearc basin. Int. J. Earth Sci. (Geol. Rundsch.) 95, 107-118, doi:10.1007/s00531-005-0005-2.

Guidoboni E., Comastri A., 2005. Catalogue of earthquakes and tsunamis in the Mediterranean area from the 11th to the 15th century. Istituto Nazionale di Geofisica e Vulcanologia, Roma, Italy.

Gutscher M.-A, Roger J., Baptista M.-A., Miranda J. M., and Tinti S.. 2006. Source of the 1693 Catania earthquake and tsunami (southern Italy): New evidence from tsunami modeling of a locked subduction fault plane. Geophysical Research Letters, vol. 33, L08309, doi:10.1029/2005GL025442

Hackl M., Malservisi R., Hugentobler U., Wonnacott R., 2011. Estimation of velocity uncertainties from GPS time series: examples from the analysis of the South African TrigNet network. J. Geophys. Res., 116, B11404, http://dx.doi.org/10.1029/2010JB008142.

Heki K., Mitsui Y., 2013. Accelerated pacific plate subduction following interplate thrust earthquakes at the Japan trench. Earth Planet. Sci. Lett., 363, 44-49, http://dx.doi.org/10.1016/j.epsl.2012.12.031.

Herring T.A., King R.W., McClusky S.C., 2010a. GAMIT Reference Manual, GPS Analysis at MIT, Release 10.4. Department of Earth, Atmospheric and Planetary Sciences, Massachusset Institute of Technology, Cambridge, USA.

Herring T.A., King R.W., McClusky S.C., 2010b. Global Kalman filter VLBI and GPS analysis program, GLOBK Reference Manual, Release 10.4. Department of Earth, Atmospheric and Planetary Sciences, Massachusetts Institute of Technology, Cambridge, USA.

Iannaccone G., Scarcella G., Scarpa R., 1985. Subduction zone geometry and stress patterns in the Tyrrhenian Sea. Pure Appl. Geophysics, 123, 819-836.

ISIDe Working Group (INGV, 2010). Italian Seismological Instrumental and parametric database: http://iside.rm.ingv.it.

Jackson J., McKenzie D., 1988. The relationship between plate motions and seismic moment tensors and the rates of active deformation in the Mediterranean and Middle East. Geophys. J., 93, 45-73.

Karnik V., 1971. Seismicity of the European area, Part II. Dordrecht, Germany.

Kastelic V., Vannoli P., Burrato P., Fracassi U., Tiberti M.M., Valensise G., 2013. Seismogenic sources in the Adriatic domain. Mar. Petrol. Geol., 42, 191-213, doi:10.1016/j.marpetgeo.2012.08.002.

Kato A., Ohnaka M., Yoshida S. and Mochizuki H., 2003. Effect of strain rate on constitutive properties for the shear failure of intact granite in seismogenic environments. Geophys. Res. Lett., 30, 2108, doi:10.1029/2003GL018372.

Kokkalas S., Xypolias P., Koukouvelas I., Doutsos T., 2006. Postcollisional contractional and extensional deformation in the Aegean region. In: Dilek Y, Pavlides S (eds.) Postcollisional tectonics and magmatism in the Mediterranean region and Asia, Geol. Soc. Am., Spec. Paper 409, 97-123, doi: 10.1130/2006.2409(06).

Kreemer C., Holt W.E., Haines A.J., 2003. An integrated global model of present-day plate motions and plate boundary deformation. Geophys. J. Int., 154, 8-34, doi:10.1046/j.1365 246X.2003.01917.x.

Kuk V., Prelogovic E., Dragicevic I., 2000. Seismotectonically active zones in the Dinarides. Geol. Croatica, 53, 295-303.

Larroque C., Mercier de Lepinay B., Migeon S., 2011. Morphotectonic and fault-earthquake relationships along the northern Ligurian margin (western Mediterranean) based on high resolution, multibeam bathymetry and multichannel seismic-reflection profiles. Mar. Geophys. Res., 32, 163-179, doi: 10.1007/s11001-010-9108-7.

Lay T., Kanamori H,, Ammon C.J., Hutko A.R., Furlong K., Rivera L., 2009. The 2006-2007 Kuril Islands great earthquake sequence. J. Geophys. Res., 114, B11308, http://dx.doi.org/10.1029/2008JB006280.

Le Pichon X., Biju-Duval B., 1990. Les fonds de la Mediterranee. Hachette-Guides bleus, Paris, sud offset-Rungis.

Lombardi A.M., Marzocchi W., 2010. A double-branching model applied to long term forecasting of Italian seismicity ($M_L \geq 5.0$) within the CSEP project. Ann. Geophysics, 53, 31-39.

Louvari E., Kiratzi A.A., Papazachos B.C., Katzidimitriou P., 2001. Fault-plane solutions determined by waveform modelling confirm tectonic collision in the eastern Adriatic. Pure Appl. Geophys., 158, 1613-1637.

Luo G., Liu M., 2010. Stress evolution and fault interactions before and after the 2008 Great Wenchuan earthquake. Tectonophysics 491, 127-140, http://dx.doi.org/10.1016/j.tecto.2009.12.019.

Makropoulos K., Kaviris G., Kouskouna V., 2012. An updated and extended earthquake catalogue for Greece and adjacent areas since 1900. Nat. Hazards Earth Syst. Sci., 12, 1425-1430, doi: 10.5194/nhess-12-1425-2012.

Mantovani E., 2005. Evolutionary reconstruction of the Mediterranean region: extrusion tectonics driven by plate convergence. In: Finetti, I.R. (Ed.), Deep Seismic Exploration of the Central Mediterranean and Italy, CROP PROJECT. Elsevier, Amsterdam, pp. 705-746 (Chapter 32).

Mantovani E., Viti M., Cenni N., Albarello D., Babbucci D., 2001. Short and long-term deformation patterns in the Aegean-Anatolian systems: insights from space geodetic data (GPS). Geophys. Res. Lett., 28, 2325-2328.

Mantovani E., Viti M., Babbucci D., Tamburelli C., Albarello D., 2006. Geodynamic connection between the indentation of Arabia and the Neogene tectonics of the central-eastern Mediterranean region. In: Dilek, Y., Pavlides, S. (Eds.) Post-Collisional Tectonics and Magmatism in the Mediterranean Region and Asia. Geological Society of America, Special Volume, 490, 15-49.

Mantovani E., Viti M., Babbucci D., Albarello D., 2007a. Nubia-Eurasia kinematics: an alternative interpretation from Mediterranean and North Atlantic evidence. Ann. Geophysics, 50, 311-336.

Mantovani E., Viti M., Babbucci D., Tamburelli C., 2007b. Major evidence on the driving mechanism of the Tyrrhenian-Apennines trench-arc-back arc system from CROP seismic data. Boll. Soc. Geol. It., 126, 459-471.

Mantovani E., Viti M., Babbucci D., Vannucchi A., 2008. Long-term prediction of major earthquakes in the Calabrian Arc. Environmental Semeiotics, 1, 190-207.

Mantovani E., Babbucci D., Tamburelli C., Viti M., 2009. A review on the driving mechanism of the Tyrrhenian-Apennines system: implications for the present seismotectonic setting in the Central-Northern Apennines. Tectonophysics, 476, 22-40, doi:10.1016/j.tecto.2008.10.032.

Mantovani E., Viti M., Babbucci D., Albarello D., Cenni N., Vannucchi A., 2010. Long-term earthquake triggering in the southern and Northern Apennines. J. Seismology, 14, 53-65, doi: 10.1007/s10950-008-9141-z.

Mantovani E., Viti M., Babbucci D., Cenni N., Tamburelli C., Vannucchi A., 2012. Middle term prediction of earthquakes in Italy: some remarks on empirical and deterministic approaches. Boll. Geofis. Teor. Appl., 53, 89-111.

Mantovani E., Viti M., Babbucci D., Tamburelli C., Cenni N., Baglione M., D'Intinosante V., 2014. Generation of back-arc basins as side effect of shortening processes: examples from the Central Mediterranean. Int. J. Geosciences, 5, 1062-1079, http://dx.doi.org/10.4236/ijg.2014.510091.

Mantovani E., Viti M., Babbucci D., Tamburelli C., Cenni N., Baglione M., D'Intinosante V., 2015a. Present tectonic setting and spatio-temporal distribution of seismicity in the Apennine belt. Int. J. Geosciences, 6, 429-454, http://dx.doi.org/10.4236/ijg. 2015.64034.

Mantovani E., Viti M., Cenni N., Babbucci D., Tamburelli C., Baglione M., D'Intinosante V., 2015b. Seismotectonics and present seismic hazard in the Tuscany-Romagna-Marche-Umbria Apennines (Italy). J. Geodynamics, 89, 1-14.

Mantovani E., Viti M., Babbucci D., Tamburelli C., Cenni N., Baglione M., D'Intinosante V., 2016. Recognition of periAdriatic seismic zones most prone to next major earthquakes: insights from a deterministic approach. In: S. D'Amico (ed.), Earthquakes and Their Impact on Society. Springer Natural Hazard, Springer International Publishing Switzerland, 43-80, doi 10.1007/978-3-319-21753-6_2.

Margottini C., Ambraseys N.N., Screpanti A., 1993. La magnitudo dei terremoti italiani del XX secolo. ENEA, Roma, Italy, 57 pp.

Markusic S., Herak M., 1999. Seismic zoning of Croatia. Nat. Hazards, 18, 269-285.

Mariotti D., Guidoboni, E., 2006. Seven missing damaging earthquakes in Upper Valtiberina (Central Italy) in 16th-18th century: Research strategies and historical sources. Ann. Geophysics, 49, 1139-1155.

Marsan D., 2005. The role of small earthquakes in redistributing crustal elastic stress. Geophys. J. Int., 163, 141-151, doi: 10.1111/j.1365-246X.2005.02700.x.

Martinis B., Pieri M., 1964. Alcune notizie sulla formazione evaporitica del Triassico Superiore nell'Italia centrale e meridionale. Mem. Soc. Geol. Ital., 4, 649-678.

Marzocchi W., 2008. Earthquake forecasting in Italy, before and after the Umbria-Marche seismic sequence 1997. A review of earthquake occurrence modeling at different spatio-temporal magnitude scales. Ann. Geophysics, 51, 405-416.

Masek J.G., Duncan C.C., 1998. Minimum-work mountain building. J. Geophys. Res., 103, 907-917, doi:10.1029/97JB03213.

Mayer L., Menichetti M., Nesci O., Savelli D., 2003. Morphotectonic approach to the drainage analysis in the North Marche region, central Italy. Quaternary Int., 101-102, 157-167.

Mazzoli S., Pierantoni P.P., Borraccini F., Paltrinieri W., Deiana G., 2005. Geometry, segmentation pattern and displacement variations along a major Apennine thrust zone, central Italy. J. Struct. Geol., 27, 1940-1953.

Mazzoli S., Macchiavelli C., Ascione A., 2014. The 2013 Marche offshore earthquakes: new insights into the active tectonic setting of the outer northern Apennines. J. Geol. Soc., http://dx.doi.org/10.1144/jgs2013-091.

Mazzoli S., Santini S., Macchiavelli C., Ascione A., 2015. Active tectonics of the outer northern Apennines: Adriatic vs. Po Plain seismicity and stress fields. J. Geodynamics, 84, 62-76, http://dx.doi.org/10.1016/j.jog.2014.10.002.

Mercier J., Sorel D., Simeakis K., 1987. Changes in the state of stress in the overriding plate of a subduction zone: The Aegean Arc from the Pliocene to the Present. Ann.Tectonicae, 1, 20-39.

Mikumo T., Yagi Y., Singh S.K., Santoyo M.A., 2002. Coseismic and post-seismic stress changes in a subducting plate: possible stress interactions between large interplate thrust and intraplate normal-faulting earthquakes. J. Geophys. Res., 107, 2023, http://dx.doi.org/10.1029/2001JB000446.

Mirabella F., Barchi M., Lupattelli A., Stucchi E., Ciaccio M.G., 2008. Insights on the seismogenic layer thickness from the upper crust structure of the Umbria-Marche Apennines (central Italy). Tectonics, 27, TC1010, doi:10.1029/2007TC002134.

Moretti I., Royden L., 1988. Deflection, gravity anomalies and tectonics of doubly subducted continental lithosphere: Adriatic and Ionian Seas. Tectonics, 7, 875-893.

Neri G., Barberi G., Oliva G., Orecchio B., 2005. Spatial variations of seismogenic stress orientations in Sicily, south Italy. Phys. Earth Planet. Int., 148, 175-191.

Niemeijer A.R., Spiers C.J., 2007. A microphysical model for strong velocity weakening in phyllosilicate-bearing fault gouges. J. Geophys. Res., 112, B10405, doi:10.1029/2007JB005008.

Ozawa S., Nishimura T., Suito H., Kobayashi T., Tobita M., Imakiire T., 2011. Coseismic and post-seismic slip of the 2011 magnitude-9 Tohoku-oki earthquake. Nature, 475, 373-376, http://dx.doi.org/10.1038/nature10227.

Papazachos B.C., Comninakis P.E., 1982. A catalogue of historical earthquakes in Greece in and surrounding area, 479 B.C.-1900 A.D.. University of Thessaloniki (Greece), Geophys. Lab. Publ. 5, pp. 24.

Papazachos B.C., Papazachos C., 1989. The earthquakes of Greece. Ziti Publ., Thessaloniki, Greece, 347 pp., in Greek.

Peccerillo A., 2005. Plio-Quaternary Volcanism in Italy. Petrology, Geochemistry, Geodynamics. Springer-Verlag, Berlin-Heidelberg, Germany, pp. 1-365.

Piccardi L., Gaudemer Y., Tapponnier P., Boccaletti M., 1999. Active oblique extension in the central Apennines (Italy): evidence from the Fucino region. Geophys. J. Int,, 139, 499-530.

Piccardi L., 2005. Paleoseismic evidence of legendary earthquakes: The apparition of Archangel Michael at Monte Sant'Angelo (Italy). Tectonophysics, 408, 113–128.

Piccardi L, Tondi G, Cello G., 2006. Geo-structural evidence for active oblique extension in South-Central Italy. In: Pinter, N. et al., (eds.) The Adria microplate: GPS Geodesy, Tectonics and Hazard. Springer Verlag, 95-108.

Poljak, M., Zivcic, M., Zupancic, P., 2000. The seismotectonic characteristics of Slovenia. Pure Appl. Geophys., 157, 37-55.

Pollitz F.F., 2003. The relationship between the instantaneous velocity field and the rate of moment release in the lithosphere. Geophys. J. Int., 153, 595-608.

Pollitz F.F., Burgmann R., Romanowicz B., 1998. Viscosity of oceanic asthenosphere inferred from remote triggering of earthquakes. Science, 280, 1245-1249.

Pollitz F., Bakun W.H., Nyst M., 2004. A physical model for strain accumulation in the San Francisco Bay region: stress evolution since 1838. J. Geophys. Res., 109, B11408, http://dx.doi.org/10.1029/2004JB003003.

Pollitz F.F., Burgmann R., Banerjee P., 2006. Postseismic relaxation following the great 2004 Sumatra-Andaman earthquake on a compressible self-gravitating Earth. Geophys. J. Int., 167, 397-420, doi: 10.1111/j.1365-246X.2006.03018.x.

Pollitz F.F., Stein R.S., Sevilgen V., Burgmann R., 2012. The 11 April 2012 east Indian Ocean earthquake triggered large aftershocks worldwide. Nature 490, 250-253, doi:10.1038/nature11504.

Ribaric V., 1982. Seismicity of Slovenia. Catalogue of earthquakes (792 A.D.-1981). Seismological Survey of the SR of Slovenia, Ljubljana, Slovenia, Series A, 1, 649 pp.

Riguzzi F., Crespi M., Devoti R., Doglioni C., Pietrantonio G., Pisani A.R., 2012. Geodetic strain rate and earthquake size: new clues for seismic hazard studies. Phys. Earth Planet. Inter., 206, 67-75, doi: 10.1016/j.pepi.2012.07.005.

Rothé J.P., 1971. Seismicité de l'Atlantique oriental, de la Méditerranée occidentale et de ses bordures. Revue de Géographie physique et de Géologie dynamique, 13, 419-428.

Rovida A., Camassi R., Gasperini P., Stucchi M. (Eds.), 2011. CPTI11, the 2011 version of the Parametric Catalogue of Italian Earthquakes. Milano, Bologna (http://emidius.mi.ingv.it/CPTI).

Rydelek P.A., Sacks I.S., 1990. Asthenospheric viscosity and stress diffusion: a mechanism to explain correlated earthquakes and surface deformation in NE Japan. Geophys. J. Int., 100:39-58

Ryder I., Parsons B., Wright T.J., Funning G.J., 2007. Post-seismic motion following the 1997 Manyi (Tibet) earthquake: InSAR observations and modelling. Geophys. J. Int., http://dx.doi.org/10.1111/j.1365-246X.2006.03312.x

Santamaría-Gómez, A., Bouin, M.N., Collilieux, X., Wöppelmann, G., 2011. Correlated errors in GPS position time series: Implications for velocity estimates. J. Geophys. Res., 116, B01405, doi:10.1029/2010JB007701.

Savage H.M., Marone C., 2007. Effects of shear velocity oscillations on stick-slip behavior in laboratory experiments. J. Geophys. Res., 112, B02301, doi:10.1029/2005JB00423.

Schorlemmer D., Mele F., Marzocchi W., 2010a. A completeness analysis of the National Seismic Network of Italy. J. Geophys. Res., 115, B04308, doi: 10.1029/2008JB006097.

Schorlemmer D., Christophersen A., Rovida A., Mele F., Stucchi M., W. Marzocchi, 2010b. Setting up an earthquake forecast experiment in Italy. Ann. Geophysics, 53, 1-9.

Scisciani V., Calamita F., 2009. Active intraplate deformation within Adria: Examples from the Adriatic region. Tectonophysics, 476, 57–72.

Shebalin N.B., Karnik B., Hadzievki D. (Eds), 1974. UNDP/ENESCO Survey of the Balkan region. Catalogue of earthquakes Part I 1901-1970. UNESCO, Paris (France).

Shebalin N.V., Leydecker G., Mokrushina N.G., Tatevossian R.E., Erteleva O.O. and Vassiliev V.Yu., 1998. Earthquake catalogue for central and southeastern Europe 342 BC - 1990 AD. Final Report to Contract ETNUCT93-0087, Brussels, Belgium, 50 pp.

Shen Z.K., Jackson D.D., Ge B.X., 1996. Crustal deformation across and beyond the Los Angeles basin from geodetic measurements. J. Geophys. Res., 101, 27957-27980.

Stucchi M., Meletti C., Montaldo V., Crowley H., Calvi G.M., Boschi E., 2011. Seismic hazard assessment (2003-2009) for the Italian Building Code. Bull. Seismol. Soc. Am., 101, 1885-1911.

Stucchi M., Rovida A., Gomez Capera A.A., Alexandre P., Camelbeeck T., Demircioglu M.B., Gasperini P., Kouskouna V., Musson R.M.W., Radulian M., Sesetvan K., Vilanova S., Baumont D., Bungum H., Fäh D., Lenhardt W., Makropoulos K., Martinez Solares J.M., Scotti O., Živčić M., Albini P., Batllo J., Papaioannou C., Tatevossian R., Locati M., Meletti C., Viganò D., Giardini D., 2012. The SHARE European Earthquake Catalogue (SHEEC) 1000-1899. J. Seismology, 17, 523-544, doi:10.1007/s10950-012-9335-2.

Tamburelli C., Babbucci D., Mantovani E., 2000. Geodynamic implications of subduction related magmatism: Insights from the Tyrrhenian-Apennines region: J. Volc. Geothermal Res., 104, 33-43, doi: 10.1016/S0377-0273(00)00198-0.

Tansi C, Iovine G., Folino Gallo M., 2005. Tettonica attiva e recente, e manifestazioni gravitative profonde, lungo il bordo orientale del graben del Fiume Crati (Calabria settentrionale). Boll. Soc. Geol. It., 124, 563-578.

Teza G., Pesci A., Galgaro A., 2008. Grid_strain and grid_strain3: software packages for strain field computation in 2D and 3D environment. Comput. Geosci., 34, 1142-1153.

Teza G., Pesci A., Casula G., 2012. Strain rate computation in northern Victoria Land (Antarctica) from episodic GPS surveys. Geophys. J. Int., 189, 851-862, doi: 10.1111/j.1365-246X.2012.05403.x.

Toda S., Stein R.S., Sagiya T., 2002. Evidence from the AD 2000 Izu islands earthquake swarm that stressing rate governs seismicity. Nature, 419, 58-61.

Tondi E., Piccardi L., Cacon S., Kontny B., Cello G., 2005. Structural and time constraints for dextral shear along the seismogenic Mattinata Fault (Gargano, southern Italy). J. Geodynamics, 40, 134-152.

Toth L., Zsiros T., Monus P., 1988. Earthquake history of the Pannonian basin and adjacent territories from 456 A.D. Eur. Earthquake Eng., 3, 44-50.

Valensise G., Pantosti D., 2001. The investigation of potential earthquake sources in peninsular Italy: a review. J. Seismology, 5, 287-306.

Valensise G., Amato A., Montone P., Pantosti D., 2003. Earthquakes in Italy: past, present and future. Episodes, 26, 245-249.

Van Dijk J.P., Scheepers P.J.J., 1995. Neogene rotations in the Calabrian Arc. Implications for a Pliocene-Recent dynamic scenario for the Central Mediterranean. Earth Sci. Rev. 39, 207-246.

Viti M., D'Onza F., Mantovani E., Albarello D., Cenni N., 2003. Post-seismic relaxation and earthquake triggering in the southern Adriatic region. Geophys. J. Int., 153, 645-657.

Viti M., Mantovani E., Babbucci D., Tamburelli C., 2006. Quaternary geodynamics and deformation pattern in the Southern Apennines: implications for seismic activity. Boll. Soc. Geol. It., 125, 273-291.

Viti M., Mantovani E., Babbucci D., Tamburelli C., 2009. Generation of trench-arc-back-arc systems in the Western Mediterranean region driven by plate convergence. Boll. Soc. Geol. It., 128, 89-106.

Viti M., Mantovani E., Babbucci D., Tamburelli C., 2011. Plate kinematics and geodynamics in the Central Mediterranean. J. Geodynamics, 51, 190-204, doi:10.1016/j.jog.2010.02.006.

Viti M., Mantovani E., Cenni N.,Vannucchi A., 2012. Post-seismic relaxation: An example of earthquake triggering in the Apennine belt (1915-1920). J. Geodynamics, 61, 57-67, http://dx.doi.org/10.1016/j.jog.2012.07.002.

Viti M., Mantovani E., Cenni N., Vannucchi A., 2013. Interaction of seismic sources in the Apennine belt. J. Phys. Chem. Earth, 63, 25-35, http://dx.doi.org/10.1016/j.pce.2013.03.005.x.

Viti M., Mantovani E., Babbucci D., Cenni N., Tamburelli C., 2015a. Where the next strong earthquake in the Italian peninsula? Insights by a deterministic approach. Boll. Geofis. Teor. Appl., 56, 329-350, doi: 10.4430/bgta0137.

Viti M., Mantovani E., Babbucci D., Tamburelli C., Cenni N., Baglione M., D'Intinosante V., 2015b. Belt-parallel shortening in the Northern Apennines and seismotectonic implications. Int. J. Geosciences, 6, 938-961, http://dx.doi.org/10.4236/ijg.2015.68075.

Wells D.L., Coppersmith K.J., 1994. New empirical relationships among magnitude, rupture length, rupture width, rupture area and surface displacement. Bull. Seism. Soc. America, 84, 974-1002.

Westaway R., 1993. Quaternary uplift of southern Italy. J. Geophys. Res., 98, 741-772.

Williams S.D.P., Bock Y., Fang P., Jamason P., Nikolaidis R-M., Prawirodirdjo L., Miller M., Johnson J., 2004. Error analysis of continuous GPS position time series, J. Geophys. Res., 109, B03412, doi:10.1029/2003JB002741.

Williams S.D.P., 2008. CATS: GPS coordinate time series analysis software. GPS Solutions, 12, 147-153, doi:10.1007/s10291-007-0086-4.

Working Group CPTI, 2004. Catalogo Parametrico dei terremoti Italiani, versione 2004 (CPTI04). INGV, Bologna, Italy, ‹http://emidius.mi.ingv.it/cpti04/›.

Zecchin M., Praeg D., Ceramicola S., Muto F., 2015. Onshore to offshore correlation of regional unconformities in the Plio-Pleistocene sedimentary successions of the Calabrian Arc (central Mediterranean). Earth-Science Reviews, 142, 60-78.

ISBN: 978-88-98161-23-2